Process planning for an Additive/Subtractive Rapid Pattern Manufacturing system

by

Xiaoming Luo

A dissertation submitted to the graduate faculty

in partial fulfillment of the requirements for the degree of

DOCTOR OF PHILOSOPHY

Major: Industrial Engineering

Program of Study Committee:
Matthew Frank, Major Professor
Frank Peters
Robert Stephenson
John Jackman
Douglas Gemmill

Iowa State University

Ames, Iowa

2009

TABLE OF CONTENTS

LIST OF FIGURES

LIST OF TABLES

ACKNOWLEDGEMENTS

I would like to express my sincere appreciation to my major professor Dr. Matthew C. Frank for guiding me into the Rapid Prototyping & Manufacturing and CAD/CAM world, for his creative suggestions, day-to-day help, support, encouragement and patience through this work.

I greatly appreciate the assistance of Dr. Frank Peters in providing important knowledge, professional experience and perspective in the casting industry, in giving constant support and encouragement during my research, and in showing me an honest and optimistic attitude.

I sincerely appreciate the great suggestions of committee members: Dr. Robert Stephenson, Dr. John Jackman, and Dr. Douglas Gemmill. They showed me the way to dig into the academic research.

I am most thankful to my wife, parents and son for their sacrifice, understanding and support during this study.

This research has also been supported by all co-workers that I have had the pleasure of interacting with as a Research Assistant over the past 3 years, thanks Ye Li, Wutthigrai Boonsuk, Alex Renner, Fanqi Meng, Joe Petrzelka, and Scott Oberbroekling.

ABSTRACT

This dissertation presents a rapid manufacturing process for sand casting patterns using a hybrid additive/subtractive approach. This includes three major areas of research that will enable highly automated process planning; a critical need for a rapid methodology.

The first research area yields a model for automatically determining the locations of layers, given the slab height, material types and part geometry. Layers are chosen such that it will avoid catastrophic failures and poor machining conditions in general. First, features that are possible thin material machining positions are defined, and methods for detecting these feature positions from an STL model are studied. Next, a layer thickness calculation model is presented according to positions of these features.

The second area focuses on tools and parameters for the subtractive side of processing each layer. A tool size and machining parameter selection model is presented that can automatically select tool sizes and machining parameters, given layer thickness, part geometry, and material types. Machining strategies and related machining parameters are studied first. Then the method for Stepdown parameter calculation is presented. Finally, an algorithm based on both accessibility and machining efficiency is proposed for the selection of tool sizes for the rough cutting operation, finish cutting operation and optional semi-rough cutting operation.

The final research area focuses on a cutting force analysis for thin material machining with additional layer thickness & tool size interaction. Popular cutting force models are reviewed, and a suitable model for cutting force calculation in this process is evaluated. Then, a cantilever beam model is used to analyze the thin material machining failure

problem, and a minimum layer thickness model is presented. Third, a combined layer thickness & tool size model is constructed based on the machining tool deflection under cutting forces.

This rapid pattern manufacturing process and related software has been implemented, and experimental data is presented to illustrate the efficacy of this system and its process planning methods.

CHAPTER 1. GENERAL INTRODUCTION

In order to meet quick-changing customer requirements, traditional sand casting pattern manufacturing would benefit from Rapid Manufacturing (RM) technology. This dissertation proposes a new Additive/Subtractive Rapid Pattern Manufacturing (RPM) system that will be effective for sand casting pattern manufacturing. This chapter presents challenges in process planning for this system and proposes a set of research objectives.

1.1 Background

Rapid Prototyping (RP) emerged only a few decades ago as an additive manufacturing technology that could create complicated 3D parts by forming /depositing discrete cross sectional slices layer by layer. This method greatly simplified 3D parts fabrication by dividing complex 3D geometries into many simple 2D entities, which can be created using relatively simple fabrication methods. Many RP technologies have been developed based on the additive manufacturing theory; where the major differences among these technologies are the material and method used to form and combine 2D slices. For example, 3D Printing (3DP) prints an adhesive onto a powder bed in order to incrementally create parts [Allen et al. (2000)]; Stereolithography (SLA) solidifies photosensitive resins with a laser or UV light [Jacobs (1995)]; and Selective Laser Sintering (SLS) fuses small particles of plastic, metal or ceramics with a high power laser [Bourell et al. (1992)]. Compared with traditional CNC machining, RP technologies have advantages over creating complex part geometries which are impossible for traditional manufacturing, such as self-reentrant structures, internal voids, etc. [Wang et al. (1999)]. However, traditional RP methods provide limited part accuracy imposed by several issues

such as the forming processes themselves, internal stresses, and post processing, to name a few. Readily available materials in RP are plastics, ceramics and a few limited metals. The limitation in available materials has kept RP technologies from being used in the manufacturing of actual functional parts. The major benefit of an RP technology is that same process planning is extremely simple and can be applied to parts with nearly any geometry without changes (creating a cross section is simple regardless of 3D complexity). Therefore, the great time saving of RP comes from the simple and automatic pre-process engineering preparation for each part, rather than the actual speed of the process itself. Processing time in RP mainly depends on the 2D layer size and number of layers; and large parts can take a significant amount of time, perhaps hours or a few days. Considering the cost and time, very small batch size production would be economic for RP but larger quantities would not be appropriate.

RM is a word originated from RP, which is targeted at the production of functional parts using "*rapid*" technologies. However, RM is not a simple technical extension of RP. RP emerged as a technology that would focus on early prototyping, in order to evaluate and examine the product design. RM is specifically targeted at generating functional parts directly from the design on the computer, once the design is believed to be finalized. It not only shortens the pre-process engineering time greatly, but also makes it nearly a "*turnkey*" operation, which does not require human intelligence. RM could have great impact on an industries ability to reduce time to market, especially where customized products are needed for cases ergonomic or biomedical requirements, but could also be effective in enabling custom designs for short-run, high value components; such as large metal castings.

An important area of RM application is to produce tooling instead of actual parts, for higher volume manufacturing, such as casting molds, injection molds, casting patterns, etc. The required volumes are obviously small; usually a single pattern or mold can create hundreds, thousands, even tens of thousands of parts. However, the production of tooling takes a very long time, and at very high costs. Design changes once parts are molded are likewise very time consuming and expensive.

CNC machining, which accommodates a variety of materials from wood to plastics, and a variety of metals, can be used to fabricate high precision, low volume, and functional parts. Unlike traditional RP processes, CNC machining is a material removal (subtractive) process which creates parts from a larger piece of stock material. RM based on CNC machining has 2 forms: Subtractive CNC Machining RM[Vouzelaud and Bagchi (1992) Shin et al. (2002) Frank et al. (2004)] and Additive/Subtractive CNC Machining RM [Merz et al. (1994) Chen and Song (2001) Cormier & Taylor (2001) Hur et al. (2002)]. The Subtractive CNC Machining RM creates parts from a single piece of material stock with the aid of flexible fixture technologies and advanced process planning [Shin et al (2002) Frank (2004)]. Additive/Subtractive CNC Machining RM decomposes the part into several layers or machinable units and performs material deposition and material removal operations layer-by-layer or unit-by-unit.

In sand casting pattern manufacturing, traditional additive RP application is severely limited in terms of both available materials and part sizes [Wang et al (1999)]. Subtractive CNC Machining RM also cannot provide enough machining capability for large sand casting pattern manufacturing. This dissertation presents a method for Additive/Subtractive CNC Machining RM that simultaneously solves the issues of both

material choice and machining capability by decomposing a large pattern into several small layers which can be handled by CNC machining without collision risk in an automated fashion.

1.2 Motivation

Sand casting is often utilized in the manufacturing of metal parts with a wide range of sizes, from one to several thousand pounds. Even though sand casting has been used for centuries, it is still one of the most important manufacturing processes today [Beeley (2001)]. A key element in the sand casting process is the pattern used to form the mold cavity in sand [Ammen (1979)]. Once a pattern is made, tens, hundreds and sometimes thousands of sand molds can be made; each producing one part.

Pattern making is considered a highly skilled task and most patterns today are made by specialty pattern shops that serve foundries, although some foundries still contain pattern fabricating departments. In early times, patterns were made manually by craftsmen using manual lathes, mills and other woodworking machines. In some cases, the pattern shop not only makes, but designs the pattern geometry given the intended part geometry. Designs for parts need to be modified to take into account parting lines, shrink and draft. This method is still being employed by many small and even larger foundries today. The advent of modern CNC machines has reduced the need for hand-made or manually processed patterns; however, this has only shifted the requirements of pattern makers to high-skilled NC programmers and machine operators. The CNC router or milling machine provides the necessary geometry creating capabilities and material needs for the pattern making industry; yet a truly automated or rapid technology is still not available.

There is a strong motivation to implement a RM technology in pattern manufacturing. However, there are limitations in current RM technologies mostly related to size and materials. An RPM system which continuously deposits thick material slabs and machines geometries in this layer with CNC milling operations layer by layer is proposed in this dissertation. This RPM process has been proven to be feasible; able to create large sand casting patterns out of wood in the laboratory. However, the process planning for CNC machining, which is affected by many factors such as material, tool selection, machining parameters and so on, is a major problem hindering the completely automatic process planning for this RPM system.

1.3 Research Objectives

The primary objective of this dissertation is to provide process planning algorithms and software to realize the automatic and optimized process planning for the RPM system. To achieve this major objective, three sub-objectives are presented.

The first sub-objective is to develop a layer thickness planning algorithm for the RPM process. The layer thickness affects the machining quality of the RPM process; where a poor choice of layer transition can leave poor surface finishes or affect the strength of the pattern. In this work, layer thickness is decided by analyzing the pattern geometry to detect emerging and disappearing features and surfaces with small slopes.

Machining parameters (such as tool size, Feed rate, Stepdown) have significant influence on the machining time and quality. The second sub-objective is to evaluate the influence of machining parameters on the machining time and quality and present an optimization model to decide tool sizes and important machining parameters automatically for patterns with different geometries and dimensions.

The cutting force is one of the most important factors in the RPM process planning. The thin material machining failure and layer thickness & tool size interaction are two key problems related to cutting forces. The third sub-objective in this research is to study the cutting force calculation method, then set up the thin material machining model and layer thickness & tool size interaction model based on cutting force analysis.

1.4 Dissertation Outline

The remainder of the dissertation is organized as follows: A detailed review of related literature is presented in chapter 2. The general system structure and process planning steps are addressed in chapter 3. A layer thickness decision algorithm is presented in chapter 4, while chapter 5 presents a tool size and machining parameter selection algorithm. Next, the cutting force analysis for thin material machining and layer thickness & tool size interaction in the RPM process is proposed in chapter 6. The conclusion and future research is illustrated in chapter 7.

CHAPTER 2. LITERATURE REVIEW

In this chapter, related researches in fields of: RP application in pattern and mold manufacturing, layer thickness decision in Additive/Subtractive Rapid Prototyping and Manufacturing, tool size and machining parameters selection, cutting force model, thin material machining and machining error prediction, are reviewed.

2.1 Rapid Prototyping Application in Pattern & Mold Manufacturing

Rapid Prototyping & Manufacturing techniques emerged only a couple of decades ago. However, it has placed great impact on product design and manufacturing. With the development of Rapid Prototyping & Manufacturing technologies, some of them have been adopted by tooling makers.

An early technology, Laminated Object Manufacturing (LOM), could create sand casting patterns which, at least in appearance and in size, were very close to patterns used in the foundry. LOM process adheres sheets of paper (or plastic, metal) to the base, layer by layer, and then used a laser to cut the cross sectional slice outline geometry of each layer by hatching patterns for support removal. LOM is appropriate for generating sand casting patterns, wax injection molds for investment casting, and master models for silicon molding process [Mueller and Kochan (1999)]. LOM is extremely economic for low volume complex metal parts which are needed in a short time. The problem of low durability and wear resistance makes LOM patterns not appropriate for high volume production. Wang et al. (1999) discussed the LOM process for sand casting patterns and concluded that: 1) LOM-based rapid tooling yields about a 50% time and cost savings compared to aluminum tooling;

2) Some geometry may not be suitable for LOM based Rapid Tooling; 3) LOM introduces a variety of additional errors into the pattern and core box fabrication process.

Selective Laser Sintering (SLS) is an additive RP technique that uses a high power laser to fuse small particles of plastics, metal or ceramics powders to create ideal 3D geometries. SLS is difficult to acquire a complete melt of the material. SLS is employed to produce injection molds [King and Tansey (2003)]. The injection molds by SLS (RapidTool^{TM}) for injection of 50,000 parts have been made by DTM corporation in Austin [Pham et al. (2000)]. As a casting pattern, parts created with amorphous material by SLS process tend to be weak and brittle as the powder is not fully melt [Liew et al. (2003)]. A low melting point metal material can be used to infiltrate the green part and make it stronger. However, the infiltration process may cause large geometry distortion. The SLS is also used to combine the foundry sand coated with combination materials to form sand casting molds directly. This technique is special good for making low-volume sand casting molds with complex geometries which are difficult to be made by traditional sand casting mold techniques [Tang et al. (2004)].

Similar to SLS, Stereolithography (SLA) is a RP process to build parts with laser. The difference between SLS and SLA is that SLA uses laser to treat resin to form parts. SLA is also an important technique in Rapid Tooling manufacturing. SLA investment casting build structure (QuickCast^{TM}) was introduced since 1993 [Jacobs (1995) Hague et al. (2001)]. Thousands of functional parts have been produced with this method in a variety of different metals. KelTool^{TM}, which infiltrates the fused metal parts with copper alloy, produces long-life injection molds quickly and economically [Smock (1995)]. SLA parts are also used as

patterns to prepare RTV molds, epoxy molds for injection molding (DirectAIM) [Karapatis et al. (1997)].

Fused Deposition Modeling (FDM) is a RP technology commonly used within engineering design. Nozzles which are heated to melt materials move in both horizontal and vertical directions by numerical control mechanism to lay down the melt model and support material [Bellini and Guceri (2003)]. FDM has been directly or indirectly used in investment casting. The direct investment casting application is to use the FDM ABS plastic parts which are treated with metal spray as investment casting patterns. And the indirect investment casting application is to produce RTV molds from FDM plastic parts first; then create wax investment casting patterns from RTV molds [Lee et al. (2004)]. The surface finishing of FDM parts is not very smooth. Therefore, the surface of the final investment casting parts is also influenced. The combination strength for FDM parts between each layer is weak, which hinders FDM technology to be used in sand casting pattern manufacturing. And FDM technology also takes a long time to make a large part.

3D printing technique builds parts by repetitively laying down a thin layer of build material and injecting bonding adhesive with ink-jet printing technique layer by layer. Metal parts combined from metal powder in 3D printing machine and infiltrated with low melting point metal can be used as plastic injection molds [Michaels et al. (1992)]. Z Corporation developed ZCast 3D printing technique to produce sand casting patterns and molds. Zp102 is the powder material for sand casting pattern printing. Printed sand casting patterns are also need to be infiltrated with epoxy to provide high strength for multiple uses [Kawola (2003)]. A report shows printed sand casting patterns meet sand casting pattern tolerance requirement well. However, the number of effective production cycles of these patterns is not mentioned.

Zcast technique is also used to print sand casting molds directly. The sand casting mold is printed with Zcast 500 direct metal casting material. Very complex part geometry which is nearly impossible to be made by traditional sand casting techniques can be created by 3D printing. However, confined by 3D printer's dimension, molds created with 3D printing technique are still small parts.

Sanders ModelMaker is also a RP technology using ink jet printing technique. Tips inject tiny droplets of thermoplastics (model material) and wax (support material) on the top of the former layer. And a plane milling operation is executed to ensure precise and fine layer thickness. The very small layer thickness makes the part surface smooth, but it also increases the manufacturing time greatly. Therefore, this technology is ideal for small parts, such as jewelry etc. [Naitove (1996)].

Walter Schaaf (2000) presented a sand mold RP technique using industrial robots. This research is still in the prototype stage. Such sand molding techniques take a long time to produce a sand mold compared with traditional sand casting mold making from sand casting patterns. Therefore they are good for low-volume sand casting production.

Main reasons why these additive Rapid Prototyping & Manufacturing techniques are not widely used by sand casting pattern industry are:

1) Sand casting is usually used to make large scale parts. Existing Rapid Prototyping & Manufacturing techniques have difficulty in making large parts. There is always a balance between the precision and time consumption in Rapid Prototyping & Manufacturing techniques. It is hard to acquire good large scale sand casting patterns or moulds quickly with these Rapid Prototyping & Manufacturing techniques.

2) When sand casting patterns are used to make sand casting molds, large pressure force is usually applied to make sand molds dense. This requires sand casting pattern materials to have good strength. Some chemical composites and water are also added into the sand to make the mold combined together well. Therefore, pattern materials are also required to be resistant to water and mold chemicals.

3) One reason for sand casting to be widely used for centuries is that it is a cheap manufacturing process. Most Rapid Prototyping & Manufacturing techniques employ expensive materials and equipments to ensure precise dimensions and good surface finishing. The high material and equipment costs hinder the application of these technologies in sand casting pattern manufacturing.

Additive/Subtractive Rapid Prototyping & Manufacturing technique imports the subtractive operation, machining, into traditional Additive Rapid Prototyping & Manufacturing field, and integrates advantages of both machining and additive manufacturing. Additive/Subtractive Rapid Prototyping & Manufacturing technique also expands the usable material variety, which improves the functional part making, in Rapid Prototyping & Manufacturing field.

Vouzelaud and Bagchi (1992) proposed an adaptive laminated machining method for prototyping of dies and molds. In this method, a complex die or mold was decomposed into simple three dimensional segments first. Then, these segments were machined layer by layer. However, they only proposed this method, and no further research and implementation was found.

Yang et al. (2000) presented a Robotic Machining RP system. An articulated robot with six-degree-of-freedom was mounted on a 2m long linear track to perform the cutting

operation. A rotary platform with clamping fixture was installed for holding work pieces. The working envelope of this system could be up to $4\times2\times2$ m ($Length\times Width\times Height$), which could be used to make large patterns.

Hur et al. (2002) created a Hybrid-RP system using machining and deposition. In this system, a flexible machining center with 6-axis parallel mechanism was used to perform the machining. A material sheet was machined on the backside first, and deposited to the base. Then another machining operation was performed on the front side. In theory, this system could create any complex geometry.

Shape Deposition Manufacturing (SDM) is a freeform fabrication process which systematically combines material deposition with material remove processes. It decomposes the Computer Aided Design (CAD) models into 2-1/2D cross sectional layer representations first. Then it deposits individual segments of a part, and of support material structure, as near-net shapes. And it machines each to net-shape before depositing and shaping additional material. SDM is a process based on existing 3-Axis or 5-Axis CNC milling machines, and intends to make precise freeform functional parts [Merz et al. (1994)]. SDM can work on a variety of soft and hard materials to create fully dense structures. Gayle et al. (1998) created a die casting inserts with SDM and run in a 600 ton die cast machine to produce 150 aluminum pieces. Another characteristic of SDM is to create multi-material parts, which is used to create injection molds for plastic production and other multi-material structures [Weiss (1998)].

Millit is the commercial software which performs the process planning for 3-axis dual-side subtractive/additive machining. The hardware requirement of this process is quite simple, which is only a 3-axis CNC milling machine. However, the process is not automated,

and a manual operation is also needed to put the machined layers together [Millit website (2007)].

One of the special characteristics of the sand casting pattern is that it does not have overhang structure, and all features can be machined out from a single building orientation. In theory, a general 3-Axis CNC milling machine is enough to create all features on sand casting patterns. However, confined by machine capability and geometry complexity, the common 3-axis or even 5-axis CNC milling machines cannot machine out a whole pattern at one time. These Subtractive/Additive Rapid Prototyping & Manufacturing systems listed above can be used to create sand casting patterns well. However, to the best knowledge of the authors, none of these Rapid Prototyping & Manufacturing technique meets sand casting pattern fabrication requirements well in industry, because:

1) These systems are complex and expensive for sand casting pattern manufacturing;
2) Most of these systems are still experimental systems.

Benefits of applying Rapid Prototyping & Manufacturing techniques into sand casting pattern production are as follows:

1) Without human participated process planning, Rapid Prototyping & Manufacturing technologies speed up reiterations of pattern making and design change greatly.
2) Rapid Prototyping & Manufacturing technologies are also special economic for low-volume pattern manufacturing.
3) Easy to operation characteristic of Rapid Prototyping & Manufacturing techniques reduces the skill requirement for pattern makers, and greatly simplifies the pattern manufacturing process.

However, due to the confinements of materials, speed, part precision, costs, system maturity etc., existing Rapid Prototyping & Manufacturing techniques have difficulty to be widely applied in sand casting pattern manufacturing.

2.2 Layer Thickness Algorithm

In conventional additive RP, thin cross sectional layer thickness is adopted to facilitate the part geometry creation and material deposition. These layer creation mechanisms usually create surfaces with stair step appearance. Additive/subtractive manufacturing processes create layers with CNC machining mechanisms which do not have the confinement of stair step appearance problem and greatly increases layer thickness to improve machining efficiency. Previous researchers have studied layer thickness in additive/subtractive manufacturing.

SDM is the rapid manufacturing process developed at Carnegie Mellon and Standford University [Merz (1994)]. In SDM, the part is decomposed into cross sectional thick layers first. Then layers are further decomposed to compacts for “single-step” geometry creation. Ramaswami, et al. (1997) presented a layer thickness method for SDM which was based on the analysis of all silhouette edges that denote transitions from non-undercut surfaces to undercut features. Surfaces were split by loops formed from these silhouette edges and other part edges.

The computer-aided manufacturing of laminated engineering materials (CAM-LEM) is one approach to directly fabricate components by assembling laser machined stock layers of engineering materials, such as metal and ceramics. CAM-LEM increases the layer thickness by inclining the laser relative to the sheet stock during cutting to avoid the stair step

appearance [Cawley et al. (1996)]. However, confined by the 1st order approximation to the part geometry curves, the layer thickness in CAM-LEM was still small.

In the layer based robot machining system presented by Chen and Song (1999), a six-degree-of-freedom articulated robot mounted on a 2m long linear track was employed to perform the machining operation, and the workpiece was fixed on a rotary platform. Geometry accessibility was the factor considered for layer thickness decision. Therefore, layer thickness was determined by continuously checking the feature visibility slice by slice. If total height of checked slices was equal to the largest material slab thickness, or some invisible regions occur, a new layer including these checked slices was formed. Then, a new search started until all slices were checked.

Hur, et al. (2002) presented a hybrid rapid prototyping system using machining and deposition based on the STEP feature model. The machining process included 2 steps: 1) back-face machining and deposition; 2) front-face machining. In this system, transition points between downward and upward faces were derived by analyzing silhouette and connection curves. Then layer thicknesses were determined based on these transition positions and the maximum material slab thickness.

The Free Form Thick Layered Object Manufacturing (FF-TLOM) is a technology that enables the fabrication of large shapes from thick layers of foam with smooth non-facetted surfaces. Targeted to fabricate large size objects, FF-TLOM breaks the large part into small components and makes these components layer by layer, then assemblies them together. This method is unique in that a heated flexible blade cutter which is able to adapt to the local curvature requirements is used to increase the layer thickness. Therefore, the layer thickness decision is based on matching part geometry curvature to available cutting blades with

certain curvatures. When no matching is found, the layer thickness is reduced to decrease the requirement for tool shape curvature. [Broek et al. (2002) Horvath (1999)].

The Solvent Welding Freeform Fabrication (SWIFT) process repeats the cycle of solvent welding and CNC contour machining on material sheets [Cormier and Taylor (2001) Taylor et al. (2001)]. Only uniform stock layer thickness in SWIFT is adopted because of the feeding system limitation, which introduces geometric error [Yang et al. (2002)].

Song, et al. (2005) presented a direct approach for freeform fabrication of metallic prototypes by 3D welding and milling. Their approach supported variable layer thickness by combining the deposition and subsequent face milling; however, the layer thickness decision in their approach was not addressed.

The hybrid adaptive layer manufacturing for rapid tooling studied by Akula and Karunakaran (2006) also integrated 3D welding and milling operations. No support structure was considered in this research because it was supposed there was no overhang structure in the objective die/mold geometry. In this research, a face milling operation was adopted to mill the top surface of the layer to attain the required layer thickness after each layer's weld deposition. This ensured the vertical z accuracy and avoided deposition defects of later layers. The layer thickness in this method was calculated from the weld bead height and step over increment to ensure the layer was fully filled of metal material.

Adaptive slicing [Tyberg and Bohn(1998)] also deals with the layer thickness problem; however, the layer thickness definition in the adaptive slicing is different from the layer thickness in this research. The objective of layer thickness decisions in adaptive slicing is to enable contours in each slice to best represent the part geometry in an efficient manner.

Layer thickness decision in the RPM process is to make sure part geometry is machined effectively, given the geometry of the pattern, and tools and materials used to create the pattern. In previous works, most researchers have considered layer thickness with a motivation of part geometry realization (to make it possible to create the geometry), while some have also considered the material slab thickness constraint. In the RPM process, geometry realization is not a problem in theory; two-part patterns for casting components with a definable parting line is not a problem. In contrast, this work is motivated by in-process failures, the final surface quality and strength of the pattern, which we believe can be significantly affected by layer thickness/layout.

2.3 Tool Size and Machining Parameter Selection

The tool size and machining parameter selection problem is a highly skilled task and has been a major problem which can hinder automated machining process planning. However, It is not easy to select cutting tools which are not only functionally correct but also optimum [Ribeiro and Coppini (1999)]. The development of software system for automatic tool selection is still in its infancy [Arezoo et al. (2000)].Many researchers have approached this problem in the literature. Some early researches focused on finding the single best milling tool for a particular feature [Lee (1994) Lee (1995)].

A geometric algorithm for finding the largest milling cutter for 2D milling operations was presented by Yao et al. (2001). The special point in this research was that a cutter feasible definition based on cutter's ability to cover the target region was proposed. Even though the application of the single cutter selection was limited, it could be the first step for multiple cutter selection.

Bala, et al. (1991) presented an automatic cutter selection and optimal cutter path generation method for prismatic parts. Prismatic parts in their research were parts which were composed by prismatic features, such as slots, steps, projections, etc. Algorithms for selecting appropriate rough and finish cutters and generating the cutter path and NC code for machining a pocket were presented in their research. An assumption for the rough and finish cutter matching was the material left behind by the rough cutter at each of convex vertices could be removed by one pass along the boundary of the finish cutter. Single cutter for rough and finish cutting made the application of this algorithm limit.

Chen et al. (1998) studied the optimal cutter selection and machining plane determination problem for die cavity rough machining operation. The integer programming and dynamic programming were adopted to search for the optimized tool set and machining plane set to minimize the total machining time.

Some researches addressed the problem of selecting multiple or a set of tools for 2D or 2½D pocket machining. A 2½D structure was composed of several 2D planes, so they could be considered as the same problem. Arya et al. (1998) proposed an approximation algorithm to select multiple tools from a set of tools for milling a particular plane based on the minimum cost. The running time and approximation ratio of this algorithm depended on the simple cover complexity of the milling region. A novel concept, Voronoi Mountain was presented by Veeramani and Gau (1997, 2000) to calculate the material volume that could be removed by a specific cutting-tool size. With the help of Voronoi Mountain, a dynamic programming model for selecting an optimal set of cutting-tool sizes for 2 ½ D pocket machining on the basis of processing time was studied. Nadjakova and Mcmains (2004) also studied the problem of finding an optimal set of cutters for 2D pocket machining on the basis

of approximation ratio and machinable area. Yao et al. (2003) expanded the cutter selection problem from the specific 2½D feature to multiple parts milling field.

Wang et al. (2005) presented a computer aided tool selection system for 3D die/mould-cavity NC machining using both a heuristic and analytical approach. This approach selected tool types, tool sizes and key parameters for dies and moulds cavity machining.

D'Souza (2006) proposed a method to solve the tool sequence selection for 2 ½ D pocket machining on setup level. This method optimized the tool path generation for all features in one setup, which might nest within each others, from perspectives of: (a) feature level optimization, (b) composite tool sequence graph optimization, (c) constrained graph optimization, and (d) sub-graph optimization. A cost model based on the actual tool path generation, which included machining tool path time, air path time, tool change time and tool life time, was developed to evaluate the tool sequence selection solutions. The complexity of the tool sequence selection problem was reduced in this paper by identifying the fact that "the accessible area of a larger tool is a strict subset of the accessible area of a smaller tool" [D'Souza (2006)].

On the basis of feature-based model, precise geometry accessibility evaluation is able to be calculated. Lim, et al (2000) developed an exact tool sizing algorithm for feature accessibility. Tool Access Distribution (TAD) and Relative Delta-Volume Clearance (RDVC) data were created from tool access algorithm, and adopted to select optimum tool automatically. The objective for tool selection and tool sizing in this algorithm was to study the geometric constraints imposed on tool selection. The input of this algorithm was feature

based digital CAD models. The result from this algorithm was able to ensure good surface accessibility.

With the development of Rapid Prototyping and Manufacturing, more and more attention is paid to tool size selection for sculpture surface or free-form surface milling.

Lee, et al. (1992) proposed a cut distribution and cutter selection for sculptured surface cavity machining. Sculptured surface was composed of some free-form curved surfaces which were difficult and expensive to produce. Sculptured surface in this paper was defined by Non-Uniform Rational B-Spline (NURBS) surfaces which provided flexibility and freedom for surface description. The curvature evaluation was employed to select the finishing cutter. Rough cutter size was based on cutters chosen for hunt planes in surface information evaluation, and semi-roughing was based on the geometric constraints and thickness of shoulders left on the surfaces. Tool selection was optimized by the objective of high Material Remove Rate (MRR). The difficulty in implementation of this system came from the determination of some system parameters.

Yang, et al. (1999) presented an interference detection and optimal tool selection solution for 3-axis NC machining of free-form surfaces. Three kinds of interference: protrusion interference, overlapping interference and boundary collision interference were defined and relative solutions were proposed. The optimal tool selection algorithm was based on the goal of minimum machining time. Objective surfaces in this paper were parametric surfaces. High computational power was needed if the grid resolution used in these algorithms was very fine.

Lin and Gian (1999) proposed a multiple tool approach to rough milling of sculptured surfaces depicted by ordered data points. In the beginning, NUB surfaces were formed from

the ordered data points, and sliced with constant z-height to acquire the boundary and island loops in each layer. Then tool sizes for linear pocketing, contour roughing, semi-roughing and new-island processing operations were selected for good machining efficiency and preventing from tool breaking.

Algorithm for decomposing machining operations for free-form surface features to minimize machining time was presented by Sun et al. (2001). Based on the decomposition of rough cutting and finish cutting, algorithms for rough cutting tool and finish cutting tool selection were also studied.

Many related researches in the optimized tool selection are based on MRR optimization [Balasubramanima (2001) Lee(1992) Yang (1999)]. The MRR is mainly concerned about the machining efficiency. With the development of CAD/CAM technology, feature-based models are widely adopted. Many feature-based algorithms have been developed since then [Joo et al. (1997) Perng and Cheng (1994) Chamberlain et al. (1993)]. By employing both the surface accessibility and MRR, feature-based algorithms acquire better precision.

Researches on machining parameters were always independent from the tool size selection problem [Chua (1993) Yazar (1994) Wang (1995)]. Rad and Bidhendi (1997) studied the optimum machining parameters determination problem for milling operations. Both single-tool and multi-tool operations were discussed in this research. A cutting force model based on two independent variables, 2D chip-load and feed rate was studied by Bae et al. (2003). Then an automatic feed rate adjustment method was proposed for optimal feed rate adjustment.

2.4 Cutting Force Models

A cutting force model is critical for machining process planning; it is also a key component in analyzing thin material machining problems and layer thickness & tool size interaction problem.

The cutting force problem is of course very old, with the first historic studies of Taylor at the turn of the last century [Taylor(1907)] After which, Merchant (1944), Zorev (1966), Trent (1977) et al. followed with proposed cutting force models. Some early researchers simulated cutting force models by fitting curves from experimental data with different machining parameter sets (spindle speed, feed, cutting depth etc.) [Boston et al. (1937) Armarego and Brown (1969)]. This experimental approach is extremely time consuming and costly; furthermore, cutting forces from these models are average cutting forces, not instantaneous. Two types of instantaneous cutting force models that have been studied include mechanistic models and mechanics models. In mechanistic models, the cutting force is proportional to the average chip load; and a set of cutting force coefficients in the model is unique for a workpiece-tool pair. Hence, a group of cutting experiments is required to calculate the cutting force coefficients for each workpiece-tool pair. These cutting force coefficients can then be used to calculate cutting forces under different machining parameters for the same workpiece-tool combination. This approach was presented by Sabberwal (1961), and adopted by later researchers such as Tlusty (1975), Sutherland (1986) and Altintas (1991).

For mechanics models, the milling process is simulated by orthogonal and oblique cutting, and cutting force coefficients can be calculated from existing orthogonal and oblique cutting force data in a data base; cutting experiments are not required. This is beneficial since

these models can be easily integrated into current CAD/CAM software systems; however, the approach also brings a certain loss of the precision. Other mechanics models have been studied, such as Armarego (1985), Budak (1996), et al. The average rigid force model is one of the more popular basic models [Wang (1988)], which is based on the relationship between Material Remove Rate (MRR) and average power consumption [Smith and Tlusty (1988)]. However, the average rigid force model can only acquire average cutting force which is not accurate in many cases. In the instantaneous rigid force model, the cutting force is proportional to the instantaneous contact between workpiece and end milling cutter [Devor and Kline (1980)], rather than the MRR. This model neglects the influence of cutting tool deformation by assuming the cutting tool is rigid. Based on the instantaneous rigid force model, Tlusty (1985), Hann (1983) and Kline (1982) calculated static tool deflection and surface error. Sutherland et al. (1986) improved the instantaneous rigid force model by considering the factor of cutter deformation in cutting force calculations. A further improvement of this model was made by including the influence of the wavy surface left by the passage of previous teeth to form the regenerative force and dynamic deflection model [Tlusty (1987)].

2.5 Thin Material Machining

Thin material machining in this paper is defined as a milling operation with a flat end mill cutter performed on thin material plates (or sheets). The thin material plate undergoes large elastic deformation under cutting forces, and intermittent material-tool contact usually causes self-excited oscillation when the material or tool has large elastic deformation [Davies and Balachandran (2000)]. Self-excited oscillation grows quickly and causes rough surface

finishing, material chipping, or even machining tool damage. Therefore, thin material machining is always undesirable machining operation.

Since thin material machining is hard to perform, punching, laser cutting, water jet cutting, and Electrical Discharge Machining (EDM) etc. are usually employed to avoid machining on thin materials. In some special situations where thin material machining cannot be avoided, special fixtures are designed to hold the thin workpiece stable to avoid excessive vibration and material fracture problems. Cameron (1989) presented a holder design for machining a thin walled cylinder. Obara et al. (2003) used low melting point alloys, whose melting point is below 100°C, to support and machine three-dimensional parts.

In recent years, thin material machining application is more and more required to produce high strength, light weight thin web structures in the aerospace industry [Bravo et al. (2005)]. Machining on thin material usually results in chatter, which may cause poor surface finish and dimension accuracy, chipping of the cutter teeth, or damage of machining tool and workpiece.

Self-excited oscillation between the workpiece and cutter is a common phenomenon in thin material machining. Tobias (1965) and Tlusty (1967) studied the basics of chatter vibrations from the aspect of regeneration of chip thickness. Their stability theories were based on orthogonal cutting where chip thickness, direction of cutting force and structural dynamics were constant [Budak and Altintas (1995)]. Extensive research efforts in the 60s and 70s were directed at understanding and modeling the dynamic machining process [Merrit (1965) Opitz et al. (1970) Tlusty et al. (1986)]. In recent years, several more models have been developed to explain chatter vibration under complicated machining situations.

Erhan and Yusuf (1995) developed a multi degree-of-freedom structure formulation to analytically predict chatter stability in milling operations. One of the benefits of the analytical prediction model was to determine chatter stability before cutting. Davies and Balachandran (2000) built a mechanics-based model with impact nonlinearities to explain the dynamic interactions between a tool and the workpiece. This model was targeted at the thin wall machining problem in high speed machining applications. Two dimensional (2D) and three dimensional (3D) chatter stability models in milling were proposed by Altintas (2000, 2001) to explain the source of chatter vibration and wave surfaces. A finite element analysis was adopted by He et al. (2003) to predict the machining deformation of thin-wall components, and an NC compensation strategy was also studied. Lacerda and Lima (2004) proposed a cutting force and chatter vibration prediction model. The time-varying directional dynamic milling forces coefficients were expanded in a Fourier series and integrated into the width of the cut, which was bound by the entry and exit angles. Experimental tests were employed to evaluate the cutting force in the contact zone between the cutting tool and workpiece. Bravo et al. (2005) presented a method for obtaining either the instability or stability lobes. This method used a three dimensional lobe diagram based on the relative movement of machine system and workpiece system. This model required that the machine structure and the machined workpiece had similar dynamic behaviors.

2.6 Machining Error Prediction

Cutting tool deflection has been and is still a focus of much research. Deflection calculation is used to predict the machining surface error and there exist two popular

approaches to calculate cutter deflection and machining surface error; the cantilever beam model and an FEM approach.

In cantilever beam models, there are two critical parameters; cutting force calculation and equivalent cutter diameter determination. A milling cutter usually has two basic components of the *shank* and *flute*, where the cutter shank is a simple cylinder whose bending deflection calculation can be easily acquired. However, the geometry of the cutter flute section is quite complex and not easy to be model. Kops and Vo (1990) proposed an equivalent diameter method to simulate the deflection behavior of the cutter flute with a standard cylinder model. This equivalent diameter method greatly simplified the cutter deflection calculation. The authors proposed an FEM method to evaluate the efficiency of the equivalent diameter model. This equivalent diameter model was adopted by Depince and Hascoet (2006). In addition, Kim et al. (2002) applied a two-step cylindrical cantilever beam model, based on the equivalent diameter model, to calculate the ball end milling deflection and form error. A similar two-step cylindrical cantilever beam model was also applied by Ryu et al. in 2003 and the cylindrical cantilever beam model was also applied by Rao et al. (2006) to study tool deflection during curved geometry milling, in which the cutting force is changing with the geometrical curvature.

Iwabe et al. (2004) applied the FEM model to predict the surface generation mechanism of a ball end mill based on deflection, where cutting force was acquired from cutting tests. Jalili Saffar et al. (2008) adopted an FEM method to simulate the end milling process and to predict the cutting tool deflection. Again cutter deflection prediction from their FEM method was validated through machining experiments. Other methods for cutter deflection and surface error prediction, such as neural networks [Ratchev (2002) Raksiri

(2004)] and measuring previously machined components [Liu and Venuvinod (1999) Lo and Hsiao (1998)] have also been used. Different neural networks models are needed for different conditions and workpiece-tool pairs; therefore, the application of this method is time consuming. On the other hand, empirical data generation makes the latter method a poor choice for determining the total deflection.

CHAPTER 3. PROCESS OVERVIEW: ADDITIVE/SUBTRACTIVE RAPID PATTERN MANUFACTURING

This chapter presents an overview of a rapid manufacturing process for sand casting patterns. The system is composed of two major process planning operations, which are: layer thickness decision, and tool size & machining parameter selection. Sections below provide details of these operations in the process planning and then an overview of three critical problems that must be solved.

3.1 The RPM Process

The Additive/Subtractive Rapid Pattern Manufacturing (RPM) system is a hybrid machining method which integrates material deposition and material removal operations in order to automatically create large patterns with ease. Basic steps of the RPM process are illustrated in Figure 3.1. The process begins by attaching a thick *slab* of material, cutting it to a defined *layer* thickness, and then creating the part geometry on this layer. In this manner, slabs are added and then turned into layers with flat surfaces on the top and complex geometry machined into the interlayer surfaces on its sides. The difference between the variable layer thickness versus the slab thickness is to create an accurate flat surface from each slab, at a specified height. This system combines the better characteristics of a traditional layer-based additive RP machine and CNC machining.

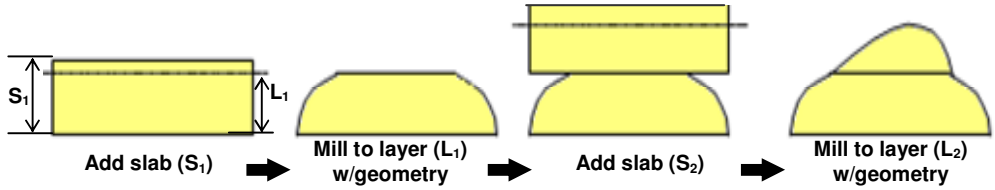

Figure 3.1 The RPM process

Sand casting patterns are usually made of wood, polyurethane or metal. Wood and polyurethane patterns are easy to fabricate, but not as durable as metal patterns. As product designs change more readily and often, the lifecycle of patterns may become shorter. In these cases, wood and polyurethane patterns are more and more appropriate due to lower cost. The RPM system proposed in this research is suitable for a wide variety of machinable materials, with a specific niche application in short-run or prototype castings where patterns can be made from foam or wood.

The RPM machine configuration is shown on the top left of Figure 3.2. The system is comprised of 5 major functional elements.

1) Work table platform: The work table is powered by a high precision servo motor which moves along the *z* direction to the specific layer position. It also increases the capacity of the system (versus a conventional CNC router), which makes the fabrication of tall patterns easily possible.

2) 3-Axis CNC router: The 3-Axis CNC router performs the function of cutting material slabs to the calculated layer thicknesses and creating part geometries on each layer. The same large face mill is adopted to cut the material slab to the specific layer thickness for each layer. Next, a special set of cutting tools are selected to create geometries on each layer.

3) Material handling system: The material handling system is designed to perform the material deposition function, which includes clamping, positioning and compressing material slabs.

4) Glue application system: The glue application system is represented by the “Glue head” in the figure. Its function is to apply glue on the bottom of material slabs for material deposition.

5) Material feed stack: The material feed stack is used to store material slabs and to feed them to the material handling system.

A sample sand casting pattern manufacturing process is also illustrated in Figure 3.2. The system performs a fabrication cycle for each layer. There are three steps in each layer fabrication cycle. To begin, a new material slab is deposited: the material handling system picks up a material slab, moves it across the glue head to apply glue on the bottom, and then positions it above the work table. Then the work table moves up to compress the base board or finished layers together with the new material slab for bonding and then the work table moves down to the specific layer position.

Second, a face milling operation is performed to machine the material slab down to the specific layer thickness. A variable layer thickness, rather than uniform layer thickness is adopted in the RPM process; where each layer has a specific thickness calculated by the layer thickness algorithm. Face milling also ensures that the top of each layer is relatively flat and parallel to the work table each time. This ensures good manufacturing precision and reduces inner stress caused by material deposition.

Lastly, a set of flat and spherical end mills are employed to machine out the part geometries in each layer. The set of tools and machining parameters are specially selected for each layer to ensure feature accessibility and reduce machining time.

Iterated like this, a sand casting pattern gradually *grows* up from the work table in the system. As a practical example, a simple sand casting pattern successfully created by the RPM process on the system is shown on the top right of Figure 3.2.

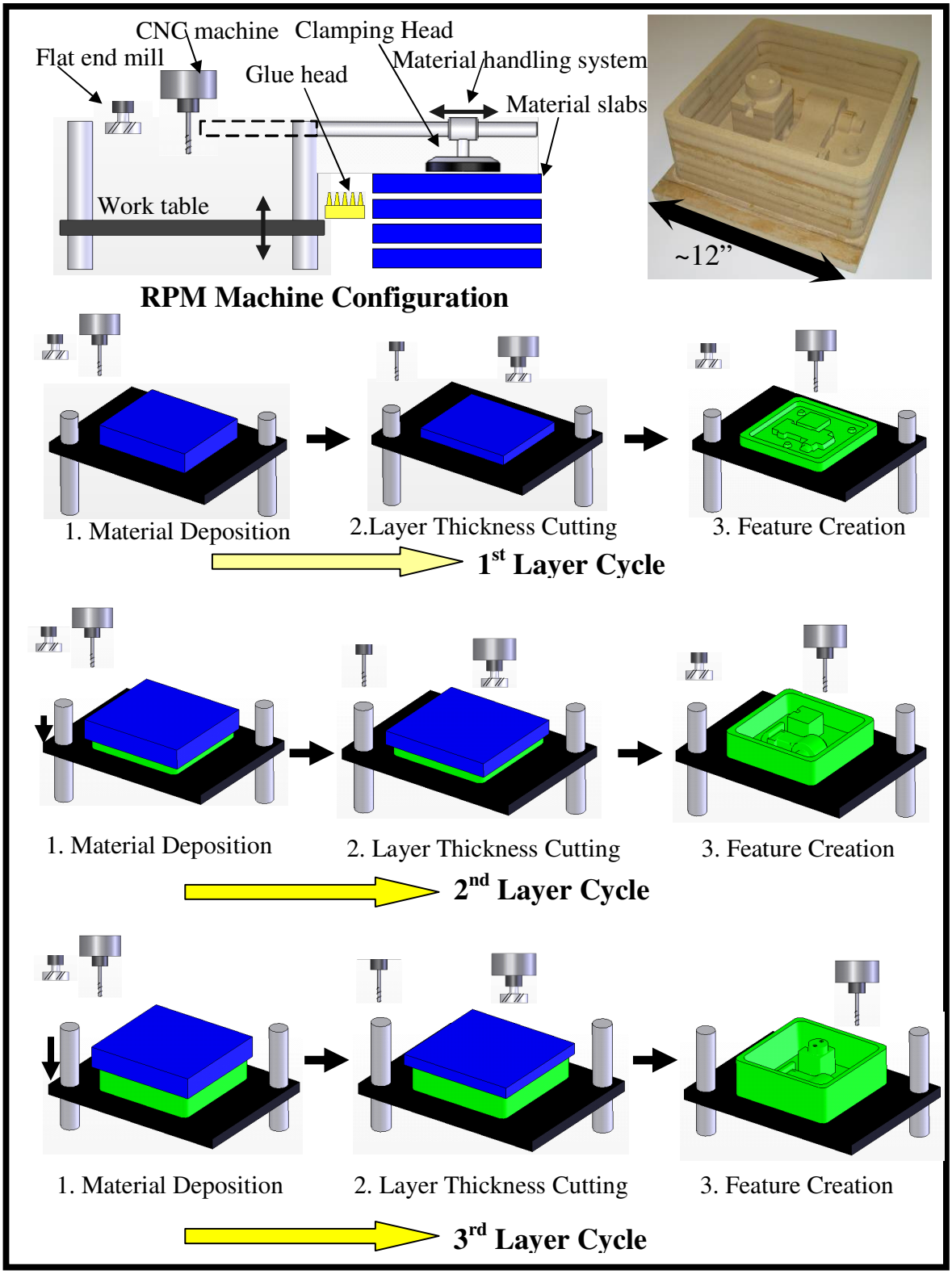

Figure 3.2 Sample part manufacturing process

3.2 Process Planning Operations

Automatic process planning is one of the most important characteristics of RP and RM systems. It not only shortens the required time from designs on the computer to real parts, but also greatly simplifies process planning to avoid the costly and time consuming skill of a technician. RP systems are, ideally, push-button machines that operate like office printers.

The function of the process planning software for the RPM system is to accept input of a 3D CAD geometry model, and output the content and sequence of a set of operations to produce high-quality final parts correctly. In the RPM process, the material used is thick material slabs, and the material deposition operation which includes clamping, applying glue and compressing, can be applied to any layer without considering the geometry differences on them. Therefore, the material deposition operation is not specially researched in the process planning as it is uniform and easy to automate.

The main task of process planning for the RPM system is to plan the actual CNC machining process. Process planning and automation for CNC machining is not new; however, since it requires some part-specific tooling and knowledge, completely automatic CNC machining process planning is still a challenge in the research field. With the addition of layered manufacturing, the process planning for Additive/Subtractive RM has some special characteristics of its own, which has not been addressed by previous researchers. Process planning for the RPM system includes 2 main operations.

1) Layer thickness analysis
2) Tool size and machining parameter selection

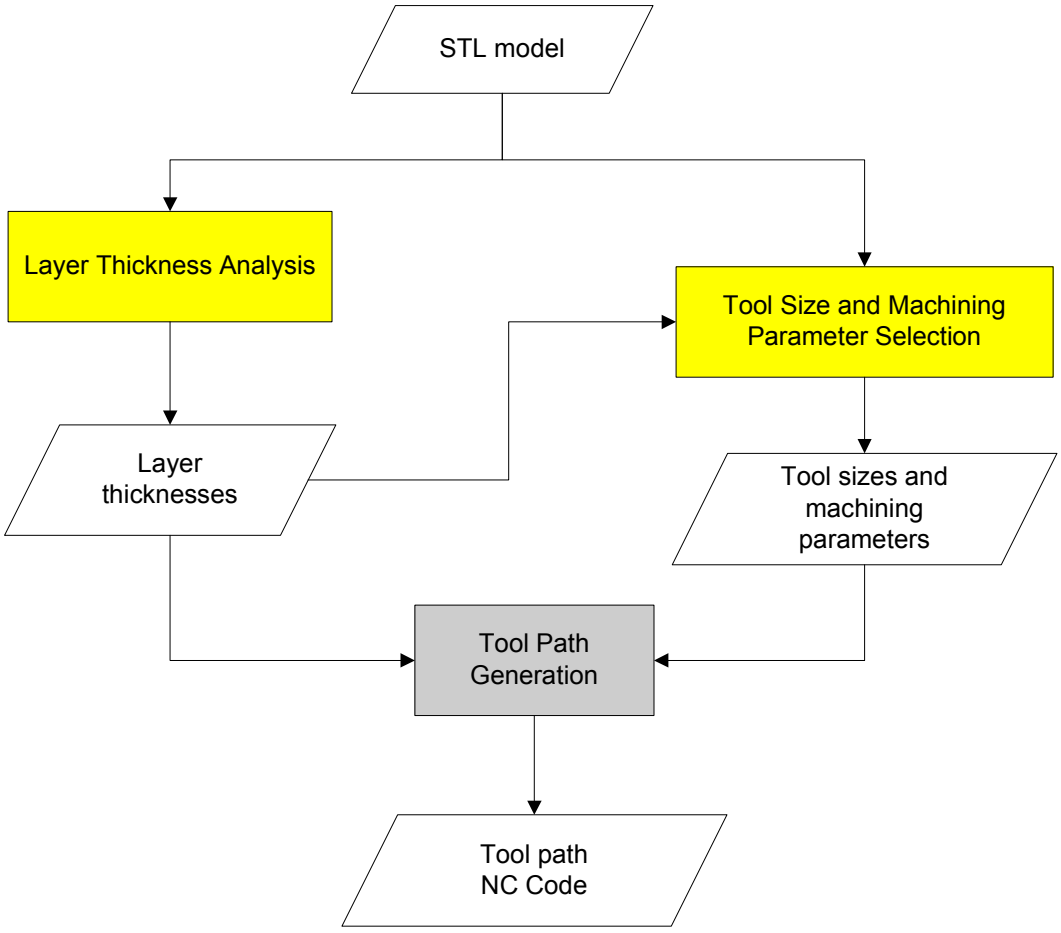

Figure 3.3 Process planning operations in the RPM process

Relationship of these two operations is shown in Figure 3.3. The process planning software accepts STL model which has been the de facto standard in RP field. This format allows input from both feature and non-feature based models. The first operation in process planning is to calculate the layer thicknesses. Next, tool sizes and machining parameters for each layer are calculated. These two fundamental operations are used to develop the overall process plan and the individual tool paths for each layer. An overview of each of these two operations and their interaction are analyzed in more detail in following sections.

3.2.1 Layer Thickness Analysis

Objective patterns for the RPM system are mostly 2-part molds and patterns which do not have overhanging structure (since we assume that sand molds must be pulled from the patterns). Hence, these patterns should be accessible via 3-axis machining from one setup orientation. However, deep cavities on the part may cause collision between the machine spindle and part geometry entities (Figure 3.4a). This problem has made it common in industry to invest in expensive and complex 5-axis systems in order to reach and access certain features on these patterns. In this research, a tall/deep pattern is divided into several layers with significantly smaller height, so collisions can be avoided altogether (Figure 3.4b). In addition, the process planning for each small individual layer is greatly simplified and more straightforward for automation.

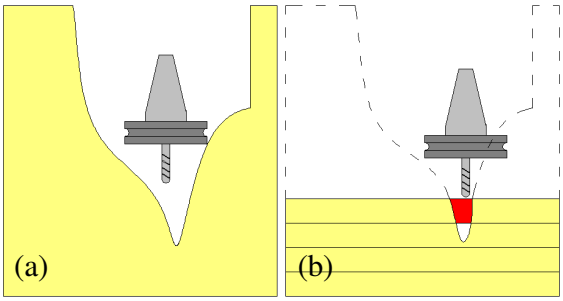

Figure 3.4 Deep cavity machining example (a) Large slab or solid block approach causes collision, (b) Layer based approach avoids collision

Although the layer-based approach is advantageous, there is a challenge of finding suitable locations to place these layers. Problems can occur if a layer is placed in some locations; such as 1) where a geometric feature emerges or disappears or 2) in areas of the pattern where small sloping surfaces exist. If a layer transition occurs at one of these locations it may cause problems such as adhesive exposure, or material failure/chipping during machining. As shown on the left of Figure 3.5, three parts created with uniform layer thickness exhibit machining problems. In Figure 3.5A, a new layer starts very close to the top

of the up-facing flat, creating a very thin upper surface. From experience, when pulling sand from a pattern such as this, any imperfections in the bonding of the layer may result in delaminating/cracking of the MDF. In contrast, the part in Figure 3.5B illustrates a considerably thicker section comprising this up-facing flat. Figures 3.5C and 3.5E are similar, except that one represents a local peak while the other represents both a local peak and an area of shallow surface slope. Failure occurred in both cases; however, the failure mode was catastrophic fracture in 3.5C versus excessive chipping in 3.5E. As expected, the bonded surfaces are intact in both cases, but the MDF material broke free in 3.5C and the edges of the shallow sloping surfaces chipped in 3.5E. In stark contrast, Figures 3.5D and 3.5F show the successful machining of these layers using the proposed layer placement algorithm.

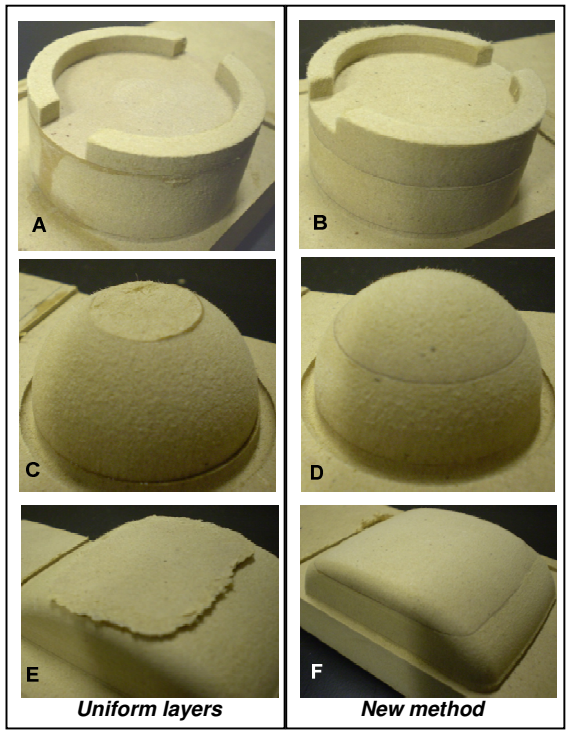

Figure 3.5 Illustrations of uniform (A,C,E) versus new (B,D,F) layer placement methods

3.2.2 Tool Size and Machining Parameter Selection

In traditional RP technologies, the same "tooling" is adopted for the fabrication of every layer in most typical applications (i.e. Laser spot diameter, extrusion tip diameter, etc.). In the RPM process, CNC machining is used to create each layer from a uniform material slab; hence different tools and parameters can be used for each layer. As shown in Figure

3.6a, a part with simple convex geometry can be created using a tool of any diameter, as long as no other contours on that layer are close to the boundary. However, the typical shape (Figure 3.6b) of a layer for a pattern will have generally more complexity and require appropriate tool diameters to be chosen automatically.

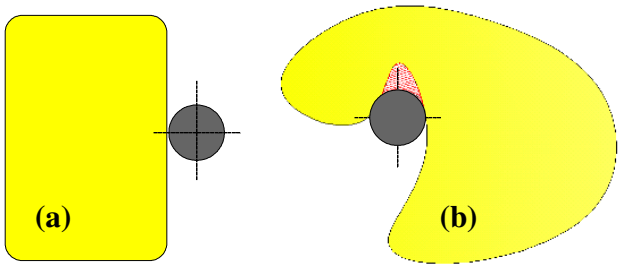

Figure 3.6 Different part geometry requires different tool size. (a) A large tool can be used to the convex shape; (b) A small tool is needed for the concave geometry

On one hand, the choice in tool size is directly related to the ability to create features. However, tool size also affects the machining time: large tools can cover a large machining area and endure larger cutting forces. Other important factors are the Stepdown (Cut depth), feeds and spindle speed chosen for each operation. Therefore, a critical issue in the RPM process is that tools and parameters are selected automatically and that those choices will result in a successfully created pattern. The selections should ensure that all geometry features are created successfully, surface finishes are sufficient for the application and the fabrication speed is efficient.

3.2.3 Thin Material Machining And Layer Thickness & Tool Size Interaction

Cutting force is the root cause of many machining problems. In the RPM process, there are 2 problems that need to be studied in terms of cutting force analysis, which are thin material machining problem, and layer thickness & tool size interaction problem.

Thin materials are easy to be deflected under large cutting forces. The deflection causes vibration, chipping and breaking of materials, which are unacceptable in machining.

However, the chance of thin material machining is large in the RPM process. Therefore, the thin material machining condition needs to be studied and avoided.

One of the restrictions for layer thickness decision is the material slab thickness, because the layer thickness must be smaller than the material slab thickness. This restriction can be resolved by combining multiple material slabs to acquire a material slab with no limit in thickness. When the material slab restriction is solved, the cutter length is the only restriction on the layer thickness decision; because the cutter length must be larger than the layer thickness to make sure the access to the bottom of the layer.

However, the tool length cannot be infinitely increased, because the deflection of the cutter under cutting forces may increase with the increase of length. To a certain degree, the deflection on the machined geometry caused by the deflection of workpiece and cutter is not acceptable. In this way, the layer thickness decision problem and tool size selection problem interact to each other when the material slab thickness limitation is solved.

To solve the interaction problem, cutting force is acquired first. Then, the cutter deflection model is needed to be setup. Finally, the layer thickness & tool size interaction model can be set up.

By resolving the material slab thickness restriction, the layer thickness can be increased greatly, which means less layers are needed. This change saves material deposition time and process planning time, improves machining quality, and also increases material usage ratio. Therefore, it is feasible and necessary to study the layer thickness & tool size interaction problem.

3.3 Summary

Process planning for the RPM system takes as input 3D CAD models and then outputs a complete manufacturing process plan. This chapter presented 3 critical problems in process planning: layer thickness analysis, tool size and machining parameter selection, and layer thickness & tool size interaction. Chapters 4, 5 and 6 of this dissertation present detailed proposals for solving these three major problems in creating a completely automated RPM process.

CHAPTER 4. A LAYER THICKNESS ALGORITHM FOR ADDITIVE/SUBTRACTIVE RAPID PATTERN MANUFACTURING

A paper accepted by the Rapid Prototyping Journal

Xiaoming Luo, Matthew C. Frank
Department of Industrial and Manufacturing Systems Engineering
Iowa State University, Ames, IA, 50011, USA

Abstract

Purpose – The purpose of this paper is to present an algorithm for an Additive/Subtractive Rapid Pattern Manufacturing process where thick slabs of material are sequentially stacked and then cut to 3D shapes. Unlike traditional rapid prototyping processes where layer thickness is typically uniform, this process is able to vary the layer thickness in order to most effectively generate feature shapes.

Design/methodology/approach – This paper discusses the factors affecting layer thickness decisions and then presents an algorithm to determine layer thicknesses for a given part model. The system is designed to import a CAD file and use the algorithm to automatically generate the set of layers based on the slab height, material and bonding properties and the process parameters used in the system.

Findings – The layer thickness algorithm was implemented and tested using an additive/subtractive manufacturing system developed in the laboratory. The algorithm has proved effective in determining appropriate layer heights for thick slab machining, taking into account a variety of geometries. Several sand casting patterns have been successfully created using the proposed system, which could significantly improve traditional sand casting pattern manufacturing.

Originality/value – The proposed Rapid Pattern Manufacturing process is a new process presented by the authors, developed for rapid sand castings. The layer thickness algorithm is an original contribution that enables automatic process planning for this new process.

Keywords – Rapid Manufacturing, Layer thickness, Sand casting patterns

Paper Type – Research paper

4.1 Background And Related Work

Sand casting is utilized in the manufacturing of a wide range of metal part sizes, from one to several thousand pounds. Even though sand casting has been used for centuries, it is still one of the most important manufacturing processes today. A key element in the sand casting process is the pattern used to form the mold cavity in sand. Once a pattern is made, tens, hundreds or sometimes thousands of molds can be made; each producing a part. There is a strong motivation to use a rapid prototyping technology for pattern manufacturing, especially for short runs or prototyping where the costs of a pattern cannot be easily justified. However, there are limitations in the current RP technologies mostly related to size constraints and materials available. Most sand casting patterns are made from wood, although some are made of urethanes and metals.

Pattern making is considered a highly skilled task and most patterns today are made by specialty pattern shops that serve the foundries, although some foundries still maintain pattern making departments. In early times, patterns were made manually by craftsmen using lathes, mills and other woodworking machines. In some cases, the pattern shop not only creates, but also designs the pattern geometry given the desired part geometry. For example, the original designs of the parts need to be modified to determine parting lines, design cores,

apply shrink rules and add draft to surfaces for the subsequent pattern geometry. The emergence of modern CNC machines has reduced the need for hand-made or manually processed patterns; however, this has only shifted the requirements of the pattern makers to high-skilled NC programmers and machine operators. Using a CNC router or milling machine provides the necessary geometric and material capabilities for the pattern industry; yet a truly automated or Rapid technology is still not available. Rapid Prototyping & Manufacturing (RP&M) techniques emerged only a few decades ago. Early adopters of some technologies were pattern making shops that needed a better method for testing part and/or pattern designs. This allowed different shrink, draft and gating systems to be tested by making a few sand molds and pouring metal. Once the design was finalized, a durable pattern could be manufactured using conventional means.

An early technology was Laminated Object Manufacturing (LOM), which could create sand casting patterns that, at least in appearance and size, were very close to patterns used in the foundry. LOM was used for generating sand casting patterns, wax injection molds for investment casting, and master models for silicone molding [Muller et al. (1999)]. LOM was seen as economic and somewhat effective for low volume complex metal parts but the problem of low durability and wear resistance made LOM ineffective for high volume production. Wang et al. (1999) discussed the LOM process for sand casting patterns and concluded that LOM-based rapid tooling yielded about a 50% time and cost savings compared to aluminum tooling, but that some geometry may not be suitable and that errors in the pattern were common. Selective Laser Sintering (SLS) has been used to directly create the sand molds using coated (*croning*) sand, which can be sintered into the mold shape. This technique can be effective for making very low-volume sand casting molds with complex

geometries which would be difficult to create using traditional sand casting mold techniques [Tang et al. (2003)]. However, since the process is making the mold directly, it can only make one part since the mold is typically destroyed in shakeout. In contrast a rapid pattern system can be used for at least several molds to ensure a good casting is created. Similar to SLS, Stereolithography (SLA) has been explored as an important technique in the rapid tooling field. The SLA investment casting build structure called QuickCast^{TM} was introduced in 1993 and has been used to create functional parts in a variety of different metals [Jacobs (1995) Hague et al. (2001)]. SLA parts have also been used as patterns to prepare RTV molds and epoxy molds for injection molding (DirectAIM) [Karapatis et al. (1997)]. Fused Deposition Modeling (FDM) has been directly or indirectly used in investment casting. The direct investment casting application is to use wax FDM parts as investment casting patterns; whereas the indirect application is to produce RTV molds from FDM plastic parts first, then create the wax investment casting pattern from RTV molds [Lee et al. (2004)]. The major limitation in FDM patterns is in the relatively rough surface finish available from relatively large layer thicknesses. Three Dimensional Printing (3DP) has also been used to create sand casting patterns and molds. Specialized powder materials for pattern printing have been developed for use with ink jet technology. The printed patterns are subsequently infiltrated with epoxy to provide suitable strength for multiple uses as patterns. The Zcast technique from ZCorp was developed in order to print sand casting molds directly [Kawola (2003)]. 3D printing allows for very complex part geometry which is nearly impossible using traditional sand casting techniques; however, confined by the 3D printer's dimensions, molds created with the 3D printing technique are typically limited to small parts. Thermojet printing such as the Sanders ModelMaker has been effectively used for investment casting through the

printing of wax. Its small layer thickness enables very smooth part surfaces, but it also increases the manufacturing time greatly and has relegated the technology to small parts such as jewelry [Naitove et al. (1996)].

There has been some research in other technologies that use subtractive methods and hybrid approaches using additive and subtractive means. Schaaf (2000) presented a sand mold RP technique using industrial robots. The technique requires a considerable amount of time to produce a sand mold compared to traditional approaches; therefore it is limited to low-volume sand casting production. Yang et al. (2002) presented a Robotic Machining RP system using a 6-axis robot on a linear track to perform the cutting operation and a rotary platform to position the workpiece. Hur et al. (2002) created a hybrid system using machining and deposition. In this system, two sided machining is executed on each deposited layer in the stack. Shape Deposition Manufacturing (SDM) is another process that combines material deposition with a material removal process. It decomposes the CAD models into sections that can be deposited as near-net shapes and then machines each to net-shape before depositing and shaping additional material [Merz et al. (1994)]. Millit is a commercial software package which performs the process planning for 3-axis dual-sided Additive/Subtractive approach; however, the process is not automated, with a manual operation to assemble the machined layers [Millit webpage (2007)].

The literature presents an array of approaches for rapid tooling, from purely additive, purely subtractive and hybrid systems. Some of the previous efforts have focused on making the mold directly instead of the pattern. This is suitable for single piece production, or very few parts; however, it leaves little room to perfect the metal pouring conditions or chemistry to ensure a good part. That said, direct RP of molds avoids a major issue of adding draft to

part surfaces in casting; an obvious advantage. To the best knowledge of the authors, there exists no clear solution to pattern making for sand casting, and certainly not for large parts. Sand casting allows for parts of relatively large scale; exceedingly large for most current RP systems. A rapid pattern making technology would allow for at least one, but more likely several molds to be created for prototypes and short-run production. There are examples in large metal casting where short production runs are typical (larger the part, smaller the production run) so an RP approach to pattern making is extraordinarily well suited. This research presents a method for rapid pattern manufacturing and in particular a layer placement algorithm that is critically important to the process.

4.2 Solution Methodology

A proposed methodology for Rapid Pattern Manufacturing (RPM) is presented in this section. The basic premise is to utilize an additive and subtractive approach in order to take advantage of accepted materials used in pattern making, while enabling very simplified toolpath and process planning so that it can be automated. The concept is to stack "slabs" of material which are subsequently machined to specified "layer" heights and with the required 3D geometry of only that layer. As such, very deep and complex patterns can be machined using considerably short tools. The process planning is reduced to a set of 2- and 2½-D toolpaths for each layer. For each layer, a face mill reduces the slab to a layer height and then a sequence of flat- and ball-milling operations using waterline toolpaths generate the 3D

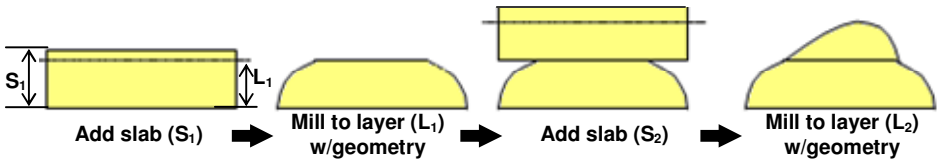

Figure 4.1 Basic steps in the RPM process

surface geometry. The basic steps of the process are illustrated in Figure 4.1.

Machining each slab to a particular layer thickness serves dual purposes; 1) it creates an accurate flat surface to ensure proper bonding of the subsequent layer and control over the part height and 2) it allows control over where the "seams" occur along the build height. The Additive/Subtractive Rapid Pattern Manufacturing system presented in this paper is designed for 3-axis, single-sided milling. As such, the process is suited mainly for the creation of two-part patterns for the metal casting industry. As partly an academic exercise, we include one undercut geometry (flat surface) for layer placement consideration, since they can be effectively created using an appropriate placement of slabs and layers. However, there are practical instances to justify this, since riser elements (used in pattern design for properly filling a casting) are sometimes implemented as loose components that may have undercut features. In these cases considering undercut flats in the algorithm has practical, albeit not straightforward uses.

The advantage of this rapid pattern manufacturing method is not obvious, as many in the industry currently use a similar approach with much larger "slabs", whereby blocks of material are glued together and then machined altogether. This is sometimes accomplished using 3- or even 5-axis CNC routers, depending on the pattern geometry and the overall depth. The advantage to our proposed method is two-fold 1) we reduce the process planning step from a large machining process plan to simpler, individual layers and 2)

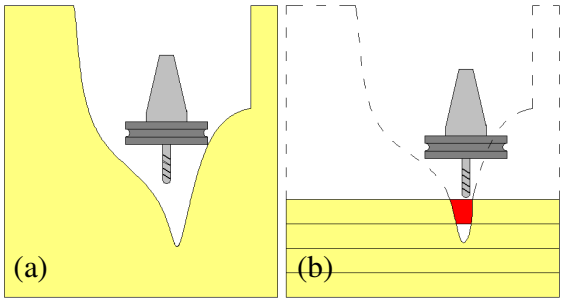

Figure 4.2 Deep cavity machining example (a) large slab or solid block approach causes collision, (b) Layer based approach avoids collision

most important, one can feasibly machine an entire pattern with very deep cavities and small features (illustrated in the example of Figure 4.2). Using this additive/subtractive approach, we can always use short, small diameter tools as needed, regardless of depth. Collision conditions usually avoided using 5-axis systems are eliminated altogether in our approach. As shown in Figure 4.2a, a large slab or solid block approach will lead to inaccessible regions. In contrast, our approach allows a small tool to access small regions, since the subsequent (higher) layers have not yet been added. In the laboratory, we have demonstrated this by making as small as 3mm features (interior radii) close to 1 meter deep in a pattern cavity. A sample pattern for a military component is illustrated in the implementation section; a smaller pattern, with only ~1meter x-y by 0.5meters deep. In theory, the system has very few limits on feature size, since we can control layer depth; hence, the maximum length tool required (short tools can have small diameters as needed, long tools cannot).

The specific problem addressed in this paper is choosing the thickness of the layers comprising each build, based on the slab thickness and the part geometry. As in many additive RP systems, a uniform layer thickness could be used, yet this may result in in-process failures and/or in the final quality of the pattern. For example, two approaches to layer thickness selection are illustrated in Figure 4.3. Option 1 shown in Figure 4.3a employs a uniform layer thickness, leading to an undesirable layout with respect to the

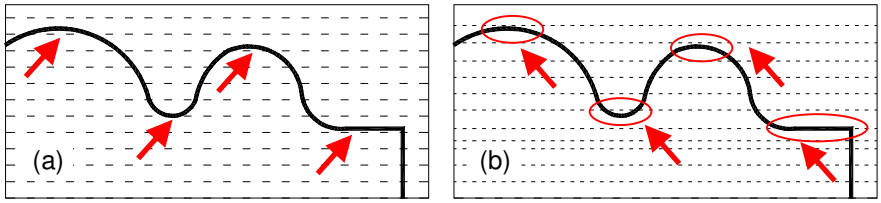

Figure 4.3 Layer thickness approaches (a) uniform layers do not locate effectively at peaks, valleys and flats, and (b) adaptive layers based on locations of features

peaks, valleys and flats found on the part geometry. Figure 4.3b illustrates an improved layout that uses variable layer thicknesses to enable more effective placement of layers to avoid poor machining conditions or resulting surfaces. These machining conditions have resulted in fractured, chipped and/or rough surfaces on wood patterns, or exposed adhesives at layer interfaces. Laboratory experiments have shown that the variable layer placement improves the process significantly; resulting in the successful processing of complex patterns with good surface finishes. The patterns have been tested using chemically bonded sand molds used to cast steel.

This problem of layer placement in RP is not new, however, it is typically not motivated by the same processing requirements. Previous researchers have studied layer thickness in additive/subtractive manufacturing, such as Hur, et al. (2002) who presented a hybrid rapid prototyping system using machining and deposition based on a STEP feature model. In their system, transition points between downward and upward faces are derived by first analyzing silhouette and connection curves and then layer thicknesses are determined based on these transition positions and the maximum material slab thickness. In a layer based robot machining system presented by Song and Chen (1999), layer thickness is determined based on the feature visibility and slab thickness. Binnard and Cutkosky (1998) utilized a pre-defined basic shape library to facilitate layer thickness planning for SDM. Pinilla, et al. (1998) presented another layer thickness method in SDM which was based on the analysis of all silhouette edges that denote transitions from non-undercut surfaces to undercut features. Chang, et al. (1999) presented a layer thickness planning approach based on surface splitting. The Free Form Thick Layered Object Manufacturing (FF-TLOM) is a technology that enables the fabrication of large shapes from thick layers of foam with smooth non-facetted

surfaces. The hierarchical decomposition of the CAD geometry in FF-TLOM describes components, segments, layers and sectors, based on morphological analysis [Broek et al. (2002)]. The Solvent Welding Freeform Fabrication (SWIFT) process repeats the cycle of solvent welding and CNC contour machining on material sheets [Cormier and Taylor (2001), Taylor et al. (2001)]. The uniform stock layer thickness in SWIFT is limited by the feeding system, which introduces geometric error [Yang et al. (2002)]. Song et al. (2005) presented a direct approach for freeform fabrication of metallic prototypes by 3D welding and milling. Their approach supports variable layer thickness by combining the deposition and subsequent face milling; however, the layer thickness decision in their approach is not addressed. Adaptive slicing [Tyberg and Bohn (1998)] also deals with the layer thickness problem; however, the layer thickness definition in the adaptive slicing is different from the layer thickness in this paper. The objective of layer thickness decisions in adaptive slicing is to enable contours in each slice to best represent the part geometry in an efficient manner. However, the layer thickness decision in the proposed Rapid Pattern Manufacturing system is to make sure part geometry is machined effectively, given the geometry of the pattern and the tools and materials used to create the pattern.

In previous work, most researchers have considered layer thickness with a motivation of part geometry realization (to make it possible to create the geometry), while some have also considered the material slab thickness constraint. In the proposed Additive/Subtractive Rapid Pattern Manufacturing system, geometry realization is not a problem in theory; two-part patterns for casting components with a definable parting line is not a problem. In contrast, this work is motivated by in-process failures and the final surface quality and strength of the pattern, which we believe can be significantly affected by layer

thickness/layout. The problem is to develop an algorithm that will take as input the surface geometry of the desired part (pattern/mold/etc.) and determine an effective sequential strategy for applying slabs and creating layer thicknesses. The general solution methodology involves several key areas of investigation including; 1) determining a set of factors affecting layer thickness decisions, 2) evaluating the input geometry to determine important "*features*" of the geometry, 3) conducting a *feature* height analysis, and 4) determining layer thicknesses appropriate for each unique combination of *feature* heights.

It should be noted that although the term "*feature*" is referred to in this paper, the goal of the research is to provide a more or less "*feature-free*" input requirement. That is, typical *feature-based* approaches assume that a part model is pre-defined by a set of "*features*" such as holes, planes, slots, cavities, bosses, etc. However, for a rapid prototyping and manufacturing process, one assumes that a platform-neutral format such as an STL file could be the CAD input. As an example, the input model could be derived from methods such as reverse engineering or medical scanning. Therefore, when this paper refers to *features*, it is in the sense of geometric characteristics of the part geometry, rather than traditional constructive solid geometry. The following section discusses factors affecting layer thickness decision criteria, followed by a description of the *feature* analysis method and then the layer thickness algorithm.

4.2.1 Factors Affecting Layer Thickness

The main factors affecting the layer thickness decision in this Rapid Pattern Manufacturing are based on a few assumptions about the general system setup. In this work, the following process and setup is proposed: 1) thick slabs of material are stacked and

bonded on a build platform 2) a 3-axis CNC mill/router machines each slab to a flat layer of designated height and forms the part surfaces within that layer, and 3) a set of cutting tools is available, with lengths as long as the slab is thick, or the maximum layer thickness, as required. This paper proposes that the layer thickness criteria are then based on 5 factors, as follows:

1) *Minimum cutting tool length*: The minimum cutting tool length determines the cutting depth for the system; therefore the maximum layer thickness is constrained by this value.

2) *Material slab thickness*: The layer thickness must obviously be less than or equal to the material slab thickness.

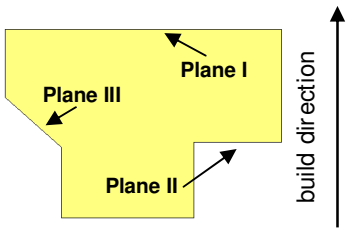

Figure 4.4 Basic part geometries

3) *Part geometries*: As shown in Figure 4.4, **Plane I** can be created; however, **Plane II** can only be created if a layer transition occurs precisely at this height. This is only possible when the plane is parallel to the faces of the slab (perpendicular to the stacking direction). Any other down-facing features, such as **Plane III,** cannot be fabricated by this system.

4) *Slab and bonding strength*: When machining, cutting forces can be sufficient to damage a very thin layer, regardless of the bonding strength of the adhesive, or the thin section may vibrate if bonding is not complete. In addition, it is undesirable to have the adhesive be exposed as a large surface on the part. In practice, these areas of exposed adhesive are potential places where chemically bonded sand could stick to the pattern. These reasons make it necessary to have a minimum criterion for the thickness of each layer. Figure

4.5 illustrates two of these cases, (a) a case where a thin layer is formed on a peak and (b) a case where a large area of exposed adhesive occurs.

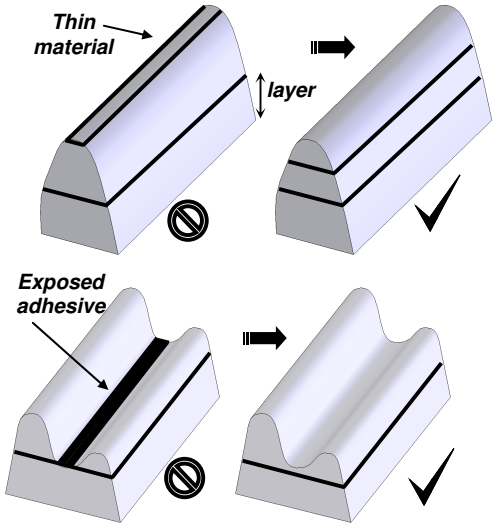

Figure 4.5 Thin material machining issues; left: poor layout, right: improved layout

5) *Freeform surface slope*: the freeform surface slope is used to describe the steep/shallow nature of a freeform surface at a point. The freeform surface slope at a certain point is defined as the reciprocal the slope of the normal at that point. As shown in Figure 4.6, *N* is the normal of the surface at point ***o***. The tangent plane T through point o is 90º to N. Therefore, the slope of tangent plane T is the reciprocal of the slope the normal at point ***o***. It should be noted that there are different slopes for the same freeform surface at different orientations. According to the experiments, if a new layer starts on the freeform surface where it has small surface slope (position (a) in Figure 4.6, thin webs that chip occur on the root of the new layer. On the other hand, it is safe for a layer to start from the freeform surface with large slope (Position (b) in Figure 4.6.

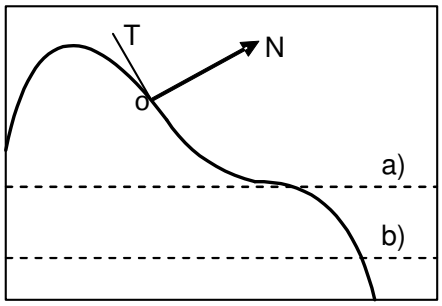

Figure 4.6 Freeform surface slope

The layer thickness algorithm for this research focuses on both manufacturing capability and part quality. It comprehensively considers the part geometry, slab and bonding material strength, slab thickness and tool length. This is accomplished by utilizing the simple

set of factors above, using only a simple input such as an STL file. The following section provides detail on the data input for the proposed layer thickness algorithm.

4.2.2 Data Input

Previous additive/subtractive methods have used a variety of CAD model formats as the system input geometry. The system presented by Hur, et al. (2002) imports STEP AP203 compatible feature models directly. The feature design information for layer thickness analysis can be directly acquired from this file format. In addition, toolpaths can be directly generated from it. The system by Chen and Song (2001) adopts the STL surface approximation model, the de facto standard in rapid prototyping. However STL format also has some shortcomings, including low accuracy and data redundancy [Leong et al. (1996)]. In this research, the STL format is utilized as the input to the layer thickness algorithm. STEP and IGES are widely used open international data exchange standards. They are effective at describing feature-based design models; however, there are many freeform models or digital models from reverse engineering which are not definable by feature-based models. In contrast, the STL format is generally compatible with both feature-based and feature-free models. It should be noted that the process described in this paper can actually avoid the argued inaccuracy of the STL approximation since we only use the STL file for analysis in the layer thickness algorithm. Once the analysis is completed (layer strategy is developed), 3-axis toolpaths can be generated from the native CAD file (if available), and not necessarily on the STL file. This approach was utilized for the example part presented in the implementation section of this paper. As such, the proposed layer algorithm was used to determine the layer sequence from an STL file, and then process and toolpath planning was

conducted based those layers using a CAM package (MasterCAM) on the original CAD model created in Solidworks.

4.2.3 Feature Analysis

A "*feature*" in this paper is loosely defined as a portion of a part having some machining significance and can be fabricated using 3-axis single-sided machining/routing. According to this definition, there are obviously countless surface shapes that could be considered *features*. In order to simplify the problem, these *features* are divided into 3 major groups, **Type I**, **Type II** and **Type III** features. **Type I** *features* include local peaks, local valleys and up-facing flats. **Type II** *features* are limited to planes having a normal in the –z direction. Finally, a **Type III** *feature* is a freeform surface with a shallow slope. As illustrated in Figure 4.7, a local valley exists as the bottom of a slot (Figure 4.7c) while local peaks exist on the top of the spherical and rounded entities (Figures 4.7a,c). The up-facing and down-facing flats are simply flat surfaces with normals in the +z or –z direction, as illustrated in Figures 4.7b,d. The position of a **Type I** feature is directly related to the thin layer problem described in the previous section. These heights along the z-axis must be found such that layer transitions at these heights are avoided. In contrast, **Type II** features (Figure 4.7d) dictate precisely where

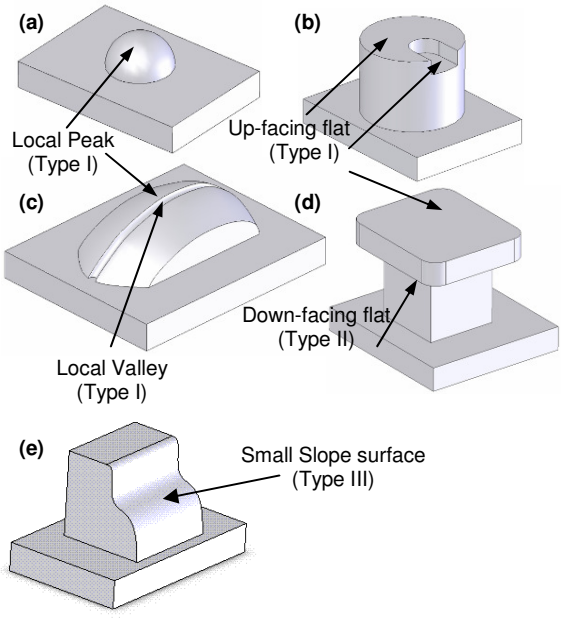

Figure 4.7 Feature Examples

a layer transition *must* occur, since it is impossible to create these undercuts by 3-axis machining along the z-axis. Therefore, the bottom side of the slab actually becomes the down-facing flat of the **Type II** feature. Of course, this also implies that the surface accuracy of the **Type II** entities is dependant on the slab surfaces, since they will not be machined surfaces. The reader will note that the **Type II** *feature* (a down facing plane) is included in this system because it is possible to create them; however, if the system is used for a purpose such as a sand casting pattern **Type II** *features* will not exist because they cannot release the sand mold, unless they are a special case of a loose piece riser that will be cut separately. A **Type III** *feature* (shallow sloping surface), affects the machining quality similar to an upfacing flat in that we can be confronted with thin material conditions and/or exposed adhesive.

The *feature* heights are the basis of the layer thickness algorithm, therefore the first step is to calculate these heights. The following section presents methods to determine the location of **Type I**, **Type II** and **Type III** *feature* heights. The location of the these feature heights along the z-direction will be used in conjunction with the slab thickness and layer parameters in order to determinethe most effective layout of layer transitions. The goal in layer positioning will be to avoid these critical features.

Type I: Local peaks and valleys

Each feature described in this work presents a different challenge in the layer based machining process. The local peak or valley presents a problem of thin materials in convex or concave surfaces. The local valleys have the potential to expose a considerable amount of adhesive. In practice, this has posed a problem if the resins used in the chemically bonded molding sand for casting react with the adhesive. The problem with peaks can be more

catastrophic, as we have experienced material failure during cutting. As shown in Figure 4.8a when an arbitrary layer placement leaves a small contact patch for the next layer, the machining of the slab may shear off the feature. Granted, the adhesive bond does not typically fail, in fact the cyanoacrylate glues used in the process are stronger than the MDF material; hence, the MDF material fails. Examples of these catastrophic failures are presented in the implementation section.

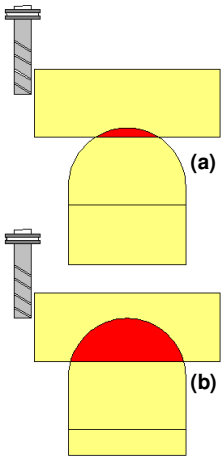

Figure 4.8 Local peak thin material machining issue

For this analysis, we simply analyze the slice geoemtry from an STL file. Each slice of an STL file contains several loops, or polygonal chains, and each chain defines part of the cross sectional slice of the object at that given layer height. When a loop *appears* or *disappears* from one slice to a successive slice of an STL file, it indicates the emergence or disappearance of what is referred to as a *feature* in this research. The *feature* heights can be obtained by locating these emerging and disappearing loops within the cross sectional slices of the part geometry as the slices are searched along the z-direction. There are several slicing algorithms available [Pandey et al. (2003) Luo et al (2001) Choi et al (2002)], thus it is easy to obtain the loops from a STL file, and then *feature* heights can be acquired by comparing these 2D loops. In previous work, Tyberg (1998) presents a contour vertical connectivity matching method. The method computes the intersection of two contours which belong to the same sub-slab [Tyberg and Bohn (1998)]. However, this approach becomes computationally expensive if many contours exist in each slice. In contrast, we will use a two-step method to speed up the local peak and valley search process. If the numbers of loops in two adjacent slices are

different, there must be a feature appearing and/or disappearing. Of course, if the number of loops in these two adjacent slices are the same, it does not necessarily follow that there are no feature changes between them. For example, if an equal number of features appear and disappear simultaneously, then the total loop count for each slice will be the same. Therefore, The first step is to check the numbers of loops in these two adjacent slices. If numbers are different, a disconnection is detected. If the loop numbers are equal a containment evaluation across the slices is performed to assess if a feature is present. This containment relationship analysis is based on a *Point Containment Assumption*, as follows:

Point Containment Assumption **-** If two points having the same coordinate value in the x-y plane are located separately in two line loops on adjacent cross sectional slices, these two loops are assumed to be from the same part body. As shown in Figure 4.9, if points p and p' with $p \subset S$, $p' \subset S'$ and line loops S and S′ are assumed to be cross sections of the same part body. This assumption is from the observation that two loops in two adjacent layers must have a common section between them (if S and S′ are from the same part body, there must be two points, p and p', with $p \subset S$ and $p' \subset S'$). However there is an exception in reverse:

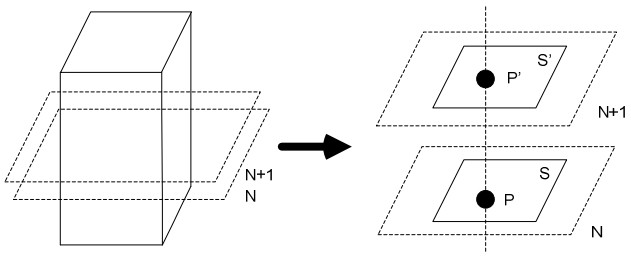

Figure 4.9 Point containment assumption

Exception **-** As shown in Figure 4.10, two loops S and S′ are from two different part bodies, and there are two points p and p' with $p \subset S$, $p' \subset S'$. This exception

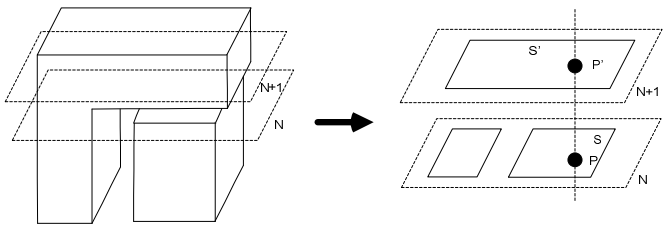

Figure 4.10 Exception to point containment assumption

exists only when the distance separating loops S and S′ is less than the resolution of the slicing algorithm. One simple, but costly method to solve this problem is to use an extremely small slice spacing; however, that could be computationally expensive for tall parts. Of course, the precision of feature detection for our algorithm is decided by the slice resolution; if slice spacing is large, feature height precision suffers. In order to quickly and accurately locate the feature heights, a *Halving Algorithm* [Matthews and Fink (2004)] is adopted. In this manner, a relatively low resolution slice spacing (~ 0.1 inch, 2.54mm) can be used to initially search for features, and then a smaller resolution (~ 0.01 inch, 0.254mm) is used to precisely locate feature heights. In reality, the probability of having the same amount of features disappear and appear at the same z height is very small. Therefore, the probability for this connectivity detection algorithm to get to step 2 is small, making the method more computationally efficient.

Figure 4.11 illustrates the halving search process (*unit: inch*). The slices being investigated (S_1, S_2 and S_3) are from a relatively large resolution (0.1 inch, 2.54mm) slice file. In this case the number of loops on S_1 and S_2 are the same. The loop on slice S_3 is obtained and compared with the loop on slice S_2. Since a difference in the number of loops on slices S_2 and S_3 is detected, the halving process begins. First, a new slice, S_{21}, which is located midway between S_2 and S_3, is obtained and the loops on slice S_{21} are compared with the loop(s) on slice S_2. Since the number of loops on these two slices is different, then another slice, S_{22}, is generated, and its loops are compared with the

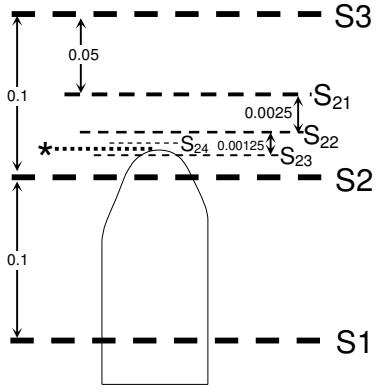

Figure 4.11 Local peak/valley feature search (approximate location of peak)

loops on S_2. Iterated as such, slices closer and closer to the feature height are generated (halving process). The stopping criteria for this iterative process is when the distance between these two slices is smaller than the minimum resolution established for the algorithm (0.01in, 0.254mm). As illustrated in Figure 4.11, the distance between S_{23} and S_{24} is 0.00625in, thus the locating process ceases (meets stopping criteria). At this point, the feature height is assumed to be midway between the last two slices generated. Hence, the final accuracy is within half of the stopping criteria resolution for this example. From a practical standpoint, this accuracy is sufficient, since we only need to find the approximate location of these peaks and valleys so that layer transitions do not occur at or near them. This arbitrary value for the stopping criteria would be defined based on the required accuracy of the layer thickness selection process, but not necessarily the required *part accuracy*. So, the resolution only needs to be enough to ensure that layers will not create poor material or adhesive conditions (described above) when the part contains up-facing peaks and valleys as is the case in a sand casting pattern. However, it should be noted that the halving algorithm resolution *would* affect part accuracy for down facing flats; since they must be precisely located. A separate approach for down facing flats will be presented later.

Type I: Up-facing flats

The halving process described above is appropriate for determining heights of local peaks and valleys; however, it is inefficient and inaccurate in finding the exact height of a horizontal plane. In the case of up-facing flat features, it is known that there must be some facet with its normal parallel to the +z axis direction (has a (0,0,1) normal vector, as illustrated in Figure 4.12a. Therefore, the facet normals of the STL file are searched to locate these potential heights of up-facing flats. In related work, Sabourin et al. (1997) searched for

continuous groups of triangle facets which share the same z height to detect horizontal areas. It should be noted, however, that some small triangular facets created to fill holes in the STL model (post-process repair algorithms), may have the same normals, but do not necessarily represent a flat planar feature (Figure 4.12b). Another issue is that a small up-facing facet could occur at the tangent "peak" of a freeform or otherwise curved feature. A method to filter these instances is as follows: 1) if two or more *adjacent* triangles have +z normal, then they exist on an up-facing flat feature (avoids detecting peaks) and 2) if only one triangle whose normal is in +z direction is found, and one dimension of the triangle is significantly small (smaller than the chordal deviation of the STL model), this triangle is not part of up-facing flat feature (avoids triangles added via repair programs). For example, vertex *P* on the triangle in Figure 4.12c is very close to the edge *L*, because this is a very thin triangle added during STL generation/repair. Obviously, this cutoff value can vary depending on the scale of the model and chordal deviation, but it should be a straightforward parameter to establish.

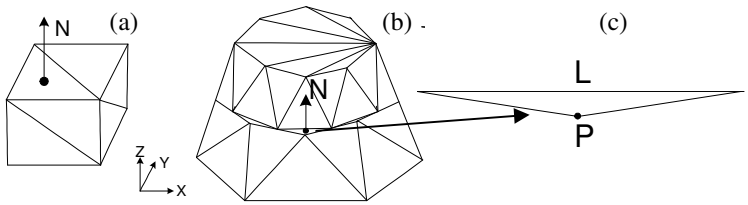

Figure 4.12 Detecting up-facing flats; (a) up facing flat, (b) small up-facing facet not on a plane, (c) parameters to define small facets

Once all local peaks and valleys and up-facing features are determined, their heights are stored into what will be called **Data Set I**. This data set helps determine candidate locations for layers to exist throughout the build height. Although they (peaks, valleys and planes) are located in one data set, they are not treated equally, depending on how close together they exist along the build height. In the case where a local peak or local valley

height is within a default distance to an up-facing plane, the local peak or local valley feature height is deleted from **Data Set I**. This approach is employed because an up-facing flat feature is more critical for layer placement as it generally has larger surface area (at the designated z-height), compared to a local peak or valley, hence it is more important to avoid a large area of exposed bonding material as a pattern surface.

Type II: Down facing flats

Both the down- and up-facing flats have normals parallel to the z axis, albeit in opposite direction. Therefore the **Type II** *feature* height analysis method is the same as the method for up-facing flat height analysis described above; but leads to placing down-facing flat heights into a second set called **Data Set II**. As opposed to the up-facing flat heights in **Data Set I**, for each down-facing flat in **Data Set II**, there must be a new layer at that height in order for the down-facing flat to be generated by the bottom face of the material slab.

Type III: Shallow Sloping Freeform Surfaces

The STL file format approximates freeform surfaces with many triangular facets; hence, the idea of analyzing slopes of surfaces is reduced to simply analyzing the triangles of the STL file, and all points in each triangle facet have the same slope. The motivation to study this freeform surface shape is similar to avoiding up facing flat, as a shallow surface approaches the same characteristic. As shown in Figure 4.13, an arbitrary layout may result in very thin material. Assuming some level of incomplete adhesion (as stated previously, experienced in the laboratory), these

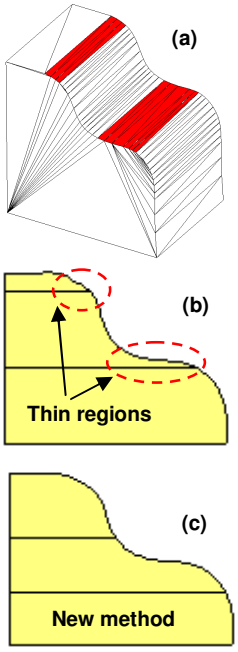

Figure 4.13 Shallow slope surfaces

thin regions are potentially sheared off during cutting. It should be noted that this problem is similar to the *local peak* condition illustrated above (Figure 4.8), where a thin section fractures under cutting forces. Figure 4.14 illustrates the normal, N, for a triangular facet, which has components N_x, N_y and N_z. The slope of the facet S_T is : $S_T = \frac{\sqrt{N_x^{\,2} + N_y^{\,2}}}{N_z}$, in practice, the angle of the facet from the plane of the layer is found: $\varphi = arctan S_T$, where a minimum value of φ can be established experimentally/experientially based on the strength of the pattern material. In laboratory experiments a nominal value of 15° has successfully avoided chipping in Medium Density Fiberboard (MDF), a material that is suitable for sand casting patterns. Higher strength materials such as hardwoods, RenBoard, or of course metals would allow smaller shallow facet angles.

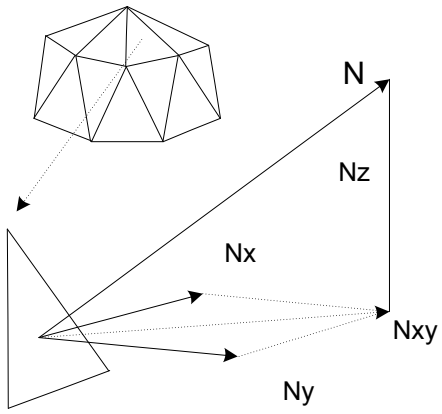

Figure 4.14 Triangle facet slope

One subtle difference between **Type III** features and the other two features discussed above is that a **Type III** feature often covers a range along the Z direction since the freeform surfaces are approximated by many small triangles in the STL file format, rather than a distinct height of a peak, valley or flat. The total range of **Type III** features along the Z direction are determined by the range of z-heights for the vertices of all shallow slope facets and these feature ranges are stored in **Data Set III**. It should be noted that material slab heights are limited therefore; a **Type III** feature may not always be avoided in layer height

calculations. In this case, the methods of the secondary approach presented in section 3.2.4.2 are utilized.

4.2.4 Layer Thickness Algorithm

The proposed layer thickness algorithm defines locations where slabs of material are bonded in the additive portion of the process. After a slab is placed and bonded onto the stack, the subtractive process not only creates the 3D geometry of the layer, but also mills the slab to the designated *layer* thickness. Although the slabs are typically of uniform thickness, layer thicknesses will vary throughout the part as required. Slab thickness could in fact also be varied, if for no other reason than to reduce waste (reduce the amount of material removed when the layer height is much smaller than the slab thickness). For each layer, the slab could simply be chosen as the smallest slab that is thicker than the current layer thickness. This small improvement is ignored in this paper, as it does not change the layer thickness algorithm development. Moreover, allowing a variety of slab thicknesses adds considerable complexity to the Rapid Pattern Manufacturing System; one would need to be able to store, pickup and place a variety of thicknesses. In the current system, we have only used a uniform slab thickness based on available pattern materials in sheet form (i.e. ~0.75" MDF boards).

To begin a presentation of the algorithm, critical parameters are defined as follows:

H_i: The z height of the i^{th} layer
MT_{min}: Minimum material thickness
H_c: Current tentative layer z height
LT_{max}: Maximum layer thickness
$H1_m$: The m^{th} **Type I** *feature* z height
$H2_n$: The n^{th} layer *Z* height in **Data Set II**
$H3_o$: The o^{th} **Type III** *feature* z height region ($H3_{o^-}$, $H3_o{}^+$)
HT_k: The k^{th} tentative layer z height

ST: Material slab thickness

TL: Minimum tool length

ND_j: Non-Deposition z height region (ND_{j-}, ND_{j+})

i: Current layer number

MT_{min} is a default value dependent on the material strength and bonding strength. The maximum layer thickness LT_{max} is set to the minimum value between the slab thickness ST and tool length TL

$$(LT_{max} = Min (ST, TL) \tag{1}$$

4.2.4.1 Primary layer thickness strategy for Type I features

The primary layer thickness strategy for each **Type I** *feature* is: there should be no deposition within a z region ($H1_m$ - MT_{min}, $H1_m$) which is called a *Non-Deposition* region. Firstly, *Non-Deposition* regions are calculated and stored in data set ND_j. Each ND_j includes two values: the upper limit ND_{j+}, and the lower limit ND_{j-}.

$$\begin{aligned} ND_{j-} &= H1_m - MT_{min} \\ ND_{j+} &= 1_m \qquad (j = m) \end{aligned} \tag{2}$$

If two *Non-Deposition* regions overlap, they are combined:

$$ND_{j-} = ND_{(j-1)-} \qquad (\text{If } ND_{j-} < ND_{(j-1)}^{+}) \tag{3}$$

If there exist **Type II** entities in the range of a *Non-Deposition* region, the *Non-Deposition* region is then divided into two *Non-Deposition* regions at these **Type II** entity z heights, since a **Type II** feature has higher priority. This division operation avoids layer placement conflicts between **Type II** entities and *Non-Deposition* regions. The sample part illustrated in Figure 4.15 has seven **Type I** *feature* entities; hence there are there are seven *Non-Deposition* regions. It happens that some *Non-Deposition* regions in this example connect; hence only two *Non-Deposition* regions are formed after combining.

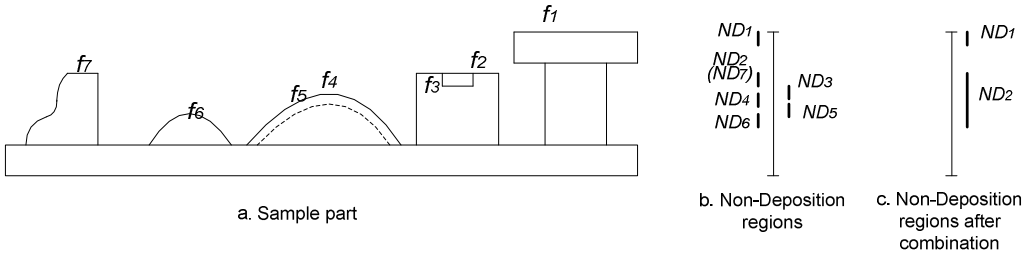

Figure 4.15 Non-Deposition region combination

4.2.4.2 Secondary layer thickness strategy for Type I features

After all combinations, some *Non-Deposition* regions may exceed the height of the material slab thickness. This indicates that it not possible to have a layer covering the entire *Non-Deposition* region. When this problem occurs, the primary layer thickness strategy for **Type I** *feature* fails, and a secondary layer thickness strategy is employed. When the height of a **Type I** *feature* is above the layer position by MT_{min}, bonding strength and material strength are assumed sufficient to ensure proper machining and part quality. However if the distance between the feature and the layer position is less than MT_{min}, the quality/value of a layer height choice is decided by two factors: 1) the distance between the feature and the layer position (*DT*), and 2) the cross section loop area (*A*) at the particular layer z height. When two **Type I** *feature* entities connect to each other, the best position to place a layer along this *Non-Deposition* region is exactly at the lower entity position, which has the largest *DT* and *A* for the upper entity. Therefore, the lower *feature* positions are evaluated with (4) to quantify the benefits of placing layers at these positions.

$$Q = \alpha * DT + \beta * A \tag{4}$$

Where:

α:	material coefficient
β:	bonding/adhesive coefficient
DT:	distance between *feature* and layer position

A: cross section loop area at the layer height

This heuristic approach does not necessarily yield an optimal solution based on *Q*-value, especially since it may result in an excessive number of layers in a *Non-Deposition* region, driving up material and adhesive costs. Consider the *Non-Deposition* region in Figure 4.14 for example. The slab thickness is assumed to be 0.8in, and the *Non-Deposition* region ND_2 in Figure 4.14c is 1.0in (which is the combination of ND_2 to ND_7 in Figure 4.14b). The *Q-value* for feature *f6* is the largest compared to *f2* through *f7*. The position of *f6* is located at 0.1inch above the minimum of ND_2. If a layer is placed at the position of *f6*, then another layer must be placed in ND_2. If a layer is placed at the position of *f5*, which is located 0.25 inch above the bottom of ND_2, and has a smaller *Q*-value than *f6*, no more layers are required in the *Non-Deposition* region ND_2. Among these two strategies, the second strategy using just one layer is obviously preferred; hence, given alternative solutions from multiple calculations, the solution with the least number of layers is chosen.

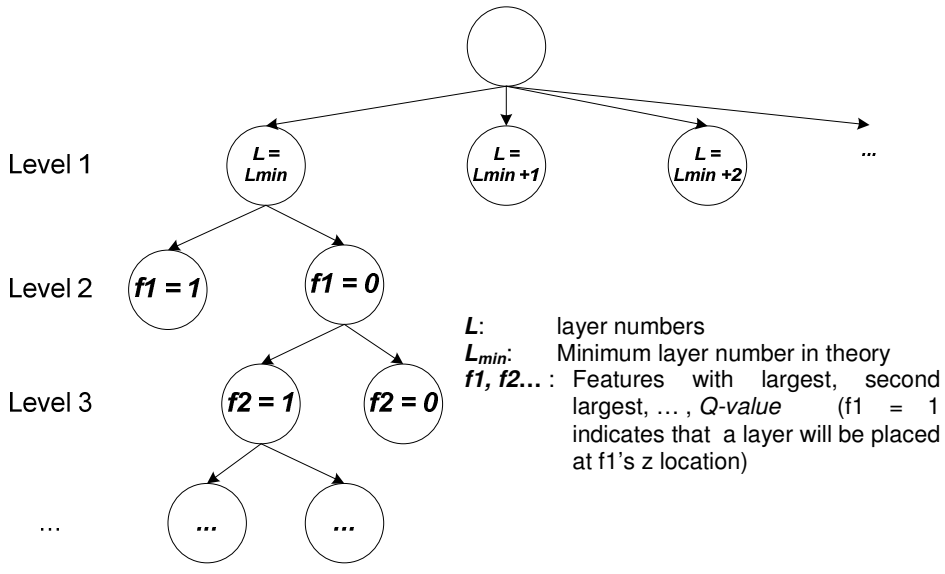

Figure 4.16 Branch-and-Bound algorithm for layer placement in Non-Deposition region

Next, a branch-and-bound algorithm (Figure 4.16) is adopted to minimize the number of layers, while maximizing the Q-value of possible positions in the *Non-Deposition* regions. The first level selects the number of layers placed in the *Non-Deposition* region. The search starts from the theoretical minimum number of layers, which is $L_{min} = UR\ [\ (\ ND_{j+} - ND_{j-}\ )\ /\ LT_{max}\ ]$, where $UR(x)$ is an operation that calculates the smallest integer $\geq x$. Next, feature heights are searched in sequence of increasing *Q*-values for possible layer placement solution.

Consider the ND_2 in Figure 4.14 for example. The height of ND_2 is 1.0 inch, LT_{max} is 0.8 inch, *f6* (which has the largest *Q-value*) is 0.1 inch from the bottom of ND_2, and *f5* has the second largest *Q-value*, which is 0.25 inch from the bottom of ND_2. For level 1, the minimum layer number needed to cover the ND_2 in theory is $UR(1.0/0.8) = 2$. Then, the level 2 starts from *f6*. If *f6* = 1, at least one more layer is required since $UR((1.0-0.1)/0.8) = 2$, and the total number of layers is greater than 3. Therefore, *f6* = 0. In level 3, if *f5* = 1, no more layers are required, since $UR((1.0-0.25)/0.8)=1$, and the total number of layers required is 2 which is equal to the minimum theoretical number of layers. At this point, the search process is completed and layer positions in the *Non-Deposition* region are stored into **Data Set II**, which stores the **Type II** *feature* heights. Layer placement in the *Non-Deposition* region is actually similar to the **Type II** *feature* problem, in which there must be layers placed at these positions to cover *Non-Deposition* regions.

4.2.5 Overall Layer Thickness Algorithm

The overall layer thickness algorithm places layers in a bottom-up fashion. To begin, the bottom of the CAD model of the pattern is positioned at $z = 0$, and the initial start position is set to $Hc = 0$. The Current layer number i is set to 1, $H1_0$ is set to 0. When the

search begins, the current tentative layer height is set to one maximum layer thickness (LT_{max}) higher than the previous layer: $Hc = H_{i-1} + LT_{max}$.

4.2.5.1 Layer Thickness for Data Set II

Type II *features* and layer positions in *Non-Deposition* regions are evaluated first since layers must correspond exactly at theses heights in order to create the down-facing flat geometry, or to provide suitable machining quality in the *Non-Deposition* regions. First, all height data in **Data Set II** are searched to determine those that are within the height range H_{i-1} to H_c. If multiple heights are possible, the height that is closest to H_{i-1} is the next layer position (H_i). If no such *feature* height is found, the search continues for **Type I** *feature* heights.

4.2.5.2 Layer thickness for Type I features

If there is a j that meets the condition: $ND_{j-} < H_c < ND_j^+$,then H_c is in the range of a *Non-Deposition* region. As such, H_c should be moved out of the *Non-Deposition* region $H_c = ND_{j-}$; else, a layer can be placed at H_c directly. The *Non-Deposition* regions here are only those less than LT_{max}. If they are greater than LT_{max}, layers are placed directly in the first step. Therefore, *Non-Deposition* regions above LT_{max} cannot be selected in the second step.

4.2.5.3 Layer thickness for Type III features

Layers are also placed based on **Type III** *features*; however, it occurs that **Type I** and **Type III** *feature*s may cause conflicts; one cannot always satisfy both Type I and III features simultaneously. Again from experimental tests, Type III features create poor machining

conditions, but Type I features more often cause catastrophic failures: hence, **Type I** *feature*s are given higher priority to be satisfied. For the H_c from step *(b)*, if there is exists an *o* for $H3_{o^-} < H_c < H3_o^+$ (that is, this H_c is Located within the range of a **Type III** *feature*), then, the height $H3_{o^-}$ is tested. If no *j* exists for: $ND_{j^-} < H3_{o^-} < ND_j^+$, then H_c is moved to $H3_{o^-}$, or, H_c is kept the same.

In this iterative manner, the **Type I**, **Type II and Type III** *feature* searching processes determine the layer thicknesses for the entire part. A flow chart illustrating the layer thickness algorithm is presented in Figure 4.17. The figure is separated into 4 main parts: **(A)** Layer thickness in *Non-Deposition* Regions, **(B)** Layer thicknesses for **Data Set II** *features*, **(C)** Layer thickness for **Type I** features, and **(D)** Layer thickness for **Type III** *features*.

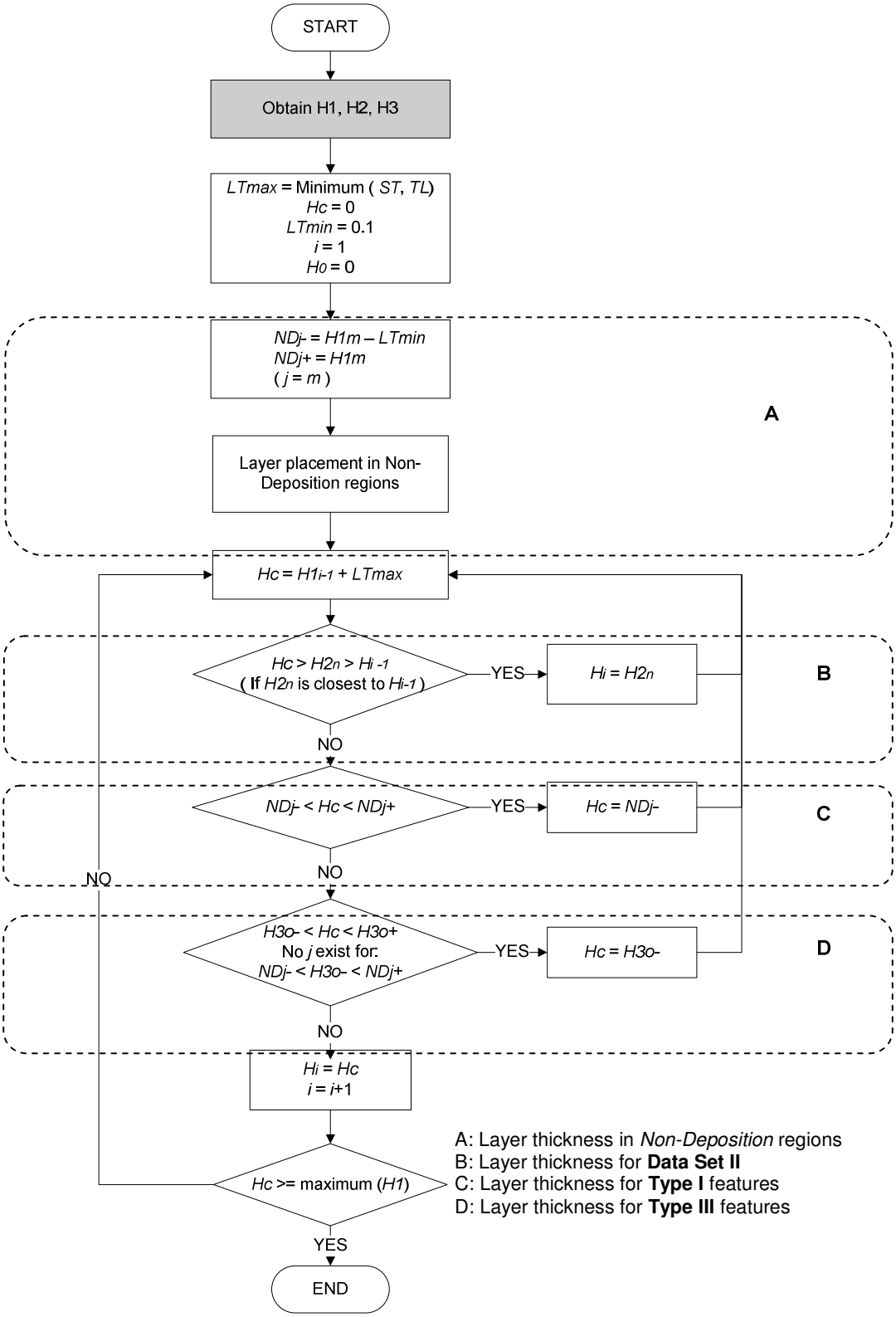

Figure 4.17 Layer thickness algorithm flow chart

4.3 Implementation

The layer thickness algorithm has been implemented and several patterns have been created in the laboratory, with chemically bonded sand molds pulled from the patterns and casting performed. The evaluation of the approach presented in this section involves 1) comparing the calculated *feature* heights from the algorithm with design *feature* heights, 2) fabricating sample test patterns to evaluate the efficacy of this layer based approach, and 3) practical testing of the methods in the creation of actual sand casting patterns for a relatively large casting.

4.3.1 Test Sample

The layer thickness algorithm was implemented in C++ on a Pentium 3.0GHz PC running Windows XP. The input to the layer thickness software was an STL file (ASCII, 0.001 inch chordal deviation). A sample part was designed to verify the layer thickness algorithm such that all steps and conditions would be tested. In this example, the material slab thickness (Medium Density Fiber board) was 0.70 inch. Tool lengths are larger than the slab thickness, so LT_{max} is set to 0.70 inch. The minimum layer thickness MT_{min} was set to 0.20 inch. The material coefficient was 0.7 (Length unit: inch), the bonding coefficient was set to 0.3 (Area unit: $inch^2$) and the small slope surface threshold angle was set to 15º. Figure 18 shows a 3D model of the sample part. Twelve machining *features* are detected by the layer thickness software, with the positions of these twelve *features* listed in Table 4.1.

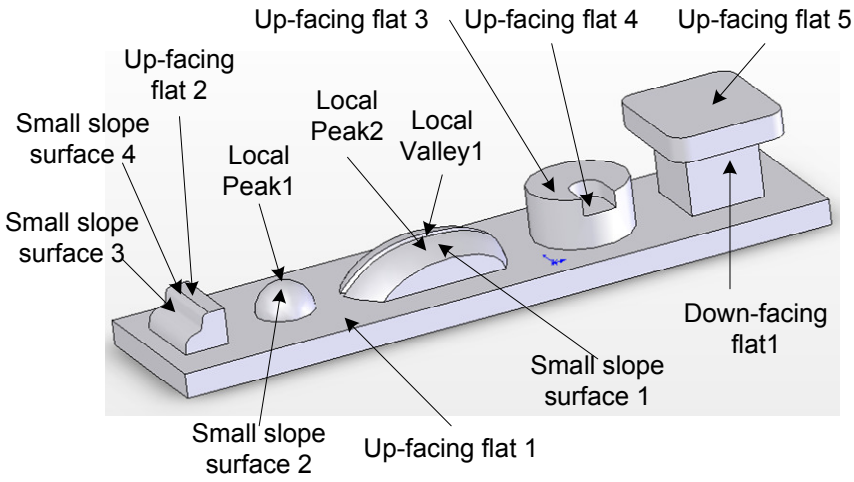

Figure 4.18 Sample part 3D model

Table 4.1 – Design feature heights and detected feature heights comparison (Unit: inch)

Feature	Detected Height	Design Height
Up-facing flat 1	0.300	0.300
Up-facing flat 2	0.700	0.700
Up-facing flat 3	1.000	1.000
Up-facing flat 4	1.180	1.180
Up-facing flat 5	1.500	1.500
Down-facing flat 1	1.200	1.200
Local peak 1	0.653	0.650
Local peak 2	0.803	0.805
Local valley 1	0.756	0.755
Small slope surface 1 & Small slope surface 4	0.638 - 0.650	0.624 - 0.650
Small slope surface 2	0.520 - 0.533	0.516 - 0.523
Small slope surface 3	0.660 - 0.744	0.652 - 0.744

The small differences between the design positions and detected positions come from two sources. One error source is the approximation inherent with an STL model while the other is from the *Halving Algorithm* which can only acquire approximate local peak or valley

positions. That being said, in this example the differences are less than 0.005 inch and consequently have little influence on the layer thickness evaluation. Layer thickness results are presented in Table 4.2, and the layer distribution on the sample part is shown in Figure 4.19.

Table 4.2 – Layer thickness result from layer thickness software (Unit: inch)

Layer No.	Layer Thickness
1	0.453 (0.0 ~ 0.453)
2	0.103 (0.453 ~ 0.556)
3	0.644 (0.556 ~ 1.200)
4	0.300 (1.200 ~ 1.500)

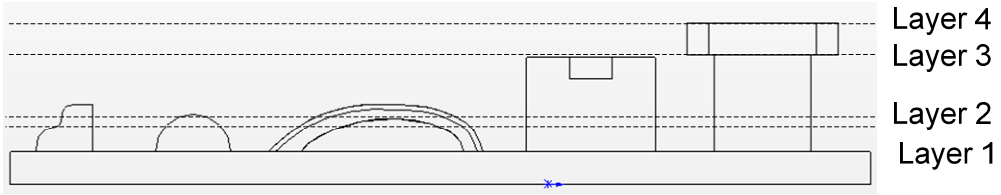

Figure 4.19 Sample part layer distribution

The first layer thickness follows the *primary* layer thickness strategy for a **Type I** feature; and is 0.2inch lower than local *peak 1*. The second layer thickness utilizes the *secondary* layer thickness approach for a **Type I** *feature*, and the layer thickness calculated from *local valley 1* meets the optimization condition (4) presented in section 2.4.2. The third layer thickness is obtained directly from the **Type II** *feature's* down-facing *flat 1*. The last layer ends at the top of the part (an up-facing plane). In this example, computation time for this model was ~3 seconds. Based on the layer thickness calculation from this algorithm, a sample part was fabricated on a 3-axis HAAS CNC milling machine. The material slabs are 0.70 inch Medium Density Fiber boards and the adhesive is cyanoacrylate. The fabrication process is illustrated in Figure 4.20. The part was machined successfully using the calculated layer thicknesses, with no de-bonding, cracking or other problems. Moreover, the resulting

part had a uniform surface with no instances where the bonding material formed a large exposed surface.

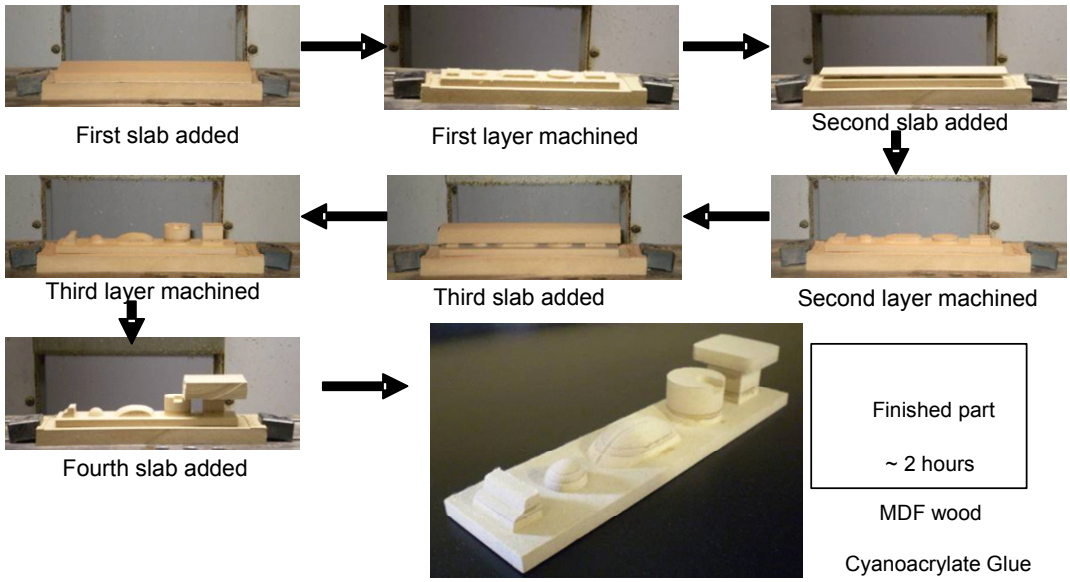

Figure 4.20 Sample part created using RPM approach

In order to at least qualitatively evaluate the methods against a control group, simple tests were conducted to compare the proposed layer thickness strategy versus simply using a uniform layer thickness strategy. The samples illustrate the problems encountered in laboratory testing of pattern making, showing how failures can occur and how the new methods avoid them.

In Figure 4.21, we illustrate side-by-side comparisons of uniform layers versus the new method. In the feature shown in Figure 4.21a, a new layer starts very close to the top of the up-facing flat, creating a very thin upper surface. From experience pulling sand from a pattern such as this, any imperfections in the bonding of the layer may result in delaminating/cracking of the MDF. In contrast, the part in Figure 4.21b illustrates a considerably thicker section comprising this up-facing flat. Figures 4.21c and 4.21e are

similar, except that one represents a local peak while the other was both a local peak and an area of shallow surface slope. Failure occurred in both cases; however, the failure mode was catastrophic fracture in 4.21c versus excessive chipping in 4.21e. As expected, the bonded surfaces are intact in both cases, but the MDF material broke free in the image 4.21c and the edges of the shallow sloping surfaces chipped in 4.21e. In stark contrast Figures 4.21d and 4.21f show the successful machining of these layers using the new method.

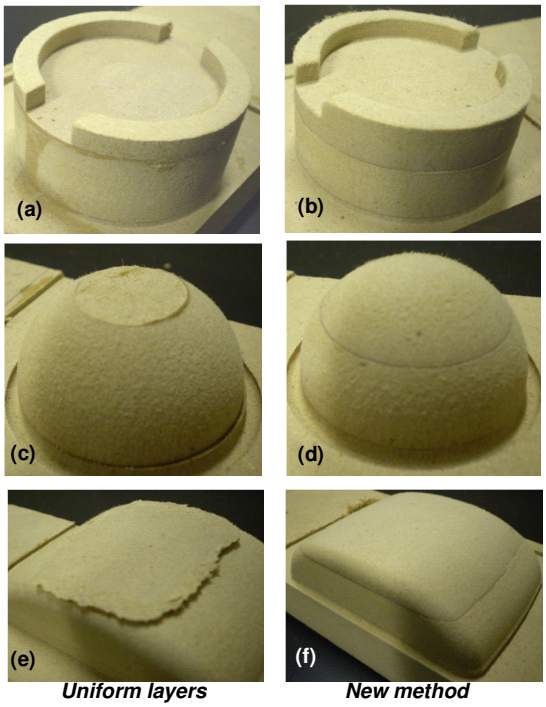

Figure 4.21 Illustrations of uniform (a,c,e) versus new (b,d,f) layer placement methods

4.3.2 Sand Casting Pattern Testing

A Rapid Pattern Manufacturing system has been developed and tested in the Rapid Manufacturing and Prototyping Laboratory at Iowa State University (Figure 4.22). The system is comprised of 4 major functional elements including; 1) two elevator platforms serving as *feed* and *build* chambers with 1.2m^3 (1440kg) capacities, 2) a material handling system to clamp, position and compress up to 1.2m^2 sheets of material, 3) a glue application system, and 4) one off-the-shelf component; a 3-Axis CNC router. A total of 7 controllable axes are utilized in the completely automated processing of patterns. The gluing system utilizes a peristaltic pump which directs cyanoacrylate adhesive through a manifold applicator head. The servo driven build table with 4 ball screws can position the pattern for

cutting operations and apply up to 17,000N of force during the 30second gluing compression cycle. The layer thickness algorithm has been implemented in software as a C-hook in the MasterCAM CAD/CAM environment. NC code for each layer and the requisite slab sequencing and facing to layer height data is output from MasterCAM and then processed using customized control system software to drive the machine elements.

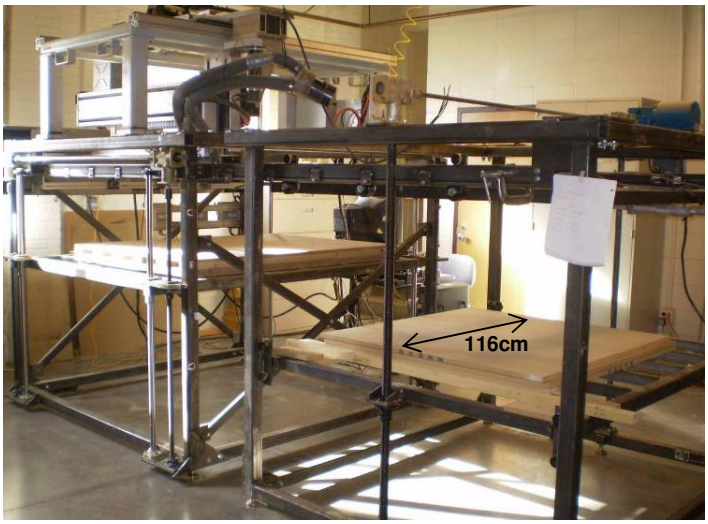

Figure 4.22 RPM machine in RP&M Lab at Iowa State University

The system has been utilized to create numerous prototype patterns and most recently for a pattern of a steel casting component measuring over 800x800x300mm. This large sand casting pattern made by the Rapid Pattern Manufacturing machine and the sand mold created from this pattern are shown in Figure 4.23. Figure 4.23A, shows the pattern in the latter stages of being machined in the system, illustrating the advantage of using a layer based approach, as it can be seen how the current layer in the picture is breaking through to reveal the deep pattern cavity below. One will note that this pattern is considerably large and deep; however, only a 1 inch (25mm) long end mill was required, since each layer is machined after being stacked. As such, we were able to use as small as a ¼”(6mm) diameter ball mill to access small corner radii, even in the deepest regions of the pattern. Total machining time for this size pattern is currently at approximately 50 hours, or roughly 2 hours per inch

(25mm) of z-height on this 116x116cm (slab dimension) pattern build. The process is currently limited by the maximum feedrate of this CNC router (a maximum of ~350ipm (9m/min)) although the pattern material could be machined faster. Figure 4.23b presents a closer image of interior of the finished pattern; while Figure 4.23c shows the resulting sand mold pulled from this pattern cavity. This pattern was used to successfully cast a large steel prototype component.

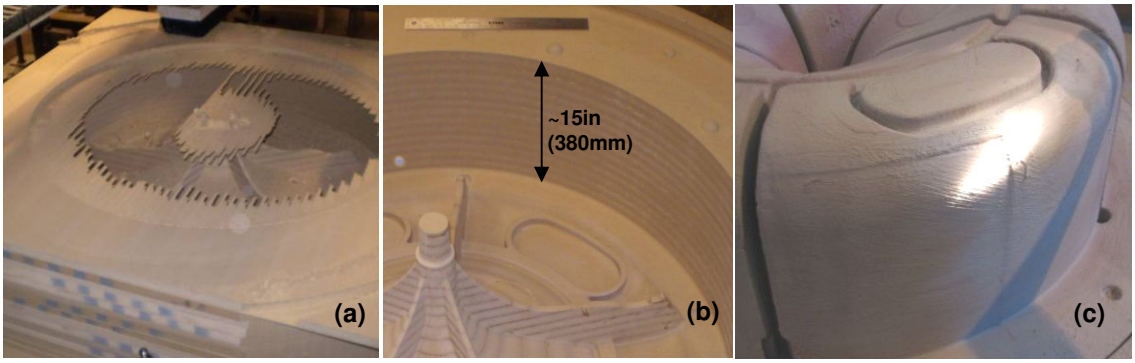

Figure 4.23 Example pattern and mold; a) Pattern in process machining through a layer and exposing the pattern cavity below, b) finished pattern showing complex geometry deep in the cavity, and c) chemically bonded sand mold pulled from pattern

4.4 Conclusion and Future Work

This paper presented a critical enabling technique in the rapid manufacturing of patterns using an additive/subtractive approach. The research addresses a need for effective layout of layers in this process, as it has been found that layer placement has a significant effect on surface quality of the patterns and more important can avoid catastrophic failure during the machining processes. The algorithm presented deals effectively with the set of feature conditions that must be addressed. Feature creation is not an inherent problem in this system; since the geometry of sand casting patterns has relatively well-known characteristics. The problem arises in the additive/subtractive nature of the process, as this creates temporary

geometric problems such as thin webs of material, potential fracture conditions, etc. However, it is also the layer based nature of the process that enables the rapid prototyping of these patterns, since the process planning is greatly simplified; being able to machine each layer with small tools capable of creating small features and no collision conditions.

The methods of this paper effectively address the problems related to this layer based system by analyzing the part features and determining a feasible solution to the layer thickness problem. The method focused on a simplified set of features including local peaks and valleys, up and down-facing flats and surfaces containing very shallow slope. Given a set of feature heights to avoid, slab thickness, pattern material, glue and tool parameters, the system is able to determine the layer placement that best avoids these critical feature transitions. The system has been implemented in terms of both software and hardware and has been extensively tested with a selective set of components that exhibit all feature types and issues. In addition, the system has been successfully used to create a variety of patterns, including a considerable large and complicated pattern for a steel prototype.

The current system is operational; however, there exist areas of improvement and further efforts to pursue. For one, the system uses a branch and bound algorithm to solve the optimization problem; however, other optimization methods may be more suitable to solve this problem, and perhaps enable us to not only avoid poor locations, but also further minimize the number of layers required. In addition, the current system uses a simple approach to tool selection, as do most rapid prototyping machines (The typical approach in other RP methods is to choose a relatively small extrusion tip (for FDM), laser spot diameter (for SLS,SLA), etc.; such that arbitrary features can be created without a priori knowledge of the new part). Similarly, we use a simple set of tools with considerably small diameters; one

face mill to machine slabs down to layer heights, one roughing *end mill* to remove much of the material, and then one finishing *ball mill*. Since a tool changer is available, we envisage a future system that chooses tools per layer and then selects them from the tool carousel for each set of NC code designated for each layer. These improvements would further optimize the system by reducing the overall processing time, which is dominated by the machining process.

Acknowledgements

Research was sponsored by the U.S. Army Benet Laboratories and was accomplished under Cooperative Agreement Number W15QKN-06-R-0501. The views and conclusions contained in this document are those of the authors and should not be interpreted as representing the official policies, either expressed or implied, of U.S. Army Benet Laboratories or the U.S. Government. The U.S. Government is authorized to reproduce and distribute reprints for Government purposes notwithstanding any copyright notation heron.

Reference

Binnard, M. Cutkosky, M. (1998). Building block design for layered shape manufacturing. *Proceedings-1998 ASME Design Engineering Technical Conference*, 1-9.

Broek, J.J. Horváth, I. Smit, B. Lennings, A.F. Rusák, Z. Vergeest, J.S.M. (2002). Free-form thick layer object manufacturing technology for large-sized physical models. *Automation in Construction*, 11(3), 335-347.

Chang, Y.C. Pinilla, J. M. Kao, J.H. Dong, J. Ramaswami, K. Prinz, F.B. (1999). Automated layer decomposition for additive/subtractive solid freeform fabrication. *Proceedings of the Solid Freeform Fabrication Symposium*, 111-120.

Chen, Y.H. Song, Y. (2001). The development of a layer based machining system. *Computer-Aided Design*, 33(4), 331-342.

Choi, S. H. Kwok, K. T. (2002). Hierarchical slice contours for layered-manufacturing. *Computers in Industry*, 48(3), 219-239.

Cormier, D. Taylor, J. B. (2001). A process for solvent welded rapid prototype tooling. *Robotics and Computer Integrated Manufacturing*, 17(1-2), 151-157.

Hague, R. D'Costa, G. (2001). Dickens PM, Structural design and resin drainage characteristics of QuickCast 2.0. *Rapid Prototyping Journal*, 7(2), 66-72.

Hur, J.H. Lee, K. Zhu-hu Kim, J. (2002). Hybrid rapid prototyping system using machining and deposition. *Computer-Aided Design*, 34(10), 741-754.

Jacobs, P.F. (1995). QuickCast 1.1 and rapid tooling. *Proceedings of 4th European Conference on Rapid Prototyping & Manufacturing*, 1-27.

Karapatis, N.P. Van Griethuysen, J.P.S. Glardon, R. (1997). Injection molds behavior and lifetime characterization. *Proceedings of the Solid Freeform Fabrication Symposium*, 317-324.

Kawola, J. (2003). Zcast direct metal casting from data to cast aluminum in 12 hours. *Website: http://www.3dprint.no*, Last accessed: October, 2008.

Lee, C.W. Chua, C.K. Cheah, C.M. Tan, L.H. Feng, C. (2004). Rapid investment casting: direct and indirect approaches via fused deposition modeling. *International Journal of Advanced Manufacturing Technology*, 23(1-2), 93-101.

Leong, K.F. Chua, C.K. Ng, Y.M. (1996). Study of stereolithography file errors and repair: part 1- generic solution. *International Journal of Advanced Manufacturing Technology*, 12(6), 407- 414.

Leong, K.F. Chua, C. Ng, Y. M. (1996). Study of stereolithography file errors and repair: part 2-special cases. *International Journal of Advanced Manufacturing Technology*, 12(6), 415- 422.

Luo, R.C. Chang, Y.C. Tzou, J.H. (2001). The development of a new adaptive slicing algorithm for layered manufacturing systems. *Proceedings of the 2001 IEEE International Conference on Robotics & Automation*, 1334-1339.

Mathews, J.H. Fink, K.D. (2004). *Numerical methods: using Matlab*. Prentice hall.

Merz, R. Prinz, F.B. Ramaswami, K. Terk, M. Weiss L. (1994). Shape deposition manufacturing. *Proceedings of the Solid Freeform Fabrication Symposium,* 1-8.

Millit webpage (2007). Millit - Rapid Prototyping durch Fräsen. *http://www.millit.net/*, November, 2007.

Mueller, B. Kochan, D. (1999). Laminated object manufacturing for rapid tooling and patternmaking in foundry industry. *Computers in Industry*, 39(1), 47-53.

Naitove, N.H. (1996). Faster, bigger desktop modeler. *Plastics Technology*, 42(12), 27.

Pandey, P.M. Reddy, N.V. Dhande, S.G. (2003). Slicing procedures in layered manufacturing: a review. *Rapid Prototyping Journal*, 9(5), 274-288.

Pinilla, J.M. Kao, J. Prinz, F.B. (1998). Process planning and automation for additive/subtractive solid freeform fabrication. *Proceedings of the Solid Freeform Fabrication Symposium*, 245-258.

Sabourin, E. Houser, S. A. Bohn, J. H. (1997). Accurate exterior, fast interior layered manufacturing. *Rapid Prototyping Journal*, 3(2), 44-52.

Schaaf, W. (2000). Robotyping-new rapid prototyping processes for sand casting moulds using industrial robots. *Assembly Automation*, 20(4), 321-329.

Song, Y.A. Park, S. Choi, D. Jee, H. (2005). 3D welding and milling: part I – a direct approach for freeform fabrication of metallic prototypes. *International Journal of Machine Tools and Manufacture*, 45(9), 1057-1062.

Song, Y.A. Park, S. Chae, S.W. (2005). 3D welding and milling: part II – optimization of the 3D welding process using an experimental design approach. *International Journal of Machine Tools and Manufacture*, 45(9), 1063-1069.

Song, Y. Chen, Y.H. (1999). Feature based robot machining for rapid prototyping. *Proceedings of the Institution of Mechanical Engineers, Part B: Journal of Engineering Manufacture*, 213(5), 451–459.

Tang, Y. Fuh, J.Y.H. Loh, H.T. Wong, Y.S. Lu, L.(2003). Direct laser sintering of a silica sand. *Materials & Design*, 24(8), 623-629.

Taylor, J.B. Cormier, D. Joshi, S. Venkataraman, V.(2001). Contoured edge slice generation in rapid prototyping via 5-axis machining. *Robotics and Computer Integrated Manufacturing*, 17(1-2), 13-18.

Tyberg, J. Bohn, J. H. (1998). Local adaptive slicing. *Rapid Prototyping Journal*, 4(3), 118 – 127.

Wang, W. Conley, J.G. Stoll, H.W. (1999). Rapid tooling for sand casting using laminated object manufacturing process. *Rapid Prototyping Journal*, 5(3), 134-141.

Yang, Z.Y. Chen, Y.H. Sze, W.S. (2002). Layer-based machining: recent development and support structure design. *Proceedings of the Institution of Mechanical Engineers, Part B: Journal of Engineering Manufacture,* 216(7), 979-991.

CHAPTER 5. A TOOL SIZE AND MACHINING PARAMETER SELECTION ALGORITHM FOR ADDITIVE/SUBTRACTIVE RAPID PATTERN MANUFACTURING

A paper to be submitted to the Rapid Prototyping Journal

Xiaoming Luo, Matthew C. Frank
Department of Industrial and Manufacturing Systems Engineering
Iowa State University, Ames, IA, 50011, USA

Abstract

This paper presents an algorithm to automatically select tool sizes and calculate machining parameters for an Additive/Subtractive Rapid Pattern Manufacturing (RPM) process. The RPM process sequentially deposits thick material slabs and then machines geometries in a layer by layer method. Although Rapid Manufacturing systems are essentially designed for flexibility and not necessarily processing speed, it is practical to choose sets of tool sizes and machining parameters specific for each layer to improve both the machining quality and efficiency. Some machining parameters are closely related to the machining strategy; therefore, the machining strategy and related machining parameters are studied first. The Stepdown (Cut depth) is a machining parameter studied next. Then, an algorithm based on both accessibility and machining efficiency is proposed for the selection of tool sizes for rough and finish machining and optimized machining parameters for each single layer. The input to the algorithm is a slice file from the CAD model. Based on the accessibility and machining efficiency analysis, a heuristic approach to select tool sizes is developed. The set of tools includes a rough cutting flat end mill, a finish cutting spherical end mill, and optional semi-roughing flat end mills. The method has been implemented in

software and the experimental result illustrates the efficacy of this algorithm to automatically choose tool sizes appropriate for the sample part. The sample part has been created using an RPM system in the laboratory.

Keywords: *Rapid Manufacturing, Layer thickness, Sand casting pattern*

5.1 Introduction

An RPM process, which attaches a thick material slab, cuts it to a certain layer thickness, then creates out the part geometry on this layer, has been proposed by authors. Basic steps of this process are illustrated in Figure 5.1. The RPM system illustrated in this paper is restricted to 3-axis, single-sided milling. It is assumed that the process mainly suited for the creation of two-part patterns for the molding and sand casting industry.

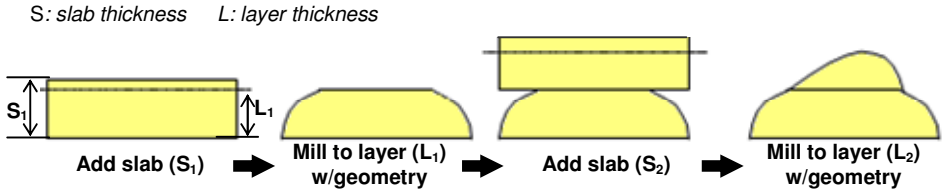

Figure 5.1 Basic steps in the RPM process

Automatic process planning is one of main advantages of Rapid Manufacturing processes [Frank et al. (2004)]. The basic steps in the automated machining process for the RPM system is further illustrated in Figure 5.2. To begin, a new material slab is deposited on the base or finished layers and then milled to the thickness calculated by a layer thickness algorithm [Luo and Frank (2009)]. A rough cutting operation removes most of the surplus material to quickly create the gross part geometry for each layer. Next, finish cutting is used to more accurately machine the surfaces and should ensure high quality surfaces and dimensions. Optional semi-rough operations may be applied between the rough cutting

operation and finish cutting operation in order to further reduce the total machining time.

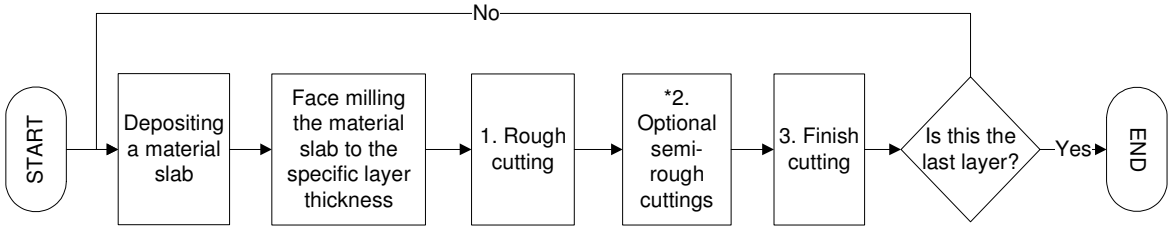

Figure 5.2 Automatic machining process flow chart of the RPM process

In this automatic Rapid Manufacturing process, the same material deposition operation and face milling operation can be applied to every layer with different geometries. However, specific cutting tools and machining parameters, such as Stepdown, should be applied to layers with different geometries in the rough cutting, finish cutting and optional semi-rough cutting operations, because different tool sizes and machining parameters have significant impact on geometry creation and cutting efficiency. The tool size and machining parameter selection problem is highly skilled task and has been a major problem which hinders automated machining process planning. However, It is not easy to select cutting tools which are not only functionally correct but also optimum [Ribeiro and Coppini (1999)]. The development of software system for automatic tool selection is still in its infancy [Arezoo et al. (2000)].Many researchers have approached this problem in the literature. Some early researches focused on finding the single best milling tool for a particular feature [Lee (1994) Lee (1995)].

A geometric algorithm for finding the largest milling cutter for 2D milling operations was presented by Yao et al. (2001). The unique point in this research was that a cutter feasible definition based on cutter's ability to cover the target region was proposed. Even

though the application of the single cutter selection was limited, it could be the first step for multiple cutter selection.

Bala, et al. (1991) presented an automatic cutter selection and optimal cutter path generation method for prismatic parts. Prismatic parts in their research were parts which were composed by prismatic features, such as slots, steps, projections, etc. Algorithms for selecting appropriate rough and finish cutters and generating the cutter path and NC code for machining a pocket were presented in their research. An assumption for the rough and finish cutter matching was the material left behind by the rough cutter at each of convex vertices could be removed by one pass along the boundary of the finish cutter. Single cutter for rough and finish cutting made the application of this algorithm limit.

Chen et al. (1998) studied the optimal cutter selection and machining plane determination problem for die cavity rough machining operation. The integer programming and dynamic programming were adopted to search for the optimized tool set and machining plane set to minimize the total machining time.

Some researches addressed the problem of selecting multiple or a set of tools for 2D or 2½D pocket machining. A 2½D structure was composed of several 2D planes, so they could be considered as the same problem. Arya et al. (1998) proposed an approximation algorithm to select multiple tools from a set of tool for milling a certain plane based on the minimum cost. The running time and approximation ratio of this algorithm depended on the simple cover complexity of the milling region. A novel concept, Voronoi Mountain was presented by Veeramani and Gau (1997, 2000) to calculate the material volume that could be removed by a specific cutting-tool size. With the help of Voronoi Mountain, a dynamic programming model for selecting an optimal set of cutting-tool sizes for 2 ½ D pocket

machining on the basis of processing time was studied. Nadjakova and Mcmains (2004) also studied the problem of finding an optimal set of cutter for 2D pocket machining on the basis of approximation ratio and machinable area. Yao et al. (2003) expanded the cutter selection problem from the specific 2½D feature to multiple parts milling field.

Wang et al. (2005) presented a computer aided tool selection system for 3D die/mould-cavity NC machining using both a heuristic and analytical approach. This approach selected tool types, tool sizes and key parameters for dies and moulds cavity machining.

D'Souza (2006) proposed a method to solve the tool sequence selection for 2 ½ D pocket machining on setup level. This method optimized the tool path generation for all features in one setup, which might nest within each others, from perspectives of: (a) feature level optimization, (b) composite tool sequence graph optimization, (c) constrained graph optimization, and (d) sub-graph optimization. A cost model based on the actual tool path generation, which included machining tool path time, air path time, tool change time and tool life time, was developed to evaluate the tool sequence selection solutions. The complexity of the tool sequence selection problem was reduced in this paper by identifying the fact that "the accessible area of a larger tool is a strict subset of the accessible area of a smaller tool" [D'Souza (2006)].

On the basis of feature-based model, precise geometry accessibility evaluation is able to be calculated. Lim, et al (2000) developed an exact tool sizing algorithm for feature accessibility. Tool Access Distribution (TAD) and Relative Delta-Volume Clearance (RDVC) data were created from tool access algorithm, and adopted to select optimum tool automatically. The objective for tool selection and tool sizing in this algorithm was to study

the geometric constraints imposed on tool selection. The input of this algorithm was feature based digital CAD models. The result from this algorithm was able to ensure good surface accessibility.

With the development of Rapid Prototyping and Manufacturing, more and more attention is paid to tool size selection for sculpture surface or free-form surface milling.

Lee, et al. (1992) proposed a cut distribution and cutter selection for sculptured surface cavity machining. Sculptured surface was composed of some free-form curved surfaces which were difficult and expensive to produce. Sculptured surface in this paper was defined by Non-Uniform Rational B-Spline (NURBS) surfaces which provided flexibility and freedom for surface description. The curvature evaluation was employed to select the finishing cutter. Rough cutter size was based on cutters chosen for hunt planes in surface information evaluation, and semi-roughing was based on the geometric constraints and thickness of shoulders left on the surfaces. Tool selection was optimized by the objective of high Material Remove Rate (MRR). The difficulty in implementation of this system came from the determination of some system parameters.

Yang, et al. (1999) presented an interference detection and optimal tool selection solution for 3-axis NC machining of free-form surfaces. Three kinds of interference: protrusion interference, overlapping interference and boundary collision interference were defined and relative solutions were proposed. The optimal tool selection algorithm was based on the goal of minimum machining time. Objective surfaces in this paper were parametric surfaces. High computational power was needed if the grid resolution used in these algorithms was very fine.

Lin and Gian (1999) proposed a multiple tool approach to rough milling of sculptured surfaces depicted by ordered data points. In the beginning, NUB surfaces were formed from the ordered data points, and sliced with constant z-height to acquire the boundary and island loops in each layer. Then tool sizes for linear pocketing, contour roughing, semi-roughing and new-island processing operations were selected for good machining efficiency and preventing from tool breaking.

Algorithm for decomposing machining operations for free-form surface features to minimize machining time was presented by Sun et al. (2001). Based on the decomposition of rough cutting and finish cutting, algorithms for rough cutting tool and finish cutting tool selection were also studied.

Many related researches in the optimized tool selection are based on MRR optimization [Balasubramanima (2001) Lee(1992) Yang (1999)]. The MRR is mainly concerned about the machining efficiency. With the development of CAD/CAM technology, feature-based models are widely adopted. Many feature-based algorithms have been developed since then [Joo et al. (1997) Perng and Cheng (1994) Chamberlain et al. (1993)]. By employing both the surface accessibility and MRR, feature-based algorithms acquire better precision.

Researches on machining parameters were always independent from the tool size selection problem [Chua (1993) Yazar (1994) Wang (1995)]. Rad and Bidhendi (1997) studied the optimum machining parameters determination problem for milling operations. Both single-tool and multi-tool operations were discussed in this research. A cutting force model based on two independent variables, 2D chip-load and federate was studied by Bae et

al. (2003). Then an automatic feed rate adjustment method was proposed for optimal feed rate adjustment.

In the RPM process, parts are machined layer by layer, and a new material slab is added for each layer. This process makes the tool size and machining parameter evaluation for each single layer both possible and necessary. In this manner tool size and machining parameter selection according to different part geometries in each layer can ensure good tool accessibility and save total machining time. Instead of attempting to use error prone feature-based methods, the RPM approach divides the models into layers; hence each layer can be treated as an individual component. In the field of Rapid Prototyping & Manufacturing, the tessellated STL file has become the de Facto standard for part geometry description. This file format breaks complex part geometry in a simple set of interconnected facets (triangles), which makes slicing and process planning simplified. In addition, the RPM process divides the whole part to many layers and produces one layer each time. This process adds flexibility to the traditional machining process planning. Most of literatures reviewed above do not provide a systematic method for tool size and machining parameters selection; and none of them are based on the layer based machining. The purpose of this paper is to present an algorithm to automatically select tool sizes and machining parameters for different geometry of each layer in the RPM process, such that the geometry is created successfully and with minimal machining time.

5.2 Problem Definition

In the RPM process, 3-axis CNC milling is the method that generates the part geometry. A face milling operation is used to cut the material slab to the pre-calculated layer

thickness. Face milling is simple and is not related to any part geometries. Materials used by the RPM process are Medium Density Fiberboard (MDF), wood, high-density foam, polyurethane, etc.

In CNC machining operations, many machining parameters affect the machining time, such as tool size, Stepdown, feed rate, spindle speeds and so on. The selection of many these parameters is highly related to the machining strategy. The machining strategy also greatly affects the machining quality. Therefore, the machining strategy adopted by the RPM process is going to be decided in the beginning; and machining time calculation for selected machining strategies will be studied.

In previous researches, the machining parameter Stepdown and feed rate are evaluated in a general machining condition and represented by MRR. In this study, Stepdown is studied separately and precisely calculated according to the part geometry.

The tool size is highly geometry related variable in the CNC machining operation. In the RPM process, tools unique for geometry in each single layer can save machining time and ensure good machining quality. The Objective of tool size selection is to decide:

1) *Rough cutting tool size;*
2) *Finish cutting tool size;*
3) *Semi-rough machining operations.*

To begin, the STL model is sliced in order to generate a set of 2D polygonal cross sections. A sample slice file is shown in Figure 5.3. These slice files serve as the basic input to the selection of the various machining parameters.

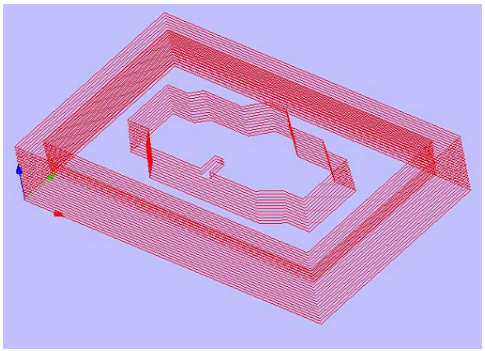

Figure 5.3 A sliced STL model

Nomenclature

SD	Stepdown (Cut depth)
R_x	Radius of the cutting tool x
L	Height of leftover material scallop
α	Slope angle of the part silhouette curve
M_{rr}	Material remove rate
f_e	Feed rate
$\overline{f_e}$	Average feed rate
t_x	Machining time (x is the tool name)
V	Material removal volume
A_{tc}	Tool cover area
AS_x	Semi rough cutting area (x is the tool name)
Tr	Total machining time for a layer
Ai	Area of each machining plane
AR	Accessibility ratio
n	Number of machining steps in a layer
L_{all}	Total length of line segments in a model or a layer
L_{ins}	Length of inaccessible line segments due to intersection
L_{cor}	Length of concave corner inaccessible line segments
W	Weight value for intersection inaccessiblility

5.3 Machining Strategy

The overall machining strategy is critical for both geometry creation and reduction in machining time. Therefore, this section provides a machining strategy used in the RPM process, where machining time calculation methods of selected machining strategies are presented.

From preliminary experiments, the machining strategy for the RPM process is selected to be: a surface rough pocket milling operation with flat end mill cutter for removing most of surplus materials, a surface finish contour milling operation with spherical end mill cutter for finishing the part surfaces, and optional surface finish contour milling with flat end mill cutter as the semi-rough cutting operation. The surface rough pocket milling and surface finish contour milling operations are introduced as follows.

5.3.1 Surface Rough Pocket Milling

Surface rough pocket tool path is a 2½D tool path strategy. In this tool path strategy, the cutting tool machines the part geometry at a specified *z*-height "Stepdowns", in a waterline approach. The cutting tool does not move in simultaneous *x*-*y*-*z* directions, therefore, it is considered only a 2½ D tool path strategy.

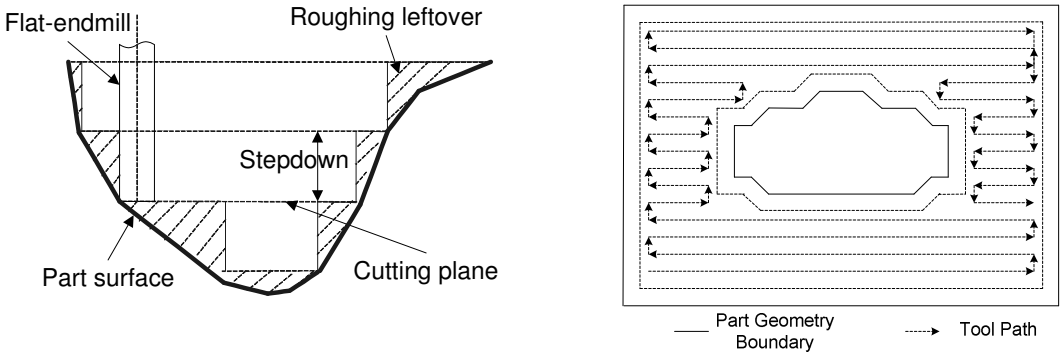

a) 2½D surface rough pocket tool path Stepdown

b) 2½D surface rough pocket tool path route in *xy* plane

Figure 5.4 2½D surface rough pocket tool path strategy

The 2½D surface rough pocket machining adopted by the RPM process is shown in Figure 5.4. Figure 5.4a shows the movement of cutting tool in the *z* direction. The tool path strategy decomposes the total *z* cutting range into several steps, and moves from the bottom to the top sequentially. The distance between 2 continuous steps is defined as Stepdown. It is common to use the same Stepdown for each single cutting operation to reduce calculation time. However, constant Stepdown may result in some machining problems, such as large material leftover and long machining time, etc. Then, the Stepdown parameter is discussed. Figure 5.4b shows the cutting tool route in each single step in the *x*-*y* plane. The cutting tool

moves simply from left to right and bottom to top to cover the whole cutting area, also known as a Zigzag machining pattern.

The MRR is a method used to evaluate the machining efficiency of tools with different tool sizes, feed rates and Stepdowns in general situations. Combining these three parameters together, MRR simplifies the machining efficiency calculation and saves computational time. However, it does not acquire precise machining time estimation for each particular situation. MRR is calculated as:

$$M_{rr} = 2R \times f_e \times SD \qquad (1)$$

In this equation, R is the tool radius. It is difficult to calculate the precise MRR, because the feed rate (*fe*) is variable during each linear and non-linear movement. In previous researches, an average feed rate is adopted, and the Stepdown *SD* is supposed to be uniform during the cutting operation. When the total volume of materials needs to be machined away in a layer is *V*, the machining time for this layer is $t = V / Mrr$.

In this research, the Tool Cover Area (TCA), rather than the MRR, is proposed to evaluate cutting efficiency, because a variable Stepdown is used. TCA is defined as the area of a tool covers in a certain unit of time.

$$A_{tc} = 2R \times \overline{f_e} \qquad (2)$$

The $\overline{f_e}$ is the average feed rate, which is acquired by machining experiments. *TCA* represents the average efficiency of a cutting tool move across a cutting plane in the 2½D surface rough pocket machining. The total time of the surface rough pocket machining is calculated by the sum of cutting time for each stepdown:

$$t_r = \sum_{i=1}^{n} \frac{A_i}{Atc} \qquad (3)$$

In this equation, n is the number of machining stepdowns in a layer, and A_i is the area of machining plane at each stepdown.

5.3.2 Surface Finish Contour Milling

The goal of surface finish contour milling is to approximate the desired part surfaces with a set of 2D contours. When these 2D contours are close to each other in z height, surfaces acquired are close to desired surfaces.

Two kinds of milling tools are usually adopted to move along these 2D contours, which are flat end mill and spherical end mill. Figure 5.6 shows surfaces acquired by using these two kinds of tools are different.

In 3-axis milling, the flat end mill can more effectively machine vertical walls; otherwise, the stair step appearance in Figure 5.5 (left) is acquired. If the Stepdown is very small, the step effect can obviously be minimized. However, very small Stepdowns greatly increase machining time. The stair step appearance in SWIFT rapid prototyping system which adopted 3-axis flat end milling with very fine Stepdown to create parts restricted the part precision; and SWIFT also takes a long time to build parts [Cormier et al. (2001)].

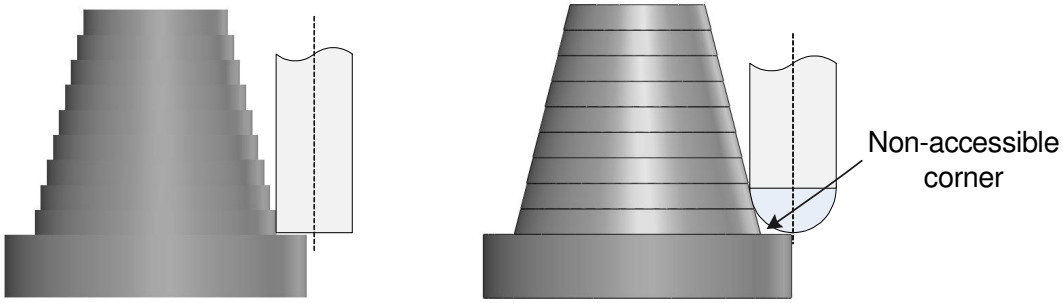

Figure 5.5 Surface finish contour milling with flat end mill (left) and spherical end mill (right)

When the tip of a spherical end mill contacts part surface, a curved shape is formed. In this way, final parts machined by spherical end mills are usually smoother than those cut by flat end mills. One problem with the spherical end mill is that: the spherical end mill does not work on multiple curvature surfaces or infinite curvature (i.e., flat surfaces) transitioning to any curved surface. As shown in Figure 5.5, the flat surface hinders the spherical end mill to move down further, and some materials cannot be cleaned in the corner which is called non-accessible corner in this paper.

In order to obtain good machining efficiency and quality, a combined surface finish contour milling strategy is adopted:

1) A spherical end mill is employed to machine the entire layer.

2) A flat end mill is adopted to clean spherical end mill non-accessible corners.

To detect spherical end mill non-accessible corners, the STL file is sliced from a direction parallel to the building orientation (x or y). Then, each contour is examined to detect slope changes between continuous line segments.

In surface finish contour milling operation, the machining tool moves along a set of contours to approximate objective surfaces. Machining time of this operation t_f can be

calculated by dividing total length of these contours L_c with the average feed speed of the machining tool:

$$t_f = \frac{L_c}{f_e} \tag{4}$$

5.3.3 Feed Rate

Feed rate is the velocity at which the cutter is fed, that is, advanced against the workpiece. Obviously, machining time is generally shortened if we can increase feed rates. Feed rate is often expressed in units of distance per time for milling (typically inches per minute or millimeters per minute).

In milling operations, feed rates are determined by workpiece material, tool material and machine capability. In the RPM process, workpiece materials are usually soft materials, such as MDF, polyurethane, wood etc, which generate limited cutting force. Tool material is usually high speed steel, which can withhold large cutting forces. Spindle speed of the router can reach 18,000 revolutions per minute (rpm), which also greatly reduces cutting forces. Therefore, the major restriction for feed rate in the system is speed of the machine and acceleration capability.

5.4 Stepdown

Stepdown is the depth of the tool which is plunged into workpiece material for each cut. Larger stepdowns obviously reduce cutting time; however, they cause larger cutting forces and rough approximation of the true 3D surface geometries.

As stated in previous sections, the cutting force restriction is not specifically considered in this paper; rather, the limitations of the Stepdown parameter are part geometries and machining tool geometry. Part geometries and machining tool geometries are analyzed in this section.

5.4.1 Spherical End Mill

In the 2½D surface finish contour milling operation, there are four possible spherical end mill contacting situations, as listed in Table 5.1. For situation 1 and 3, when α and the allowable tolerance are determined, the material leftover (surface roughness) reduces with increasing tool diameter *R*. This means a larger tool should always be selected, if the accessibility requirement can be satisfied. Larger tools also save machining time, because larger tools obviously cover larger areas in the machining plane for the same feed rate, and larger *SD* is always applied to larger tools. In situation 2, the spherical end mill contacts on the vertical wall position during 2 continuous machining planes. The height of leftover material scallop is:

$$L = \sin\partial\left(\frac{R}{\sin\partial} - ctg\partial\sqrt{2Rctg\partial SD - SD^2}\right) \qquad (5)$$

In this situation, tools with different radius *R* have different limitations for *SD*. Therefore, the relationship between leftover versus tool radius cannot be simply obtained. Figure 5.6a shows the leftover increase relatively with the increase of tool radius. The 1/8 inch spherical end mill is always the smallest tool adopted in the RPM process. From figure 5.6b, the smallest leftover in this situation is larger than 0.02 inch, which is twice of the general sand casting pattern tolerance requirement. Therefore, it can be concluded that the

leftover for larger tools are much larger than 0.02 inch. The leftover dimension in this situation is unacceptable for sand casting patterns.

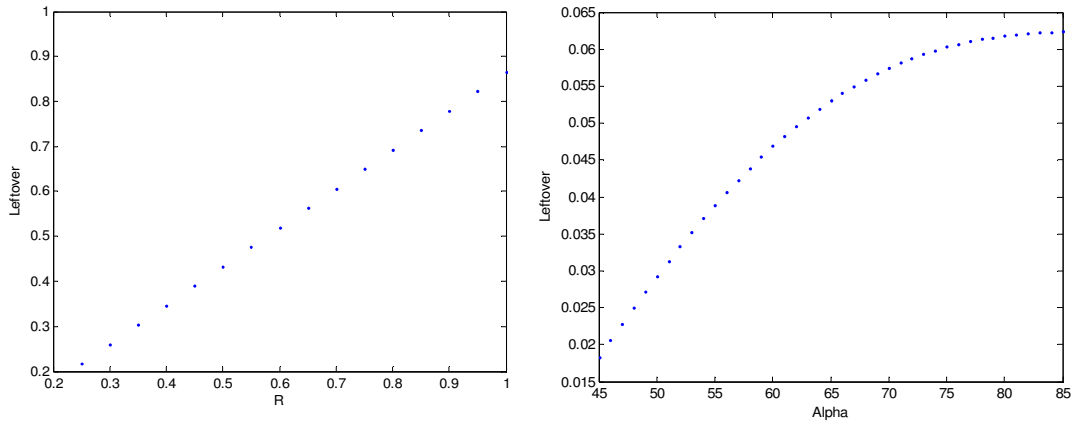

a) Relationship between *R* and *L*

b) Relationship between α and *L* for 1/8 inch tool

Figure 5.6 Relationships of *R*, α and *L*

Table 5.1 Spherical end mill Stepdown calculation

NO	Condition	*SD*	Note
1	$\partial \geq 45^{\circ}$ and $SD <= R\cos(2\partial - 90^{\circ})$	$SD = \dfrac{2ctg\partial\sqrt{R^2 - h^2} - 2h}{1 + ctg^2\partial}$ Where $h = \dfrac{2ctg\partial\dfrac{R-L}{\sin\partial} \pm \sqrt{4ctg^2\partial(\dfrac{R-L}{\sin\partial})^2 - 4(1+ctg^2\partial)[(\dfrac{R-L}{\sin\partial})^2 - R^2]}}{2(1+ctg^2\partial)}$	The allowable Stepdown increases with the increase of tool radius *R*, when α and allowable leftover (*L*) is determined. Therefore, a larger tool should be selected to save machining time with the same allowable surface tolerance requirement.
	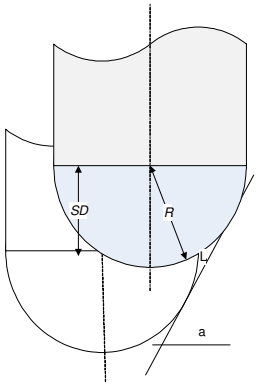	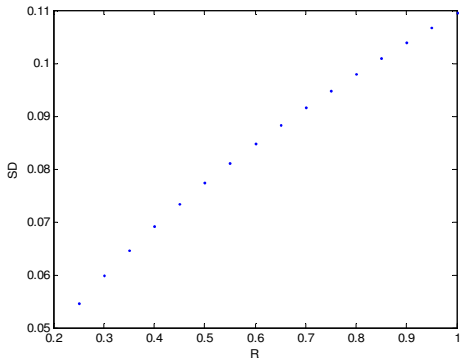	
2	$\partial \geq 45^{\circ}$ and $SD > R\cos(2\partial - 90^{\circ})$	*The leftover is always larger than the sand casting pattern tolerance requirement in the RPM process. Therefore, it is not considered.*	

Table 5.1 (continued)

NO	Condition	*SD*	Note
3	$\partial < 45^{\circ}$ **and** $SD \le R\sin(2\partial)$	$SD = \dfrac{2ctg\partial\sqrt{R^2 - h^2} - 2h}{1 + ctg^2\partial}$ Where $h = \dfrac{2ctg\partial\dfrac{R-L}{\sin\partial} \pm \sqrt{4ctg^2\partial(\dfrac{R-L}{\sin\partial})^2 - 4(1+ctg^2\partial)[(\dfrac{R-L}{\sin\partial})^2 - R^2]}}{2(1+ctg^2\partial)}$	The allowable Stepdown increases with the increase of tool radius *R*, when α and allowable leftover (*L*) are determined. Therefore, larger tool should be selected to save cutting time with the same allowable surface tolerance requirement.
	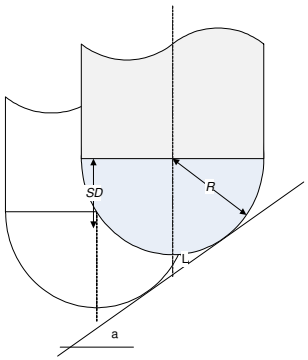	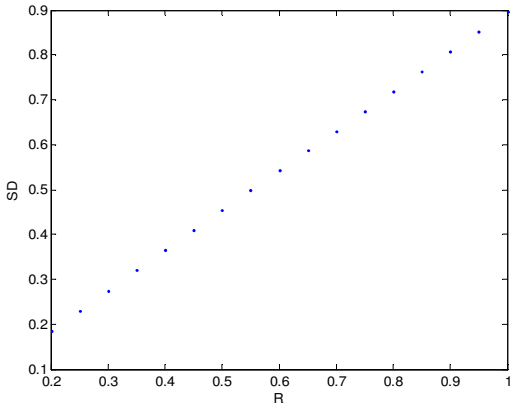	
4	$\partial < 45^{\circ}$ **and** $SD > R\sin(2\partial)$	*In this situation, surfaces cannot be machined properly; and Is not allowed*	

The tool does not overlap during 2 continuous machining planes in situation 4 and the surface will not be machined properly, so this condition should be avoided.

5.4.2 Flat End Mill

Figure 5.7 illustrates the overlap of two continuous machining planes for a flat end mill. The leftover is calculated by:

$L = SD\cos\partial$ Where $L < 2R\sin\partial$

The Stepdown is determined once the leftover is established.

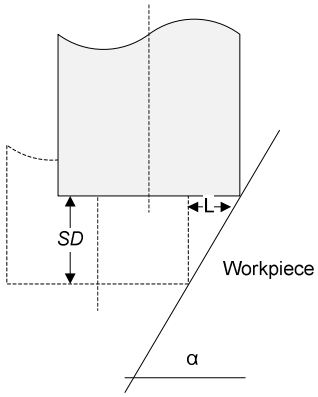

Figure 5.7 Flat end mill overlapping

$$SD = \frac{L}{\cos\partial} \qquad (6)$$

This equation shows that leftover is only affected by *SD* and α, and not by the tool radius. Therefore, the Stepdown of the flat end mill is only decided by the required surface tolerance and surface slope angle α.

5.4.3 Surface Slope Angle α

The surface slope angle α is one of the key parameters required in order to calculate the Stepdown.

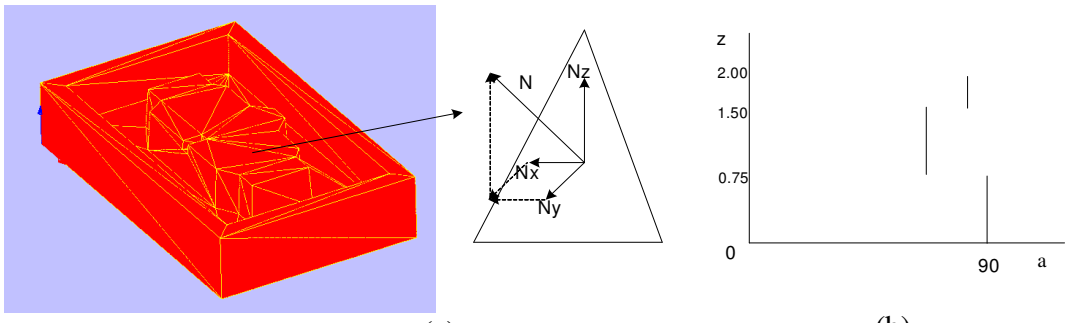

(a) (b)

Figure 5.8 Surface Slop angle α calculation from STL model (a) and α-mapping for a part (b)

In each triangle of the STL model, there is a normal vector *N* which is composed by *Nx*, *Ny* and *Nz* in the 3D coordinate system (Figure 5.8a). From normal vector components *Nx*, *Ny* and *Nz*, the angle between the triangle normal and horizontal plane is $\beta = arctg(Nz/\sqrt{Nx^2 + Ny^2})$. And α = 90º – β, then the surface slope angle of this facet (triangle) is:

$$\alpha = 90^{o} - arctg(Nz/\sqrt{Nx^2 + Ny^2}) \qquad (7)$$

By evaluating all triangles in the STL model, and choosing the smallest α at each Z position, a "α-mapping" (Figure 5.8b) is acquired for each part. Using the α-mapping, the Stepdown *SD* for each layer can be calculated using the chosen tool.

5.5 Tool Size Selection

In general, larger tools allow for larger Stepdowns and higher possible feed rates, thereby reducing machining time; since they can endure larger cutting forces without deflection or failure. On the other hand, larger tools cannot create very small radii features due to decreased accessibility. In the first and second sections of this chapter, a method is presented to calculate the accessibility ratio from the STL slice model. Section 3 and 4 illustrate how to determine the finish and rough cutting tool sizes based on the accessibility ratio and machining time.

5.5.1 Accessibility Ratio Calculation

Accessibility is defined by how much of a surface can be accessed by a specific size of tool, therefore, it is an important index of machining quality. In the RPM process, only the

finish cutting tool is employed to create the net shape of the pattern surface. Therefore, the accessibility ratio is the indicator for finish cutting tool selection. Accessibility can be calculated using the polygonal geometry of the STL slice model. In this work, the accessibility is represented by the accessibility ratio, which is the percentage of the part surfaces that can be accessed by a certain size of tool. The accessibility ratio is defined as:

$$AR = \frac{Length\ of\ accessible\ line\ segments}{Total\ length\ of\ line\ segments\ in\ the\ model} \times 100\%$$

In the beginning of the accessibility ratio calculation, the total length of line segments in a model or a layer of the model is calculated and represented by L_{all}.

5.5.1.1 Undercuts Evaluation

The first step is to evaluate the undercut accessibility. Consider the part in Figure 5.9, where the current slice is covered by the union of slices above it. In this example, line segments of the current slice cannot be machined, if they are within the range of upper slices.

The undercut line segment accessibility has no relationship to the tool size; therefore in this analysis, these undercut geometries are neglected in the remainder of the analysis

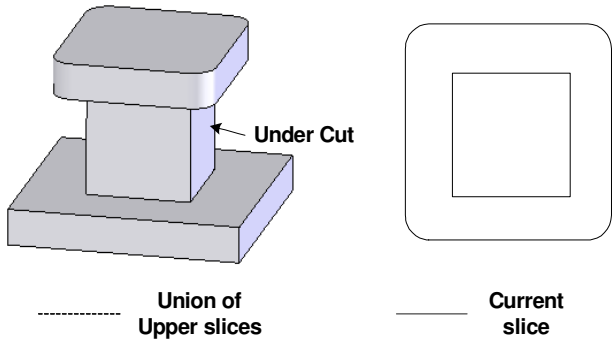

Figure 5.9 An undercut example

5.5.1.2 Line Segment Intersection

The path of the finish cutting tool can be obtained by offsetting pattern boundaries by the tool radius. After offsetting, some line segments intersect, which implies the distance between these features are small, and a tool with this radius will result in an overcut in these areas. Therefore, these intersected line segments are inaccessible by tools with the given radius. Length of these inaccessible line segments due to intersection are represented by L_{ins}.

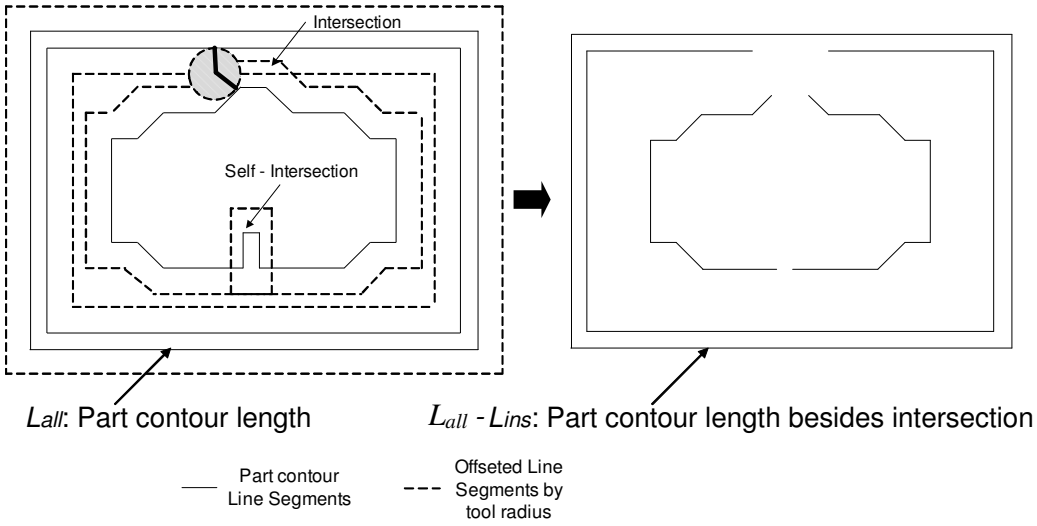

Figure 5.10 Intersection evaluation

Figure 5.10 shows the self-intersection and intersection between line segments on the cutting tool route. These line segments which cause intersection are inaccessible line segments. The part component polygons after filtering inaccessible line segments is also shown in Figure 5.10 (right).

5.5.1.3 Concave Corners

As shown in Figure 5.11, concave corners are partially or totally inaccessible. In this step, the accessibility of line segments left from step 1 and 2 are assessed by evaluating corner angles formed by them. If the angle of a corner composed of two line segments is greater than 180° (Convex corner), all line segments around the corner are accessible. However, if the angle of the corner formed by them is less than 180°, some sections of these line segments are inaccessible. The length of the inaccessible line segments depends on the tool size and the angle of the corner formed by these line segments. L_{cor} is the inaccessible corner length calculated in this step. Figure 5.11 illustrates the accessible line segments after filtering inaccessible corner sections in a particular slice.

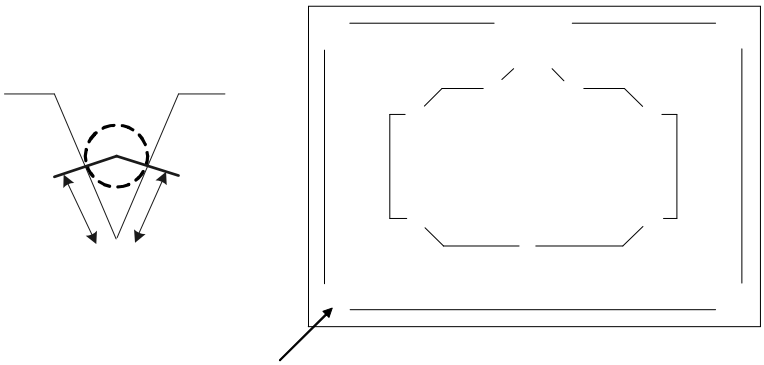

Lcor: Inaccessible line segments length around concave corners

Figure 5.11 Line segment accessibility assessment

According to the definition, the accessibility ratio can be calculated by:

$$AR = \frac{L_{all} - L_{ins} - L_{cor}}{L_{all}} \times 100\% \qquad (8)$$

Usually, the inaccessible due to intersection is more important than the inaccessible around concave corners for the tool selection; because inaccessible due to intersection can be

eliminated or reduced by selecting small tools, but inaccessibility around concave corners is inevitable. Therefore, a weight value *W* can be applied to balance the importance of these two kinds of inaccessible line segments. Then, the accessibility ratio formula becomes:

$$AR = \frac{L_{all} - L_{ins} \times W - L_{cor}}{L_{all}} \times 100\% \qquad (9)$$

Slices from an STL model use line segments to approximate curves. This approximation may impart small errors in the accessibility calculation. One method to reduce these errors is to accommodate a certain degree of allowable deviation. A threshold accessibility ratio can be acquired by experience.

5.5.2 Rough & Finish Tool Matching

Figure 5.4 shows the surface rough pocket milling process. Objective of surface rough pocket milling is to remove most of the surplus material and prepare for the finish contour cutting operation. Surface rough pocket milling leaves some materials with stair step appearance which is called rough cutting leftover in this paper. If too much leftover material remains after rough cutting operation, surfaces of the pattern may not be successfully created by single pass of the surface finish contour milling operations; worse, it could cause tool failure.

1) Rough cutting leftover

Large Stepdowns during rough cutting and the slope of part surfaces can cause considerable leftover material (Figure 5.12). In different positions, the leftover material amounts are also different; however, the largest leftover typically occurs at the top of each

stepdown. Therefore, the largest rough cutting leftover is searched in each layer for rough & finish tool matching calculation.

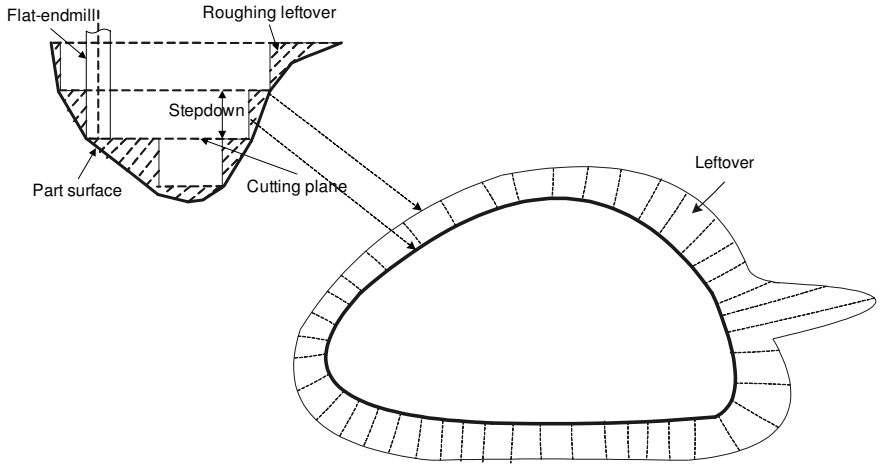

Figure 5.12 Rough cutting leftover

2) Semi-rough cutting area calculation

The semi-rough cutting area is the area of the material between the rough cutting leftover and the path of the finish cutting. The finish cutting area is acquired by offsetting the pattern boundary by the finish cutting tool diameter.

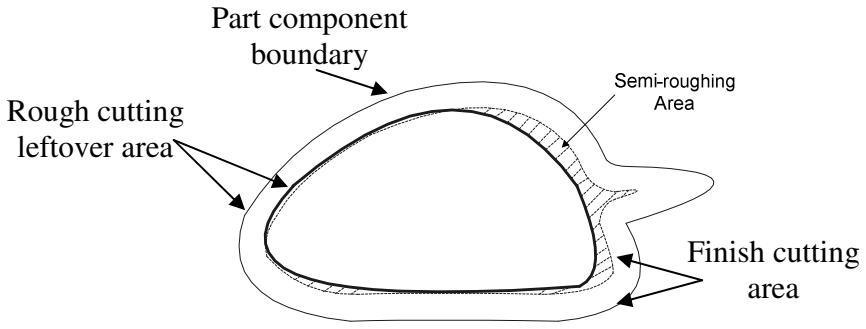

Figure 5.13 Semi-roughing area

As shown in Figure 5.13, a finish cutting tool is selected to remove the remaining material left by the rough cutting operation. The area of surplus material left after both the

rough cutting and finish cutting operations can be calculated by subtracting the rough cutting leftover area by the finish cutting area. A parameter *AS* is defined to be the area of rough cutting leftover minus the finish cutting area, which is the semi-rough cutting area.

If $AS > 0$, it means there are still some rough cutting leftover materials left after the finishing cutting operation. Then, this leftover material created by the rough cutting tool is too large for the finish cutting tool. Therefore, a smaller rough cutting tool should be searched.

5.5.3 Tool Size Selection

The tool size is highly related to the geometry being created and is also an important factor in determining machining time. To begin, a tool size selection algorithm is presented in Figure 5.14.

In the RPM process, there are 3 milling operations: face milling, surface rough pocket milling and surface finish contour milling. Because the face milling has no relationship to part geometries, the tool size selection algorithm only decides the rough cutting, finish cutting and optional semi-rough cutting tool sizes.

The tool size selection algorithm in this paper has four steps

1) *Allowable finish cutting tool size calculation*
2) *Vertical wall analysis*
3) *Roughing cutting tool matching**
4) *Semi-rough cutting tools selection **

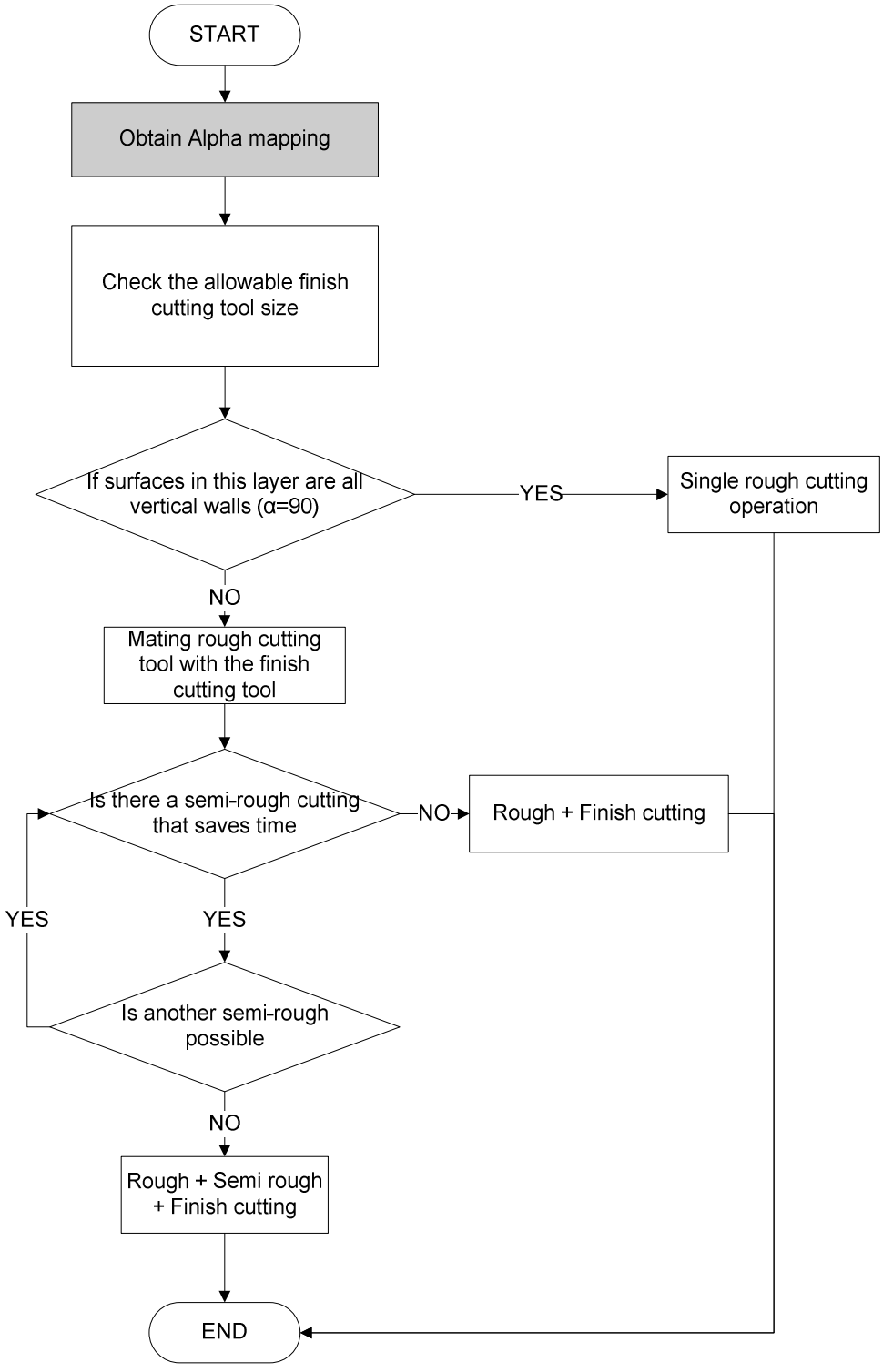

Figure 5.14 Tool size selection algorithm work flow

Step 3 and 4 are not necessary if a vertical wall is detected in the second step. An assumption in this algorithm is that all tools in the database have lengths larger than the slab thickness.

5.5.3.1 Step 1: allowable finish cutting tool size calculation

As mentioned above, a surface finish contour tool path is employed in the finish cutting operation in the RPM process. In surface finish contour milling, the tool moves directly along contours or "waterlines" along the pattern. For a certain surface finish contour operation, the machining efficiency is mainly decided by its Stepdown. However, the final part quality is mainly influenced by tool size and Stepdown. Therefore objectives of finish cutting tool selection are:

1) The finish cutting tool meets the threshold accessibility requirement.

2) The finish cutting tool has high cutting efficiency.

To begin, all the finish cutting tools are sorted by diameters. Next, the part is sliced and the accessibility ratio of the tool is calculated from finish cutting tools ranging from large to small diameter. If the accessibility ratio of a certain size of tool is equal to or exceeds the threshold accessibility ratio, all tools with smaller diameters are eligible for the finish cutting operation of this part, because all tools with smaller diameters have a better accessibility ratio for this part. If no finish cutting tool can meet the threshold accessibility requirement, the smallest finish cutting tool in the tool library is selected. Finally, the Stepdown is calculated using the equations in table 5.1. In some layers, more than one Stepdown values are adopted according to the α-mapping in this range.

5.5.3.2 Step 2: vertical wall analysis

Vertical walls are surfaces perpendicular to build platform or *xy* plane in the RPM process. In the STL file, vertical surfaces are represented by triangle facets with α=90°. For the vertical wall, no finishing is necessary, because the flat end mill can machine the surfaces most efficiently. From α-mapping, if vertical facets cover the entire layer, only rough cutting is required for this layer. A flat end mill with the calculated diameter in *Step 1* is adopted (It is assumed there is always a rough cutting tool with the same diameter for each finish cutting tool) and the Stepdown is the maximum allowable for this tool. If not all vertical surfaces in this layer, the vertical surface region and non-vertical surface region are divided and planned for tool paths separately.

5.5.3.3 Step 3: Rough cutting tool selection

The finish cutting tool selected from step 1 ensures good machining quality. The objective of this step is to select an optimal rough cutting tool to mate with the finish cutting tool (AS = 0) and ensure good machining efficiency. The rough cutting tools are evaluated from two aspects: the semi-rough cutting area and the Stepdown. As shown in Figure 5.13, the Stepdown and semi-rough cutting area are related to each other for a certain size of tool. A decrease in Stepdown may result in a decrease of the Semi-rough cutting area, and as shown in equation (6), the Stepdown for rough cutter has no relationship to the tool diameter. In this manner, there are infinite selections for the rough cutting tool. In order to simplify the selection problem, an allowable Stepdown range $[SD_i^-, SD_i^+]$, where i is the tool name, is

pre-determined for each rough cutting tool. Then, the rough cutting tool selection algorithm is as follows:

1) *Calculate the rough cutting tool Stepdown (SD_{rough}) with equations (6), where L = R_f.*
2) *Searching for rough cutting tools with $SD_i^- \leq SD_{rough}$.*
3) *For tool i, if AS_{rough} = 0, it is the rough cutting tool. And the Stepdown is searched between SD^+ and SD_{rough} with Halving Algorithm.*
4) *If $AS_{rough} \neq 0$, AS_{SD-} is calculated. If AS_{SD-}=0, the rough cutting tool is selected. And the Stepdown is searched between SD- and SD_{rough} with Halving Algorithm.*
5) *If $AS_{SD-} \neq 0$, the next large tool with $R>R_f$ in step 2 is selected, and calculated from step 3. If no tool left in step 2. The next large tools with $R>R_f$ are calculated in sequence. If no tool with $R>R_f$ are selected, the tool with $R=R_f$ is the rough cutting tool, and the Stepdown is min(SD_{rough}, SD_i^+).*

5.5.3.4 Step 4: Optional semi-rough cutting evaluation

The semi-rough cutting operation is used to reduce leftover materials left by the rough cutting operation to enable the usage of larger rough cutting tool to save rough cutting time. The semi-rough cutting is in fact conducting a surface finish cutting operation using a selected rough cutting flat end mill. The semi-rough cutting operation evaluation process includes two steps:

1) Larger rough cutting tool selection. The selected rough cutting tool (NO. *r1*) in step 3 is supposed to be the semi-rough cutting tool; then another larger rough cutting tool is

selected. The same rough cutting tool selection method in step 3 is adopted, and the finish cutting tool radius in step 3 is R_{r1}.

2) *Time saving evaluation.* When the new rough cutting tool is selected, a new machining strategy with the rough cutting operation is formed. In the new machining strategy, a larger rough cutting tool is added and the previous rough cutting tool is transferred to perform a surface finish contour machining which is the semi-rough cutting operation. The machining time of the new machining strategy is compared to the previous strategy to evaluate the machining time saving. From equation 3 and 4, the rough cutting time and semi-rough cutting time can be calculated. The t_{r2}, t_{f1} and t_{r1} are defined as new rough cutting time, semi-rough cutting time and original rough cutting time. If the sum of new rough cutting time and semi-rough cutting time is shorter than the original rough cutting time (Equation 7), it means the new strategy saves machining time and the semi-rough cutting operation is adopted; else the original machining strategy should be kept.

$$t_{r2} + t_{f1} < t_{r1} \qquad (7)$$

If a semi-rough cutting operation is proved to save machining time, it is possible that one more semi-rough cutting operation may save machining time further. In this case, step 4 in the algorithm can be repeated to test the possibility of another semi-rough cutting operation.

5.6 Implementation

The tool size and machining parameter selection algorithm presented in this paper has been implemented, and some sample parts have been machined. In this section, a sample pattern is machined with both the strategy output from the proposed algorithm and the

existing fixed tool set strategy, and compared with respect to machining quality and machining time.

By referring to the "Pattern maker's manual" (AFS, 1970), basic surface tolerance requirements for sand casting patterns are shown in Table 5.2.

Table 5.2 Tolerance requirement for sand casting patterns (Unit: inch)

Part Size	Tolerance
Up to 6 inches	± 0.010
Additional each inch over 6 inches	± 0.003

The sample part adopted in this study is shown in Figure 5.15. The 0.75 inch thick 10×8 inch MDF is the raw material used to create the part. From the layer thickness decision software [Luo and Frank (2009)], three layers are needed to create this part (Table 5.3).

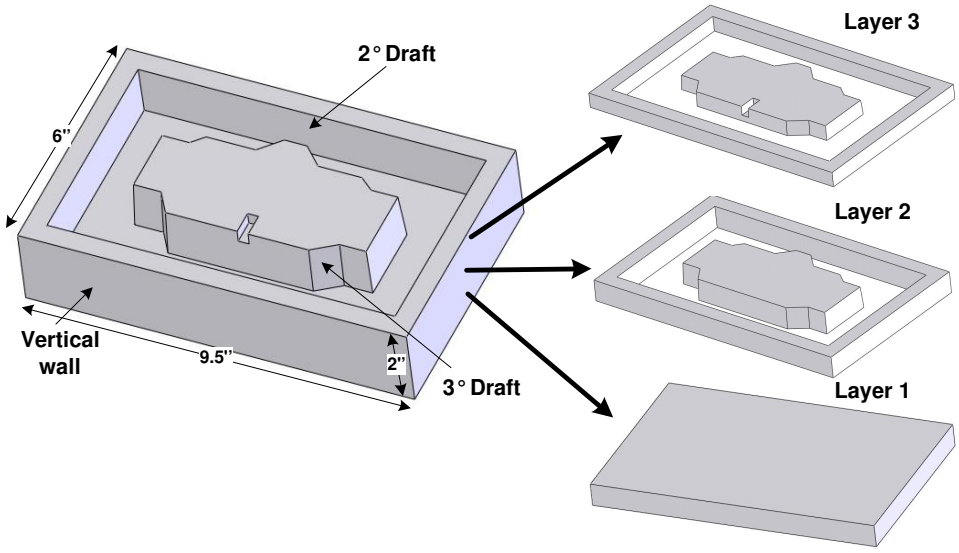

Figure 5.15 Sample pattern design

The first layer covers the whole bottom of the pattern; therefore, the geometry of this layer is a plate with vertical outside walls. The second layer contains vertical wall, 2° draft

and 3° draft geometries. In the last layer, there is a small slot which forces the system to select a small tool, and test the possibility of semi-rough cutting operation.

Table 5.3 Layer thicknesses of the sample part (Unit: inch)

Layer NO.	Layer Thickness
1	0.75 (0.00~0.75)
2	0.75 (0.75~1.50)
3	0.50 (1.50 ~ 2.00)

In the tool library, there are 5 groups of tools from 0.125 to 1 inch diameter for selection. In each group, there is a spherical end mill and a flat end mill with the same diameter. The length of each tool is larger than the material slab thickness. Available tool sizes and the "Stepdown" ranges for rough cutting tools are listed in Table 5.4.

The threshold accessibility rate is set to be 97.50%. The weight for inaccessible line segment intersection is determined to be 2.0 .

Table 5.4 Available tools in the tool library (Unit: inch)

Tool NO.	1	2	3	4	5
Diameter	0.125	0.25	0.5	0.75	1.00
Stepdown	(0~0.0625]	[0.0625 ~ 0.125]	[0.1 ~ 0.15]	[0.12 ~ 0.2]	[0.16~0.25]

1) First Layer

The first layer has only vertical wall geometry, and the layer does not have the convex geometry; therefore, the cutting tool with any diameter has 100% accessibility ratio. The largest cutting tool with 1 inch diameter is selected. A single rough cutting operation is the machining plan for this layer.

The maximum Stepdown 0.25 inch of 1 inch diameter rough cutting tool is the Stepdown value for this layer.

2) Second Layer

In the second layer, there are some concave corners; therefore, the accessibility ratio of tools from large to small are calculated to select the finish cutting tool.

Table 5.5 Finish cutting tool accessibility ratio for the second layer (Unit: inch)

Tool	Accessibility Ratio
1	88.29 %
0.75	96.18 %
0.50	97.00 %
0.25	97.82 %

The tool with 0.25 inch diameter is selected to do the finish cutting, because it is the largest tool which has accessibility ratio larger than 97.50%. The accessibility ratios of tools with diameter from 1.00 inch to 0.25 inch are shown in Table 5.5. According to the Stepdown calculation method, the Stepdown for the finish cutting operation is 0.0445 inch.

From Alpha-Mapping, the minimum alpha angle for this layer is 87 degree. According to equation (6), the allowable Stepdown for the rough cutting operation is 0.191 inch, which is larger than the allowable Stepdown of tools which have diameter smaller than 1 inch. Then, the *AS* of each tool is checked form the 1 inch diameter tool to smaller ones. Finally the 0.50 inch diameter flat end mill is selected, because flat end mills with 1 inch diameter and 0.75 inch diameter cannot meet the requirement of $AS = 0$. The allowable Stepdown (0.191 inch) is not within the Stepdown range of 0.50 inch diameter tool, then, the Stepdown for the rough cutting operation is 0.15 inch which is the maximum allowable Stepdown for the 0.50 inch diameter rough cutting tool.

If the 0.50 inch diameter tool is used to be a semi-rough cutting tool, the other larger rough cutting tools cannot meet the $AS = 0$ condition; therefore, there is no semi-rough cutting operation for this layer.

3) Third layer

The accessibility ratio evaluation for the third layer is shown in Table 5.6. Evaluated from the threshold accessibility ratio, the 0.125 inch diameter spherical end mill is used to do the finish cutting.

Table 5.6 Finish cutting tool accessibility ratio for the third layer (Unit: inch)

Tool	Accessibility Ratio
1	92.12 %
0.75	95.36 %
0.50	96.17 %
0.25	96.99 %
0.125	99.58 %

In the Alpha-mapping, the minimum alpha angle in this layer is 87 degree. According to the equation (6), the allowable Stepdown of rough cutting tool is 0.191 inch. Tools with diameter smaller than 1 inch can meet the Stepdown condition, however, only the 0.125 inch diameter flat end mill meets the $AS = 0$ condition; Therefore, the 0.125 inch diameter flat end mill cutter is employed to do the rough cutting operation.

If the 0.125 inch diameter flat end mill cutter is the semi-rough cutting tool, then another rough cutting tool is evaluated. And the 0.50 inch diameter tool can meet the $AS = 0$ condition. In theory, the rough cutting time of 0.50 inch diameter tool is 195s; and the semi-rough cutting time of 0.125 inch tool is 56s. The original rough cutting time of 0.125 inch diameter tool is 624s. Therefore, the semi-rough cutting operation is adopted, because it greatly saves the total process time. The Stepdown for the semi-rough cutting operation is 0.0625 inch. The rough cutting flat end mill has the 0.50 inch diameter, and the Stepdown is 0.15 inch.

This sample pattern is machined with both the original fixed tool set strategy and the tool size selection strategy studied in this paper. The fixed tool set strategy machines every layer with a 0.25 inch finish cutting tool and a 0.5 inch rough cutting tool. The machining

times of these two methods are shown in Table 5.7. The tool size selection strategy saves 43% of the total machining time comparing to the original fixed tool set strategy in the RPM process. Machined patterns with these two strategies are shown in Figure 5.16. The fixed tool set strategy cannot create the small slot feature in the third layer; however, the tool size selection strategy detected this small feature and machined it correctly. The surface finish of the first and second layer machined from tool size selection strategy is rougher than those machined with fixed tool set strategy; however, the surface finish created by this method satisfied the surface tolerance requirement. Therefore, by considering the machining quality and machining time, the tool size selection strategy is better than the fixed tool set strategy.

Table 5.7 Machining time of different strategies (Unit: minute)

	FIXED TOOL SET	TOOL SIZE SELECTION
Layer 1	29	11
Layer 2	60	32
Layer 3	48	39
Total	137	82

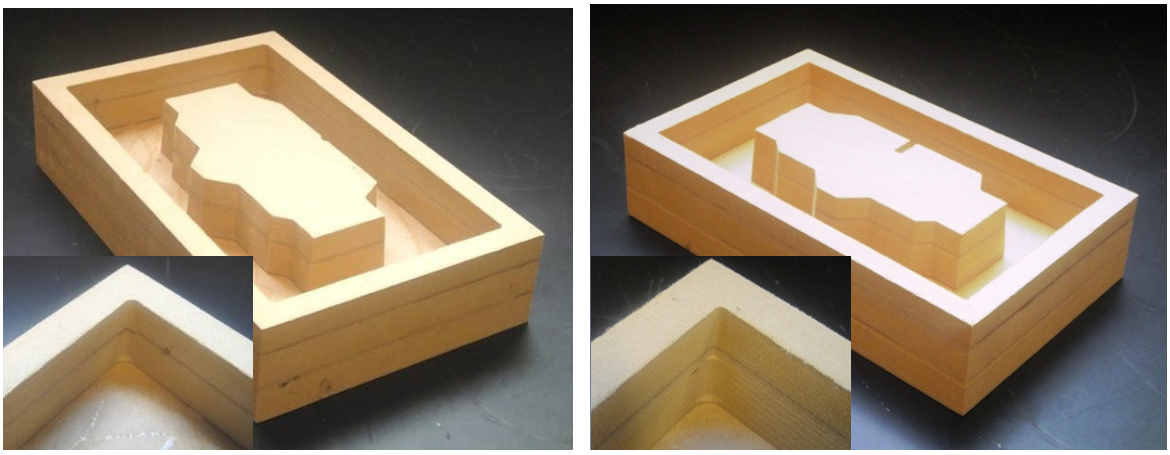

Figure 5.16 Machined sample patterns. (a) Pattern machined with fixed tool set strategy (b) Pattern machined with tool size selection strategy.

5.7 Conclusion

This paper presented a key enabling technique for the purpose of geometry realization and machining time savings in the Additive/Subtractive Rapid Pattern Manufacturing process. As it has been found, different tool size and machining parameter combinations have significant impact on the geometry realization and machining time.

Even though high processing speed is not necessary for Rapid Prototyping/Manufacturing techniques, slow fabrication speed inhibits the creation of large parts, such as sand casting patterns, with existing rapid prototyping/manufacturing methods. Therefore, the machining efficiency improvement for the RPM process is meaningful.

The methods of this paper effectively address the problem by analyzing three key aspects: machining strategy, Stepdown and tool sizes. The surface rough pocket machining is selected to be the rough cutting method, and the flat end mill cutter is employed. The surface finish contour is the finish cutting solution. The spherical end mill is used to machine all the geometry in the layer, and flat end mill is adopted to clean the spherical end mill inaccessible corners. The Stepdown parameter for both spherical end mill cutter in finish cutting operation and flat end mill cutter in rough cutting operation are studied. A tool size selection algorithm based on both accessibility and machining efficiency is proposed for the selection of tools for both rough and finish cutting operations.

The algorithm has been implemented in software and has been tested. A sample part is machined with both the fixed tool set strategy and the tool size selection strategy. The experimental result shows the proposed algorithm has better performance with respect to both machining quality and time over the existing fixed tool set strategy.

This algorithm is functional and has better performance than the arbitrary fixed tool set approach; however, there exist areas of improvement to pursue. For one, geometry is the key factor to determine tool size and machining parameter selection and in this regard a *feature* is the index to represent different geometries. Selecting tool sizes and machining parameters based on *features* may further improve the machining quality and machining efficiency. In addition, although a single pass of finish cutting was used to calculate the semi-roughing area in this work, a multi-pass approach to finishing machining may further reduce machining time.

Reference

AFS (1970). Pattern Maker's Manual. *American Foundrymen's Society*.

Arezoo, B. Ridgway, K. Al-Ahmari, A. M. A. (2000). Selection of cutting tools and conditions of machining operations using an expert system. *Computers in Industry*, 42(1), 2000.

Arya, S. Cheng, S. W. Mount, D. M. (1998). Approximation algorithms for multiple tool milling. *Proceedings of the Fourteenth Annual Symposium on Computational Geometry*, 297-306.

Bae, S. H. Ko, K. Kim, B. H. Choi, B. K. (2003). Automatic feedrate adjustment for pocket machining. *Computer-Aided Design*, 35(5), 495-500.

Bala, M. Chang, T. C. (1991). Automatic cutter selection and optimal cutter path generation for prismatic parts. *International Journal of Production Research*, 29(11), 2163-2176.

Balasubramanima, M. Joshi, Y. Engels, D. Sarma, S. Shaikh, Z. (2001). Tool selection in three-axis rough machining. *International Journal of Production Research*, 39(18), 4215-4238.

Chamberlain, M. A. Joneja, A. Chang, T. C. (1993). Protrusion features handling in design and manufacturing planning. *Computer Aided Design*, 25(1), 19-28.

Chen, Y. H. Lee, Y. S. Fang, S. C. (1998). Optimal cutter selection and machine plane determination for process planning and NC machining of complex surfaces. *Journal of Machining Systems*, 17(5), 371-388.

Chua, M. S. Rahman, M. Wong, Y. S. Loh, H. T. (1993). Determination of optimal cutting conditions using design of experiments and optimization techniques. *International Journal of Machine Tools & Manufacture*, 33(2), 297-305

Cormier, D. Taylor, J. (2001). A process for solvent welded rapid prototype tooling. *Robotics and Computer Integrated Manufacturing*, 17(1-2), 151-157.

D'Souza, R. M. (2006). One setup level tool selection for 2.5-D pocket milling. *Robotics and Computer Integrated Manufacturing*, 22(3), 256-266.

Frank, M. C. Wysk, R. A. Joshi, S. B. (2004). Rapid planning for CNC milling – a new approach for rapid prototyping. *Journal of Manufacturing Systems*, 23(3), 242-255.

Joo, J. Cho, H. Yun, W. (1997). Efficient feature-based process planning for sculptured pocket machining. *Computers &Industrial Engineering*, 33(3-4), 493-496.

Lee, Y. S. Choi, B. K. Chang, T. C. (1992). Cut distribution and cutter selection for sculptured surface cavity machining. *International Journal of Production Research*, 30(6), 1447-1470.

Lee, Y. S. Chang, T. C. (1994). Using virtual boundaries for the planning and machining of protrusion freeform features. *Computers in Industry*, 25(2), 173-187.

Lee, Y. S. Chang, T. C. (1995). Application of computational geometry in optimizing 2.5D and 3D NC surface machining. *Computers in Industry*, 26(1), 41-59.

Lim, T. Corney, J. Clark, D. E. R. (2000). Exact tool sizing for feature accessibility. *International Journal of Advanced Manufacturing Technology*, 16(11), 791-802.

Lin, A. C. Gian, R. (1999). A multiple-tool approach to rough machining of sculptured surfaces. *The International Journal of Advanced Manufacturing Technology*, 15(6), 387-398.

Luo, X. M. Frank, M. C. (2009). A layer thickness algorithm for Additive/Subtractive Rapid Pattern Manufacturing. *Rapid Prototyping Journal, (*Accepted).

Nadjakova, I. Mcmains, S. (2004). Finding an optimal set of cutter radii for 2D pocket machining. *Proceedings of International Mechanical Engineering Congress and RD&D Expo*, 1-8.

Perng, D. B. Cheng, C. T. (1994). Feature based process plan generation from 3D DSG inputs. *Computers & Industrial Engineering*, 26(3), 423-435

Rad, M. T. Bidhendi, I. M. (1997). On the optimization of machining parameters for milling operations. *International Journal of Machine Tools and Manufacture*. 37(1), 1-16.

Ribeiro, M. V. Coppini, N. L (1999). An applied database system for the optimization of cutting conditions and tool selection. *Journal of Materials Processing Technology*, 92-93, 371-374.

Sun, G. P. Sequin, C. H. Wright, P. K. (2001). Operation decomposition for freeform surface features in process planning. *Computer Aided Design*, 33(9), 621-636.

Taylor, J. B. Cormier, D. R. Joshi, S. Venkataraman, V. (2001). Contoured edge slice generation in rapid prototyping via 5-axis machining. *Robotics and computer integrated manufacturing*, 17(1-2), 13-18.

Veeramani, D. Gau, Y. S. (1997). Selection of an optimal set of cutting-tool sizes for 2 ½ D pocket machining. *Computer Aided Design*, 29(12), 869-877.

Veeramani, D. Gau, Y. S. (2000). Cutter-path generation using multiple cutting-tool sizes for 2 ½ D pocket machining. *IIE transactions*, 32(7), 661-675.

Wang, J. Armarego, E. J. A. (1995). Optimisation strategies and CAM software for multiple constraint face milling operations. *Proceedings of the 6th International Conference on Manufacturing Engineering*, 535-540.

Wang, Y. Ma, H. J. Gao, C. H. Xu, H. G. Zhou, X. H. (2005). A computer aided tool selection system for 3D die/mould-cavity NC machining using both a heuristic and analytical approach. *International Journal of Computer Integrated Manufacturing*, 18(8), 686-701

Yang, D. C. H. Han, Z. (1999). Interference detection and optimal tool selection in 3-axis NC machining of free-form surfaces. *Computer-Aided Design*, 31(5), 303-315.

Yao, Z. Y. Gupta, S. K. Nau, D. S. (2001). A geometric algorithm for finding the largest milling cutter. *Journal of Manufacturing Processes*, 3(1), 1-16.

Yao, Z. Y. Gupta, S. K. Nau, D. S. (2003). Algorithm for selecting cutters in multi-part milling problems. *Computer-Aided Design*, 35(9), 825-839.

Yazar, Z. Koch, K. F. Merrick, T. Altan, T. (1994) Feed rate optimization based on cutting force calculations in 3-axis milling of dies and moulds with sculptures surfaces. *International Journal of Machine Tools & Manufacture*. 34(3), 365-377.

CHAPTER 6. CUTTING FORCE, LAYER THICKNESS AND TOOL SIZE ANALYSIS FOR A RAPID PATTERN MANUFACTURING PROCESS

A paper to be submitted to the Rapid Prototyping Journal

Xiaoming Luo, Matthew C. Frank
Department of Industrial and Manufacturing Systems Engineering
Iowa State University, Ames, IA, 50011, USA

Abstract

Cutting force is a key factor in the process planning for machining operations. In this paper, two process planning problems in an Additive/Subtractive Rapid Pattern Manufacturing (RPM) process are presented: the thin material machining problem and layer thickness & tool size interaction problem. Both of these problems are analyzed in terms of cutting force. First, popular cutting force models are reviewed, and a suitable model for cutting force calculation in the RPM process is evaluated. A study of thin material machining failure helps to eliminate or reduce fracture failure in the RPM process, and a thin material machining failure model is developed. By using the thin material machining model, the minimum layer thickness for a material in the RPM process is determined. Third, related work by the authors for the layer thickness decision problem and tool size selection problem is incorporated. These two problems interact when the material slab thickness constraint is resolved. The removal of the material slab thickness constraint enables the use of fewer layers; however, the layer thickness and tool size interaction must be evaluated. A solution model to the layer thickness & tool size interaction problem according to machining tool deflection under cutting forces is presented. Finally, implementations of these two models are presented to evaluate the efficiency.

Keywords: Rapid Manufacturing, Thin material machining, Layer thickness, Tool size selection

6.1 Introduction

A hybrid process for the rapid manufacturing of casting patterns has been proposed by the authors. This Additive/Subtractive Rapid Pattern Manufacturing (RPM) process adds a thick material slab, cuts it to a certain layer thickness, then machines the part geometry on each layer incrementally. In this manner, process planning is greatly simplified, and moreover, very deep cavities in patterns can be machined using simple small diameter tools. The process overcomes traditional challenges in pattern making that normally force the use of 5-axis machining in order to complete large patterns, even though those sand casting patterns are undercut-free and 3-axis machinable, necessarily. The most basic steps of this process are illustrated in Figure 6.1.

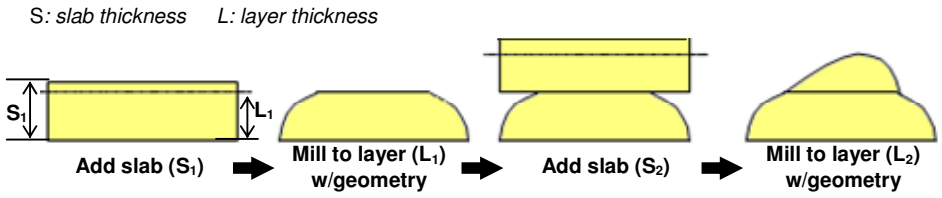

Figure 6.1 Basic steps in the RPM process

In a CNC milling operation, cutting force is a critical parameter that affects process planning; it is an important index that is useful in evaluating the material and cutter distortion. In the proposed Additive/Subtractive Rapid Pattern Manufacturing (RPM) process, there are two critical problems: thin material machining problem, and layer thickness & tool size interaction problem. Thin material machining failure in the form of a fracture, is a major problem affecting the machining quality in the RPM process. When the material slab thickness constraint is resolved, layer thickness increases, resulting in fewer layers and less material deposition time. However, the layer thickness and tool size interaction problem must be resolved when the layer thickness becomes overly larger. Both of these problems need to be studied while considering

the cutting force parameter. In this RPM process, a complete sand casting pattern is constructed layer by layer, generally using wood, although other materials are possible. Layer thicknesses in the RPM process are considerably thicker than conventional RP systems, which usually range from 0.001" to 0.010". In contrast, the RPM process uses thick slabs of material like wood, up to 0.75" thick or more. However, the traditional "stair-step" problem in additive-only RP systems is avoided altogether since every larger slab is machined sequentially using a 3 axis milling system (3-axis CNC router). These slabs are cut to the aforementioned "layer" thicknesses; a major problem addressed in this paper. Many issues arise when machining through these layers; and the proper selection of layer thickness and tooling choices are critical.

6.1.1 Thin Material Machining

Thin material machining in this paper is defined as a milling operation with a flat end mill cutter performed on thin material plates (or sheets). The thin material plate undergoes large elastic deformation under cutting forces, and intermittent material-tool contact usually causes self-excited oscillation when the material or tool has large elastic deformation [Davies and Balachandran (2000)]. Self-excited oscillation grows quickly and causes rough surface finishing, material chipping, or even machining tool damage. Therefore, thin material machining is always undesirable machining operation.

Since thin material machining is hard to perform, punching, laser cutting, water jet cutting, and Electrical Discharge Machining (EDM) etc. are usually employed to avoid machining on thin materials. In some special situations where thin material machining cannot be avoided, special fixtures are designed to hold the thin workpiece stable to avoid excessive vibration and material fracture problems. Cameron (1989) presented a holder design for

machining a thin walled cylinder. Obara et al. (2003) used low melting point alloys, whose melting point is below 100°C, to support and machine three-dimensional parts.

In recent years, thin material machining application is more and more required to produce high strength, light weight thin web structures in the aerospace industry [Bravo et al. (2005)]. Machining on thin material usually results in chatter, which may cause poor surface finish and dimension accuracy, chipping of the cutter teeth, or damage of machining tool and workpiece.

Self-excited oscillation between the workpiece and cutter is a common phenomenon in thin material machining. Tobias (1965) and Tlusty (1967) studied the basics of chatter vibrations from the aspect of regeneration of chip thickness. Their stability theories were based on orthogonal cutting where chip thickness, direction of cutting force and structural dynamics were constant [Budak and Altintas (1995)]. Extensive research efforts in the 60s and 70s were directed at understanding and modeling the dynamic machining process [Merrit (1965) Opitz et al. (1970) Tlusty et al. (1986)]. In recent years, several more models have been developed to explain chatter vibration under complicated machining situations.

Erhan and Yusuf (1995) developed a multi degree-of-freedom structure formulation to analytically predict chatter stability in milling operations. One of the benefits of the analytical prediction model was to determine chatter stability before cutting. Davies and Balachandran (2000) built a mechanics-based model with impact nonlinearities to explain the dynamic interactions between a tool and the workpiece. This model was targeted at the thin wall machining problem in high speed machining applications. Two dimensional (2D) and three dimensional (3D) chatter stability models in milling were proposed by Altintas (2000, 2001) to explain the source of chatter vibration and wave surfaces. A finite element analysis was adopted by He et al. (2003) to predict the machining deformation of thin-wall components, and an NC

compensation strategy was also studied. Lacerda and Lima (2004) proposed a cutting force and chatter vibration prediction model. The time-varying directional dynamic milling forces coefficients were expanded in a Fourier series and integrated into the width of the cut, which was bound by the entry and exit angles. Experimental tests were employed to evaluate the cutting force in the contact zone between the cutting tool and workpiece. Bravo et al. (2005) presented a method for obtaining either the instability or stability lobes. This method used a three dimensional lobe diagram based on the relative movement of machine system and workpiece system. This model required that the machine structure and the machined workpiece had similar dynamic behaviors.

The thin material machining is a critical problem that needs to be considered in the RPM process, since it can cause catastrophic fracture failure in the middle of an automated process. The machining operation in the RPM process is called a thick slab layer-based machining. As shown in Figure 6.2, both single block machining and thick slab layer based machining have aspects of thin material machining. However, the thin material machining only occurs when machining is performed on the bottom of the workpiece in single block machining; and thin material machining occurs at the bottom of each layer in thick slab layer based machining.

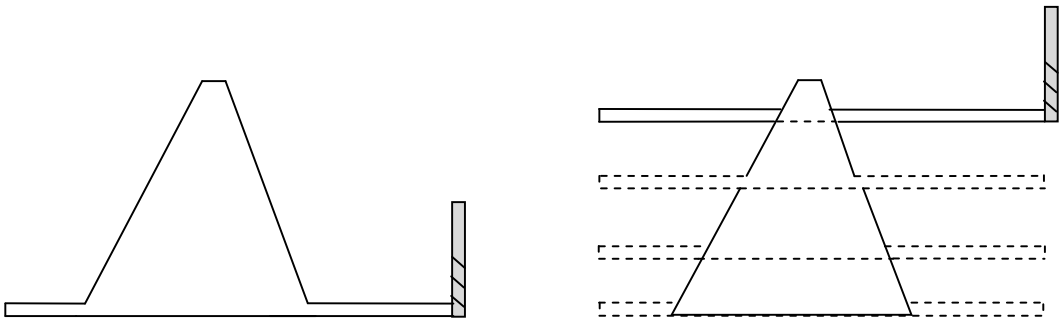

a. Thin material machining in single block machining

b. Thin material machining in thick slab layer based machining

Figure 6.2 Thin material machining problem in single block machining and thick slab layer based machining

In previous research, the cutting plane of thin material machining is usually parallel to the machining tool axis. This means the machining is mainly performed by flank of the milling cutter, which is also called thin wall machining. However, the machining plane in the RPM process is perpendicular to the machining tool axis; therefore, cutting forces on the side of the milling cutter is focused on a certain small area. This paper specifically targets the thin material machining problem of the proposed RPM process.

6.1.2 Layer Thickness & Tool Size Interaction

The layer thickness decision and tool size selection problems have been evaluated previously by authors [Luo and Frank (2009)]. However, these two problems are not mutually exclusive; their solutions are dependent on the cutting force variable. A solution to the layer thickness and tool size interaction problem can further reduce the machining times of the RPM process.

One restriction for the layer thickness decision is the material slab thickness, which must be greater than or equal to the layer thickness. However, the restriction can be resolved by combining multiple slabs to acquire a much thicker material slab with no theoretical limit in material slab thickness. In that case, layer thickness is only dependent on the cutting tool length. Of course, the tool length is limited by deflection problems under cutting forces. Cutting tool deflection has been and is still a focus of much research. Deflection calculation is used to predict the machining surface error and there exist two popular approaches to calculate cutter deflection and machining surface error; the cantilever beam model and an FEM approach.

In cantilever beam models, there are two critical parameters; cutting force calculation and equivalent cutter diameter determination. A milling cutter usually has two basic components of the *shank* and *flute*, where the cutter shank is a simple cylinder whose bending deflection

calculation can be easily acquired. However, the geometry of the cutter flute section is quite complex and not easy to be model. Kops and Vo (1990) proposed an equivalent diameter method to simulate the deflection behavior of the cutter flute with a standard cylinder model. This equivalent diameter method greatly simplified the cutter deflection calculation. The authors proposed an FEM method to evaluate the efficiency of the equivalent diameter model. This equivalent diameter model was adopted by Depince and Hascoet (2006). In addition, Kim et al. (2002) applied a two-step cylindrical cantilever beam model, based on the equivalent diameter model, to calculate the ball end milling deflection and form error. A similar two-step cylindrical cantilever beam model was also applied by Ryu et al. in 2003 and the cylindrical cantilever beam model was also applied by Rao et al. (2006) to study tool deflection during curved geometry milling, in which the cutting force is changing with the geometrical curvature.

Iwabe et al. (2004) applied the FEM model to predict the surface generation mechanism of a ball end mill based on deflection, where cutting force was acquired from cutting tests. Jalili Saffar et al. (2008) adopted an FEM method to simulate the end milling process and to predict the cutting tool deflection. Again cutter deflection prediction from their FEM method was validated through machining experiments. Other methods for cutter deflection and surface error prediction, such as neural networks [Ratchev (2002) Raksiri (2004)] and measuring previously machined components [Liu and Venuvinod (1999) Lo and Hsiao (1998)] have also been used. Different neural networks models are needed for different conditions and workpiece-tool pairs; therefore, the application of this method is time consuming. On the other hand, empirical data generation makes the latter method a poor choice for determining the total deflection.

6.1.3 Cutting Force Models

A cutting force model is critical for machining process planning; it is also a key component in analyzing thin material machining problems and layer thickness & tool size interaction problem. The cutting force problem is of course very old, with the first historic studies of Taylor at the turn of the last century [Taylor(1907)] After which, Merchant (1944), Zorev (1966), Trent (1977) et al. followed with proposed cutting force models. Some early researchers simulated cutting force models by fitting curves from experimental data with different machining parameter sets (spindle speed, feed, cutting depth etc.) [Boston et al. (1937) Armarego and Brown (1969)]. This experimental approach is extremely time consuming and costly; furthermore, cutting forces from these models are average cutting forces, not instantaneous. Two types of instantaneous cutting force models that have been studied include mechanistic models and mechanics models. In mechanistic models, the cutting force is proportional to the average chip load; and a set of cutting force coefficients in the model is unique for a workpiece-tool pair. Hence, a group of cutting experiments is required to calculate the cutting force coefficients for each workpiece-tool pair. These cutting force coefficients can then be used to calculate cutting forces under different machining parameters for the same workpiece-tool combination. This approach was presented by Sabberwal (1961), and adopted by later researchers such as Tlusty (1975), Sutherland (1986) and Altintas (1991).

For mechanics models, the milling process is simulated by orthogonal and oblique cutting, and cutting force coefficients can be calculated from existing orthogonal and oblique cutting force data in a data base; cutting experiments are not required. This is beneficial since these models can be easily integrated into current CAD/CAM software systems; however, the approach also brings a certain loss of the precision. Other mechanics models have been studied,

such as Armarego (1985), Budak (1996), et al. The average rigid force model is one of the more popular basic models [Wang (1988)], which is based on the relationship between Material Remove Rate (MRR) and average power consumption [Smith and Tlusty (1988)]. However, the average rigid force model can only acquire average cutting force which is not accurate in many cases. In the instantaneous rigid force model, the cutting force is proportional to the instantaneous contact between workpiece and end milling cutter [Devor and Kline (1980)], rather than the MRR. This model neglects the influence of cutting tool deformation by assuming the cutting tool is rigid. Based on the instantaneous rigid force model, Tlusty (1985), Hann (1983) and Kline (1982) calculated static tool deflection and surface error. Sutherland et al. (1986) improved the instantaneous rigid force model by considering the factor of cutter deformation in cutting force calculations. A further improvement of this model was made by including the influence of the wavy surface left by the passage of previous teeth to form the regenerative force and dynamic deflection model [Tlusty (1987)].

6.1.4 Summary

Two key problems in the proposed process of this paper; the thin material machining problem, and the layer thickness & tool size interaction problem, where both, need to be analyzed with respect to cutting forces. An understanding of the thin material machining failure mode helps to eliminate or reduce fracture failure in the process, therefore machining quality could be improved. A solution to layer thickness and tool size interaction is a way of enhancing the efficiency of the RPM process. The objectives of this paper are; 1) to set up a cantilever beam mechanics model to analyze thin material machining failure to calculate an appropriate minimum layer thickness, and 2) to develop a solution for the layer thickness & tool size

interaction problem to meet the specific implementation requirements of this hybrid rapid pattern making process.

6.2 A Cutting Force Approach for the RPM Process

In this paper, the purpose of the cutting force calculation is to calculate the thin material machining failure condition and the layer thickness & tool size interaction problem. Since we wish to avoid excessive experiments the edge force model proposed by Altintas (2000), a mechanics approach, is employed.

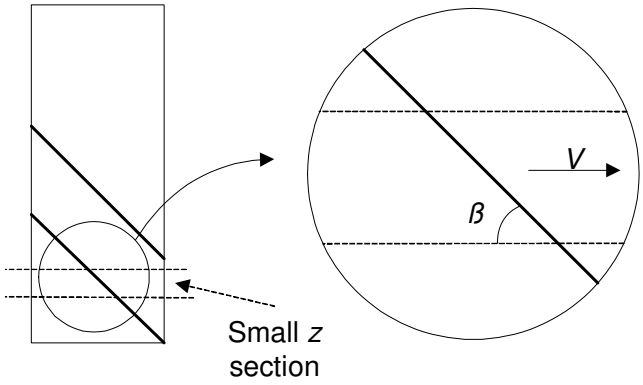

Figure 6.3 Small z section in helix end milling

As shown in Figure 6.3, in a helix milling operation, for a small section in the z direction on one flute of a milling cutter, the cutting operation can be approximated by classic oblique cutting, since the cutting angle changes due to the helix angle on one flute of the cutter can be neglected for a small z section.

In the edge cutting force model, there are three fundamental cutting force elements acting on the oblique cutting edge, which are the elemental tangential (dF_t), radial (dF_r) and axial (dF_a) cutting forces. On the cutter flute j, the elemental cutting forces are:

$$\begin{cases} dF_{t,j} = dF_{tc} + dF_{te} = K_{tc}\, h(\Phi_j)\, d_z + K_{te}\, d_z \\ dF_{r,j} = dF_{rc} + dF_{re} = K_{rc} h(\Phi_j)\, d_z + K_{re}\, d_z \\ dF_{a,j} = dF_{ac} + dF_{ae} = K_{ac} h(\Phi_j)\, d_z + K_{ae}\, d_z \end{cases} \quad (1)$$

Each elemental cutting force is composed of 2 components: a cutting force component and an edge force component. The cutting force component is caused by shearing on the rake face; and the edge force component is due to the friction between machined surfaces and the

flank face. The term $h(\Phi_j)$ is the uncut area of the chip and K_{tc}, K_{rc}, K_{ac}, K_{te}, K_{re} and K_{ae} are cutting force coefficients that are dependent on the material and cutting tool edge geometry. The elemental cutting forces can be resolved into the feed (x), normal (y), and axial (z) directions:

$$\begin{cases} dF_{x,j} = -dF_{t,j}\, cos\Phi_j(z) - dF_{r,j}\, sin\Phi_j(z) \\ dF_{y,j} = +dF_{t,j}\, sin\Phi_j(z) - dF_{r,j}\, cos\Phi_j(z) \\ dF_{z,j} = dF_{a,j} \end{cases} \tag{2}$$

Where $\Phi_j(z)$ is angular immersion of flute j at vertical height z and cutting forces along each cutting edge j can be acquired by integrating the differential cutting forces. All of these cutting forces on each cutting edge can be summed to obtain the total cutting forces applied on the cutter in x, y and z directions.

$$\begin{cases} Fx(\phi_j(z)) = \int_{z_j,1}^{z_j,2} dFx(\phi_j(z))dz \\ Fy(\phi_j(z)) = \int_{z_j,1}^{z_j,2} dFy(\phi_j(z))dz \\ Fz(\phi_j(z)) = \int_{z_j,1}^{z_j,2} dFz(\phi_j(z))dz \end{cases} \tag{3}$$

$$\begin{cases} F_x(\phi) = \sum_{j=0}^{N-1} F_{xj}(\phi) \\ F_y(\phi) = \sum_{j=0}^{N-1} F_{yj}(\phi) \\ F_z(\phi) = \sum_{j=0}^{N-1} F_{zj}(\phi) \end{cases} \quad \text{where } N \text{ is the flute number} \tag{4}$$

The cutting force coefficients can be acquired from the transformation matrix as follows [Engin (2000)].

$$\begin{bmatrix} K_{r,oblique} \\ K_{t,oblique} \\ K_{a,oblique} \end{bmatrix} = \begin{bmatrix} \sin k(z) & \cos \beta(z) & \cos k(z) \\ \sin k(z) & \cos \beta(z) & \cos k(z) \\ \cos k(z) & \sin \beta(z) & \sin k(z) \end{bmatrix} \begin{bmatrix} K_{r,orthogonal} \\ K_{t,orthogonal} \\ K_{a,orthogoanl} \end{bmatrix}$$

Details of this mechanics and dynamics of milling force model with complex cutters can be found in previous publications [Altintas (2000) Engin (2001)].

Based on this cutting force model, a cutting force calculation process for the RPM system is designed as follows.

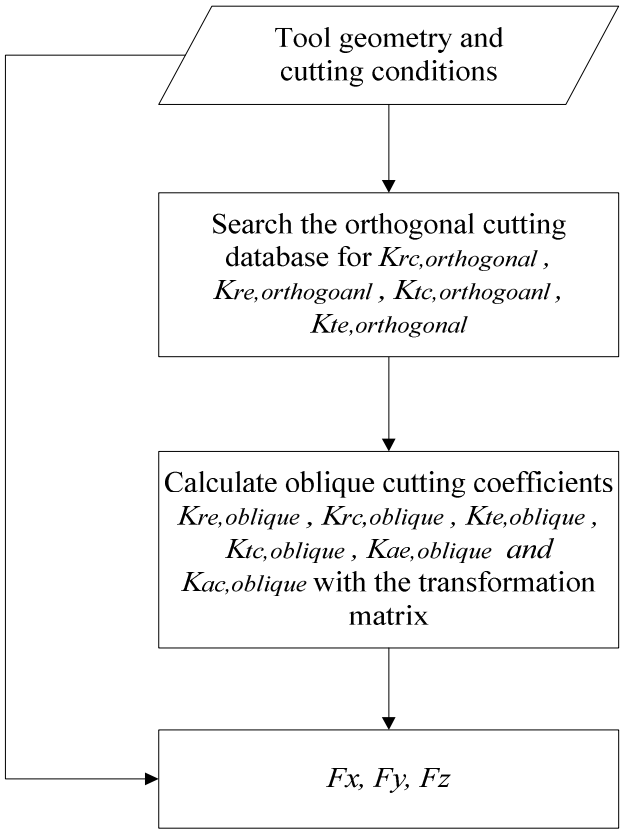

Figure 6.4 Cutting force calculation for the RPM process

As shown in Figure 6.4, some parameters about the cutting tool geometry and cutting condition are extracted from the helix milling operation first. Then the orthogonal cutting force coefficients are found in the database according to cutting tool geometry and cutting condition

parameters. Oblique cutting force coefficients can be calculated from orthogonal cutting force coefficients by the transformation matrix. Finally, the helix milling forces are calculated from the cutting force model.

6.3 Minimum layer thickness in the RPM process

For this work, the thin material machining condition is represented by a cantilever beam model. In this section, a machining structure and minimum layer thickness model for the RPM process are presented.

6.3.1 Machining Structure

In the RPM process, a new material slab which is equal to or larger than the objective part geometry is deposited on the top of finished layers, and then machined. As shown in Figure 6.5, when the milling cutter moves from the edge of material slab to the center, the worst machining condition happens when the cutter is cutting on the farthest edge of the material slab (which has the largest distance to the edge of finished part geometries).

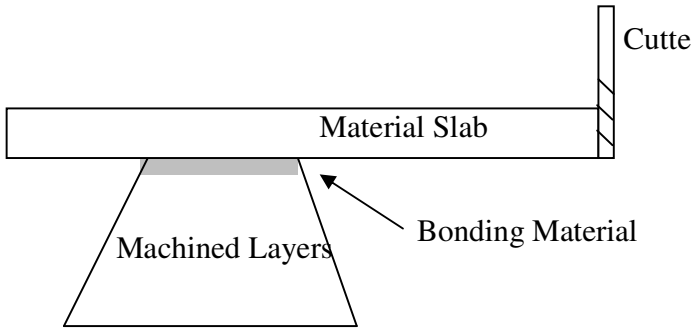

Figure 6.5 Machining condition in the RPM process

During machining, some portions of the material slab overhang of the finished part geometries; thus the basic cantilevered beam model, as illustrated in Figure 6.6. The horizontal section of the cantilever beam with length "*b*" represents the overhanging material slab cantilevered beam. The vertical beam with length "*a*" is a rigid beam from the material deposition *z* position to the cutting force *z* position. This *z* height difference between the material

deposition plane and cutting force position causes a bending torque generated by cutting force *Fy* on the workpiece. The deposition plane, as referred to in this work, is the plane representing the top of the previously machined layer. This is the contact patch onto which the subsequent slab is bonded. In this work, we assume the previously finished parts of wood pattern are rigid bodies, and that deflection is negligible compared to next overhanging layer being machined. Three elemental cutting forces are applied to the end of the cantilevered beam where the cutting process occurs.

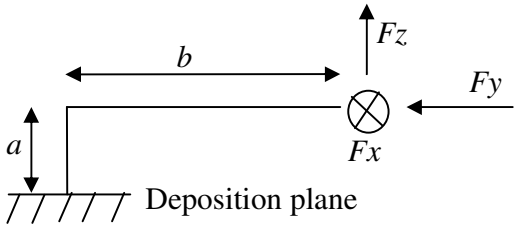

Figure 6.6 Machining structure model in the RPM process

In the RPM process, the router spindle structure is assumed to be much stronger than the workpiece cantilevered beam structure. In addition, the machining tool is usually short (usually less than 3 inches); therefore, the machining tool assembly is assumed to be a rigid structure also. Both forms of addition deflection are ignored compared to the rigidity, or lack thereof, of the thin web materials during layer based cutting. .

6.3.2 Minimum Layer Thickness Calculations For The RPM Process

In previous work by the authors, a “minimum layer thickness” parameter was adopted to ensure good machining quality. These minimum layer thicknesses for different materials were acquired in a more ad-hoc manner through machining experiments in the lab. In this section, the “minimum layer thickness” is treated more formally and calculated from cutting force calculations.

Materials adopted to date for the RPM process are primarily woods, such as Medium Density Fiberboard (MDF), but it could also be applicable for plastics, aluminum etc. Although MDF wood is an excellent choice for pattern making and machines easily, it is quite fragile when

thin. In the machining structure model illustrated in Figure 6.6, the weakest position is on the deposition position, or finished part body right under the deposition position, as most glue bonds are stronger than the MDF slab material. This is because when the cutter starts to machine on the bottom of a layer, the cantilever beam structure has a large cross section area in the beginning, which places a large load on the contact surfaces. Therefore, the failure position of MDF is at the deposition plane, or interface to the layer below, rather than on the overhanging cantilever beam.

As shown in Figure 6.6, force *Fx*, *Fy* and *Fz* are applied at the machining position of the workpiece. *Fz* is assumed too small to cause tensile failure. In this model, we assume *Fx,* which generates the bending torque on the deposition plane (weakest position), and *Fy* and *Fz* cause counter clockwise bending torques on the deposition plane. In order to ensure safe machining, the stress condition as follows should be met.

$$\sigma_{max\text{-}x} = \frac{M_{\max}}{W_{z1}} = \frac{Fx * b}{W_{z1}} \le [\sigma] \tag{5}$$

$$\sigma_{max\text{-}yz} = \frac{M_{\max}}{W_{z2}} = \frac{Fz * b + Fy * a}{W_{z2}} \le [\sigma] \tag{6}$$

W_{z1} and W_{z2} are the section modulus in bending. The cross section of the beam could be represented by a rectangle with a length of the *cut depth d*, and a width of the *cutter radius R*:

$$W_{z1} = \frac{d * R^2}{6} \tag{7}$$

$$W_{z2} = \frac{R * d^2}{6} \tag{8}$$

In this manner, the minimum layer thickness can be calculated by:

$$minimum\left(\frac{Fx * b * 6}{R^2 * [\sigma]}, \sqrt{\frac{(Fz * b + Fy * a) * 6}{R * [\sigma]}}\right) \tag{9}$$

6.4 Layer Thickness & Tool Size Interaction

This section presents the interaction between layer thickness decision and tool size selection. Since the layer thickness is restricted by cutter length, there is an obvious interaction between the layer thickness decision problem and the tool size selection problem. In theory, the layer thickness is unlimited, so long as a same length cutter can be found. However, cutter lengths are of course limited; cutting forces cause deflection on both the cutter and workpiece. As shown in Figure 6.5, when the workpiece is tall and thin or the tool shank is long, deflections of them under cutting forces could be large. When the total deflection of workpiece and cutter is larger than the dimension tolerance, machined geometries will not be acceptable. In the proposed RPM process, the deflection on workpiece is assumed small, therefore only cutter deflection is considered in this study. Although this appears to be a bold assumption, wood patterns for metal casting using chemically bonded sand do not generally contain very thin or otherwise fragile geometries. In this section, cutter deflection under cutting forces during machining is studied first, and then a model for layer thickness & tool size interaction problem is presented.

6.4.1 Cutter Deflection During Machining

From the literature, cutter deflection during machining has been given much attention, where two main approaches have emerged; the cylindrical cantilever beam model [Kops and Vo (1990) Kim et al. (2002) Rao et al. (2006)] and the FEM method [Iwabe et al. (2004) Jalili Saffar et al. (2008)]. The cylindrical cantilever beam model is shown to be simple to calculate, and the results are shown to be precise; therefore, it is employed to calculate the cutter deflection in this study.

The two-step cylindrical cantilever beam model proposed by Kim et al. (2003) is one such model that represents the cutter deflection condition well. In the two-step cylindrical cantilever beam model, a cutter is divided into 2 sections: shank and flute. The shank section has a full cylindrical structure, whose diameter is equal to the milling cutter diameter, while the cutter flute section is obviously not a full cylinder. In previous research, a cylinder with equivalent diameter is used to approximate the flute structure. The equivalent cylinder diameter was studied both experimentally with strain gauges and on a finite element model by Kops and Vo (1990), and it was concluded to be approximately 80% of the cutter diameter.

In the RPM process, in order to make the tool length as small as possible, the length of cutter shank beyond the collet or tool holder should be near zero; because only the cutter flute section performs the cutting function, and tools do not need to "reach" into deep cavities in the RPM process. That is, in the RPM process, the hybrid additive/subtractive methods only requires the cutter to plunge into and cut one layer thickness, not reach into the actual cavities of the pattern. Geometry on any depth within the pattern, regardless of total pattern height, will only ever be as much as the layer depth. As such, cutter deflection can be simplified by the model shown in Figure 6.7.

$$\delta_t = \frac{FL^3}{3EJ} \qquad (10)$$

Where J is moment of inertia of cutter flute:

$J = \frac{\pi d_{=}^{\ 4}}{64}$ ($d_{=}$ is the equivalent diameter)

.

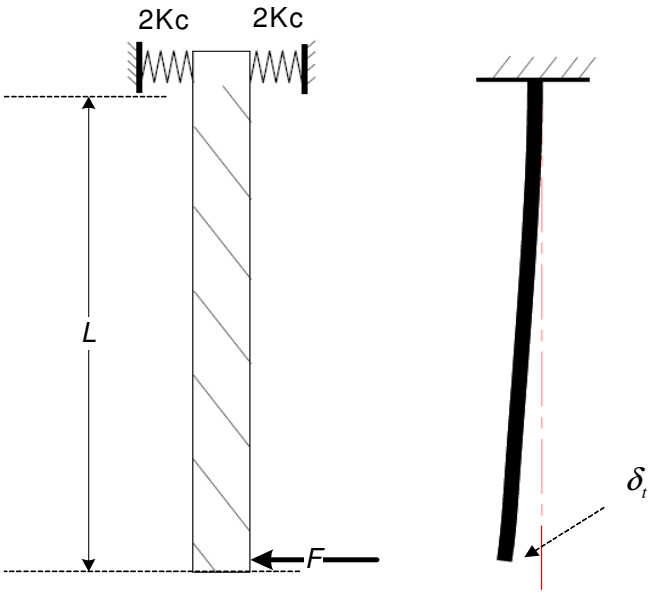

Figure 6.7 Cutter deflection in the RPM process

6.4.2 Combined Layer Thickness & Tool Size Model

According to equation (10), when the tool diameter and surface tolerance (allowable machining error) are fixed, allowable tool length could be calculated from equation 11:

$$L = \sqrt[3]{\frac{\delta_t * 3 * E * J}{F}} \qquad (11)$$

The cutting force F can be determined using the method of Section 6.2.

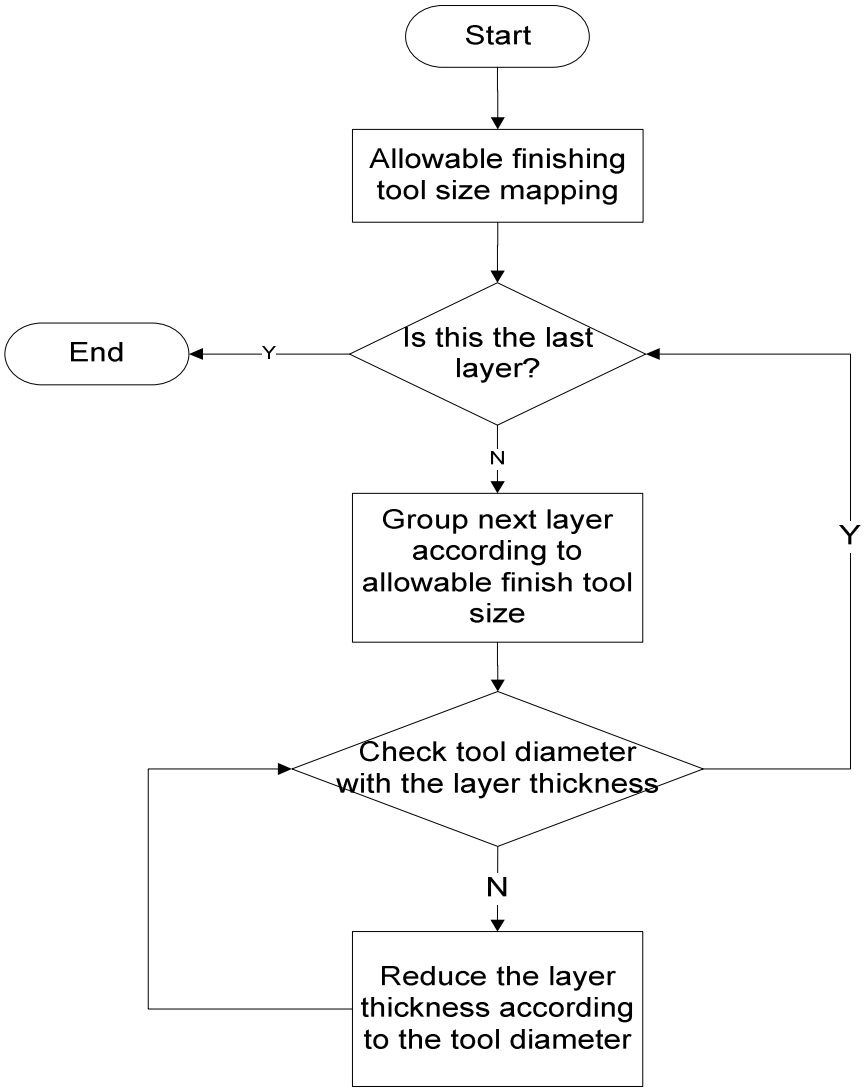

Figure 6.8 Combined layer thickness & tool size model

A combined layer thickness & tool size model is therefore presented, according to the cutter deflection (Figure 6.8). First, the STL model of the pattern is sliced, and the allowable finishing tool size for each slice is calculated. Next, allowable finishing tool sizes for the entire pattern are grouped together, and mapped to an allowable finishing tool size-z height diagram. Second, continuous slices with the same or similar allowable finishing tool size are combined together to be a layer. The allowable tool size of the layer is checked against the layer thickness.

If the layer thickness is too thick for the finishing tool, the layer thickness will be reduced to the allowable length of the selected finishing tool. This second step repeats until the layer thickness decision and tool size selection for the whole part are finished.

6.5 Implementation

Experiments have been conducted in order to evaluate the minimum layer thickness model and the combined layer thickness & tool size model. The implementation includes three sections: 1) cutting forces for a machining condition are calculated with the selected cutting force model; 2) the minimum layer thickness for MDF in the RPM process is calculated and the machining test is performed to evaluate the model and finally, 3) layer thicknesses and tool sizes for a sample part is calculated with the combined layer thickness & tool size model, and the pattern is machined to evaluate the model.

6.5.1 Cutting Force Calculation

A two flute helical flat end milling cutter is used in rough machining step the RPM process. Cutting forces for this cutter are calculated with the cutting force model found in section 6.2. Relevant cutting parameters are as follows:

Rake Angle:	15°
Helix Angle:	30°
Spindle speed:	4000 rpm
a (cutting depth):	3mm
c (Feed per tooth):	0.635 mm/tooth/rev

The orthogonal cutting data in the research of Dippon (2000) was employed. This cutting force model has been illustrated by Engin et al. (2000), and the model has been applied in the

commercial MILLPRO program [MillPro (1998)]. We employ the same model in this section and use the resulting data in successive sections. According to machining condition parameters listed above, orthogonal cutting force coefficients are:

K_{te} = 1.1268 N/mm K_{tc} = 8.8575 N/mm^2

K_{fe} = 2.4948 N/mm K_{fc} = 0.6188 N/mm^2

Calculated from the transformation matrix, oblique cutting force coefficients are:

K_{te} = 3.4706 N/mm K_{tc} = 8.2894 N/mm^2

K_{fe} = 3.4706 N/mm K_{fc} = 8.2894 N/mm^2

K_{ae} = 0.5634 N/mm K_{ac} = 4.4288 N/mm^2

Calculated from the cutting force model, instantaneous cutting forces in a 360 degree cycle are shown in Figure 6.9.

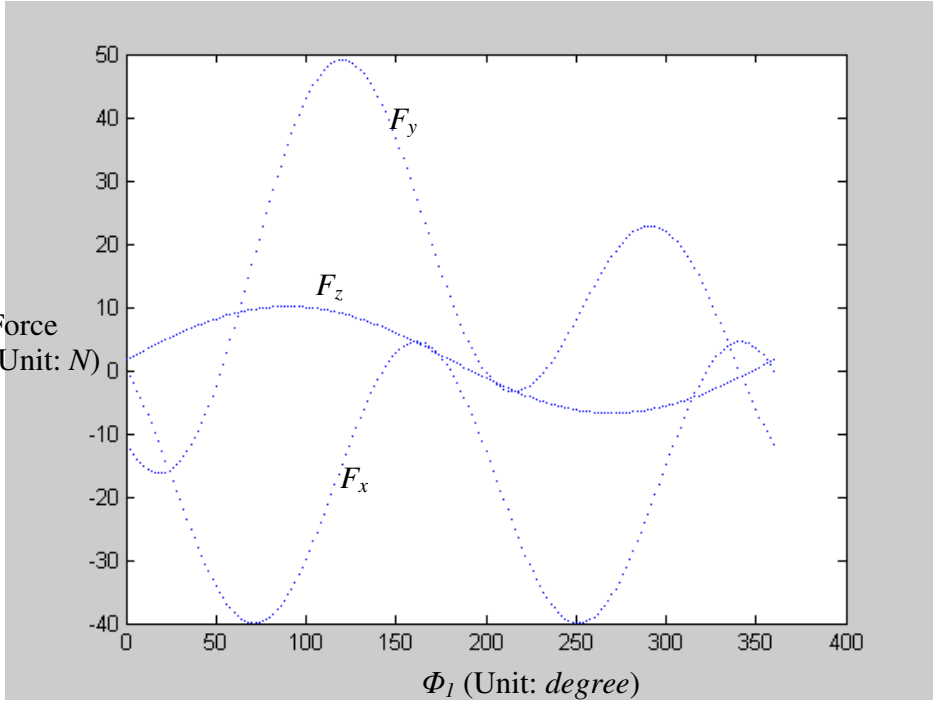

Figure 6.9 Dynamic cutting forces in a 360 degree cycle

In this 360 degree cutting force cycle, peak cutting forces are:

$F_{x\text{-}max}$ = 40.00 N

$F_{y\text{-}max}$ = 49.07 N

$F_{z\text{-}max}$ = 10.13 N

6.5.2 Minimum Layer Thickness Experiment

In minimum layer thickness experiment, the same cutters as that in the cutting force experiment in 6.5.1 and MDF raw material are used. The method to evaluate the minimum layer thickness model is to simulate the minimum layer thickness failure condition and then conduct machining experiments to determine if predicted failure occurs. The test condition is as follows:

MDF rupture strength: 27 MPa [MDF Standard (1999)]

Cutting depth: d = 0.12 inch

MDF specimen length: b = 2 inch

MDF specimen width: R = 0.50 inch

The cutting height: a = 0.06 inch

The experiment setting is shown in Figure 6.10. The specimen is deposited on a base. The length of the overhang portion on the specimen is b=2 inches. The failure of the specimen in this experiment is defined as the fracture of the specimen.

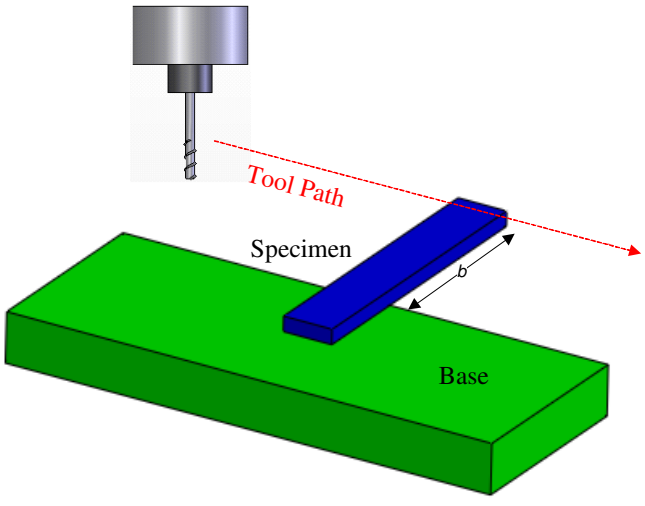

Figure 6.10 Minimum layer thickness machining experiment setting

According to the minimum layer thickness model, the failure layer

thickness is 0.124 inch. Therefore, 2 groups of cutting experiments with two different layer thicknesses, which are 0.120 inch and 0.130 inch, are tested. For each group, 6 specimens are tested. The result is shown in Table 6.1. The experiment result shows that all cutting on 0.12 inch thick layers failed, which matches the calculation from the minimum layer thickness model. When the layer thickness is increased, it should not fail during machining. However, one failure did occur in this group; owing most likely to the inhomogeneous and inconsistent qualities of MDF material.

Table 6.1 Thin material machining experiment result (Unit: inch)

NO.	Layer Thickness	Fail (F) / Not Fail (NF)		Layer Thickness	Fail (F) / Not Fail (NF)
1	0.12	F		0.13	NF
2		F			NF
3		F			NF
4		F			NF
5		F			F
6		F			NF

According to the experiment results, machining on material which is thicker than 0.124 inch will not have fracture failure under the designed machining conditions. Then, the related machining parameters could be adjusted to avoid machining on materials thinner than 0.124 inch to improve the machining quality.

6.5.3 Combined Layer Thickness & Tool Size Model Experiment

A sample pattern shown in Figure 6.11 is used to test the combined layer thickness & tool size model.

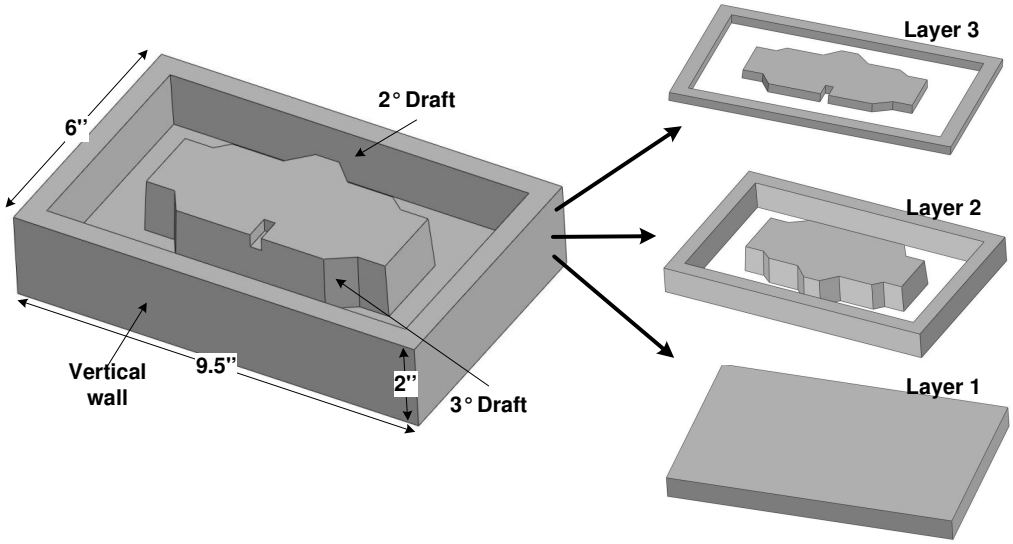

Figure 6.11 Sample pattern design

Diameters of available Tools in the tool library are from 0.125 to 1 inch (Table 6.2).

Table 6.2 Tool diameters in tool library (Unit: inch)

Tool NO.	1	2	3	4	5
Diameter	0.125	0.25	0.5	0.75	1.0

Finishing tool size mapping for the pattern is shown in Table 6.3. The allowable finishing tool sizes are combined into 3 sections. From the bottom to 0.75 inch height, the 1 inch tool is the selected finishing tool size according to the accessibility ratio. From 0.75 to 1.7 inch height, the 0.25 inch tool is the maximum finishing tool size. The section above 1.70 inch can accommodate a 0.125 inch finishing tool, and meet the accessibility ratio [Luo and Frank (2009)].

Table 6.3 Allowable finishing tool size mapping (Unit: inch)

Z (inch)	Maximum Tool Size
0~0.75	1 .00
0.75 ~ 1.70	0.25
1.70 ~ 2.00	0.125

E = 200 GPa

$\delta_t = 0.002$

According to the finishing tool size mapping, the first layer is from 0 to 0.75. Because cutting forces for the MDF material are considerably small, for 1 inch diameter tool, the allowable tool length (layer thickness) within δ_t deflection is 8.0 inch. Therefore, the first layer is 0 to 0.75 inch. For the second layer, the allowable tool length for the 0.25 inch diameter tool with δ_t deflection is 3.4 inch, therefore, the layer covers 0.75 to 1.70 of z height and is within the allowed machining error. The allowable tool length for 0.125 inch diameter tool in the RPM process is 0.57 inch, then the last layer is from 1.70 z height to the top of the part.

A sample pattern was machined using the previous tool size selection strategy [Luo and Frank (2009)] and machining plan from the combined layer thickness & tool size model. Picture 6.12 shows these machined 3-layer patterns.

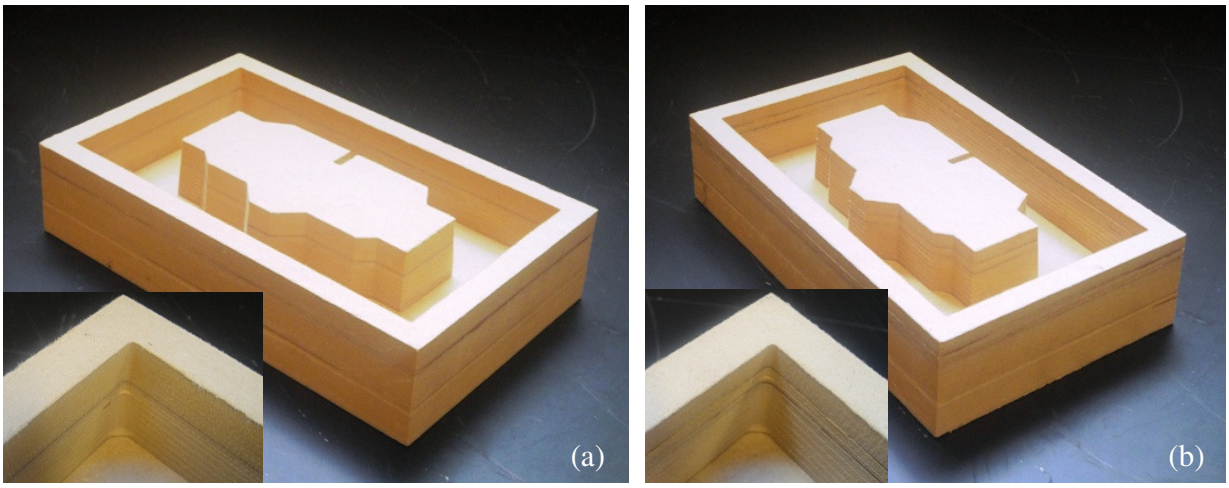

Figure 6.12 Machined sample patterns. (a) Tool size selection strategy; (b) Layer thickness & tool size interaction strategy

The pattern machined with the machining plan from combined layer thickness & tool size model has the same quality as that machined from the tool size selection strategy. However, the combined layer thickness & tool size method required 10 minutes less to machine. This sample

pattern has only 3 layers, therefore, the machining time and potential material saving is not outstanding. However, it illustrates the potential improvement in machining time when determining layer thickness and tool size by considering their interaction.

6.6 Conclusion

Fracture is a major problem that affects machining quality in the RPM process, where it usually occurs when machining on thin materials. Analyzing from the aspect of cutting force, bending failure is the major reason for facture of thin materials during machining. Therefore, a minimum layer thickness model is set up to calculate the minimum safe material thickness that will avoid fracture failure in the RPM process. A machining experiment showed the correctness of this model and this solution to fracture failure can improve the machining quality of the RPM process.

Material slab thickness is not a constraint for the layer thickness decision when multiple material slabs can be attached together to form a thick material slab. When the material slab thickness restriction is resolved, layer thickness in the RPM process increases. However, deflection of the cutter must be considered to ensure good machining quality when the layer thickness increases. Therefore, a combined layer thickness and tool size interaction model was presented to address this problem. The cutter deflection model is studied first, then a combined layer thickness and tool size interaction model which decides layer thicknesses and tool sizes together by making sure acceptable cutter deflection is presented. The implementation example shows the combined layer thickness and tool size model requires less machining time compared to the method of an independent layer thickness decision and tool size selection method.

Reference

Altintas, Y. Spence, A. (1991). End milling force algorithm for CAD systems. *Annals of the CIRP*, 40(1), 31-34.

Altintas, Y. (2000). *Manufacturing Automation: Metal Cutting Mechanics, Machine Tool Vibration and CNC Design*. New York: Cambridge University Press.

Altintas, Y. (2001). Analytical prediction of three dimensional chatter stability in milling. *JSME International Journal*, 44(3), 717-723.

Armarego, E.J.A. Brown, R.H. (1969). *The Machining of Metals*. Prentice-Hall Inc.

Armarego, E. J. A. Witfield, R. C. (1985). Computer based modeling of popular machining operations for force and power prediction. *Annals of the CIRP*, 34(1), 65-69.

Boston, O. W. Gilbert, W. W. Kaiser, K. B. (1937). Power and forces in milling SAD 3150 with helical mills. *Transaction of the ASME*, 59(2), 545.

Bravo, U. Altuzarra, O. Lopez de Lacalle, L. N. Sanchez, J. A. Campa, F.J. (2005). Stability limits of milling considering the flexibility of the workpiece and the machine. *International Journal of Machine Tools & Manufacture*, 45(15), 1669-1680.

Budak, E. Altintas, Y.(1995). Analytical prediction of chatter stability in milling Part I : general formulation. *Proceedings of ASME Dynamic Systems and Control Division*, 57(1), 545-556.

Budak, E. Altintas, Y. (1995). Analytical prediction of chatter stability in milling Part II : application of the general formulation to common milling systems. *Proceedings of ASME Dynamic Systems and Control Division*, 57(1), 557 -565.

Budak, E. Altintas, Y. Armarego, E.J.A (1996). Prediction of cutting force coefficients from orthogonal cutting data. *Transaction of the ASME*, 118(2), 216-224.

Cameron Jr. (1989). US Patent 4,811,962.

Davies, M. A. Balachandran, B. (2000). Impact dynamics in milling of thin-walled structures. *Nonlinear Dynamics*, 22(4), 375-392.

Depince, P. Hascoet, J. Y. (2006). Active integration of tool deflection effects in end miiling. Part I. Prediction of milled surfaces. *International Journal of Machine Tools & Manufacture*, 46(9), 937-944.

Devor, R. E. Kline, W. A. (1980). A mechanistic model for the force system in end milling. *Proceeding of NAMRC* 8^{th}, 297-303.

Dippon, J. Ren, H. Ben Amara, F. Altintas, Y. (2000). Orthogonal cutting mechanics of medium density fiberboards. *Forest Products Journal*, 50(7-8), 25-30.

Engin, S. Altinatas, Y. Amara, F. B. (2000). Mechanics of routing medium density fiberboard. *Composites and Manufactured Products*, 50(9), 65-69.

Engin, S. Altintas, Y. (2001). Mechanics and dynamics of general milling cutters: Part I: helical end mills. *Internatioanl Journal of Machine Tools and Manufacture*, 41(15), 2195-2212.

Hann, V. (1983). *Kinetic de Schaftrasens*. Ph.D dissertation, Aschen: Technischen Hochschule.

He, N. Wang, Z. G. Jiang, C. Y. Zhang, B. (2003). Finite element method analysis and control stratagem for machining deformation of thin-walled components. *Journal of Material Processing Technology*, 139(1-3), 332-336.

Iwabe, H. Natori, S. Masuda, M. Miyaquchi, T. (2004). Analysis of surface generation mechanism of ball end mill based on deflection by FEM. *JSME International Journal, Series C: Mechanical Systems, Machine Elements and Manufacturing*, 47(1), 8-13.

Jalili Saffar, R. Razfar, M. R. Zarei, O. Ghassemieh, E. (2008). Simulation of three-dimension cutting force and tool deflection in end milling operation based on finite element method. *Simulation Modeling Practice and Theory*, 16(10), 1677-1688.

Kim, G. M. Kim, B. H. Chu, C.N. (2002). Estimation of cutter deflection and form error in ball-end milling processes. *International Journal of Machine Tools & Manufacture*, 43(9), 917-924.

Kline, W.A. Devor, R. E. Shareef, I.A. (1982). The prediction of surface accuracy in end milling. *Transaction of the ASME Journal of Engineering for Industry*, 104, 272-278.

Koenigsberger, F. Tlusty, J. (1967). *Machine Tool Structure-Vol. 1: Stability Against Chatter*. Pergamon Press.

Kops, L. Vo, D. T. (1990). Determination of equivalent diameter of an end mill based on its compliance. *Annals of the CIRP*, 39(1), 93-96.

Lacerda, H. B. Lima, V. T.(2004). Evaluation of cutting forces and prediction of chatter vibrations in milling. *Journal of the Brazil Society of Mechanical Science & Engineering*, XXVI (1) , 74-81.

Liu, Z. Q Venuvinod, P. K. (1999). Error compensation in CNC turning solely from dimensional measurements of previously machined parts. *Annals of the CIRP*,48(1), 429-432.

Lo, C. C. Hsiao, C. Y. (1998). CNC machine tool interpolator with path compensation for repeated contour machining. *Computer Aided Design*, 30(1), 55-62.

Luo, X. M. Frank, M. C. (2009). A layer thickness algorithm for Additive/Subtractive Rapid Pattern Manufacturing. *Rapid Prototyping Journal, (*Accepted).

Luo, X. M. Frank, M. C. (2009). A tool size and machining parameter selection algorithm for Additive/Subtractive Rapid Pattern Manufacturing. *Rapid Prototyping Journal*, (To be submitted).

MDF Standard (1999). *China: GB/T 11718-1999*.

Merchant, M. E. (1944). Basic Mechanics of the metal cutting process. *Transaction of the ASME Journal of Applied Mechanics*, A11, 168-175.

Merrit, H. E. (1965). Theory of self-exited machine tool chatter. *Transaction of the ASME Journal of Engineering for Industry*, 87, 447-454.

MillPro webpage (1998). Machine tool testing software and machining problem diagnosis software. *http://www.maline.com*, March, 2009.

Obara, H. Watanabe, T. Osumi, T. Hatano, M. Ninomiya, E. (2003). A Method to Machine Three-Dimensional Thin Parts. *Journal of the Japan Society for Precision Engineering*, 69(3), 375-379.

Opitz, H. Bernardi, F. (1970). Investigation and calculation of the chatter behavior of lathe and milling machines. *Annals of the CIRP*, 18, 335~343.

Rao, V. S. Rao, P. V. M. (2006). Tool deflection compensation in peripheral milling of curved geometries. *International Journal of Machine Tools & Manufacture*, 46(15), 2036-2043.

Ryu, S. H. Lee, H. S. Chu, C. N. (2003). The form error prediction in side wall machining considering tool deflection. *International Journal of Machine Tools & Manufacture*, 43(14), 1405-1411.

Sabberwal, A. J. P. (1961). Chip Section and cutting force during the milling operation. *Annals of the CIRP*, 10, 197-203.

Salgado, M. A. Lopez de Lecalle, L. N. Lamikiz, A. Munoa, J. Sanchez, J. A. (2005). Evaluation of the stiffness chain on the deflection of end-mills under cutting forces. *International Journal of Machine Tools & Manufacture*, 45(6), 727-739.

Smith, S. Tlusty J. (1988). Modeling and simulation of the milling process. *Proceeding of Winter Annual Meeting of the American Society of Mechanical Engineer*, 17-26.

Sutherland, J. W. Devor, R. E. (1986). An improved method for cutting force and surface error prediction in flexible end milling systems. *Transaction of the ASME Journal of Engineering for Industry*, 108(4), 269-279.

Taylor, F. W.(1907). *On the Art of Cutting Metals*. Transaction of the ASME, 28.

Tlusty, J. MacNeil, P. (1975). Dynamics of cutting forces in end milling. *Annals of the CIRP*, 24(1), 21-25.

Tlusty, J. (1985). *Machine dynamics, handbook of high speed machining technology*. New York: Chapman and Hall.

Tlusty, J. (1986). Dynamics of high-speed milling. *Transaction of the ASME Journal of Engineering for Industry*, 108(2), 59-67.

Tlusty, J. Hernadez, I. Smith, S. Zamudio, c. (1987). High speed high power spindles with roller bearings. *Annals of the CIRP*, 36(1),267-272.

Tobias, S. A (1965). *Machine tool Vibration*. Blackie and Sons Ltd.

Trent, E. M.(1977). *Mteal cutting*. Butterworths.

Wang W. P. (1988). Solid modeling for optimizing metal removal of three-dimensional NC end milling. *Journal of Manufacturing Systems*, 7(1), 57-65.

Zorev, N. N. (1966). *Metal Cutting Mechanics*. Pregamon Press.

CHAPTER 7. CONCLUSIONS, LIMITATIONS AND FUTURE WORK

Sand casting continues to be one of the most important manufacturing processes, and sand casting patterns are the key tool in production. In this dissertation, an RPM process, which integrates traditional Rapid Manufacturing technology and CNC machining, is proposed; and three key problems in its automatic process planning are studied. Results and contributions of this dissertation research can be summarized as follows.

The RPM process is a thick slab layer based machining process, which creates parts by continuously and automatically attaching a thick slab of material, cutting it to a defined layer thickness, and then creating the part geometry with selected tools and parameters for the layer. The RPM process provides good sand casting pattern quality while reducing the time and skill required from the time of definitive pattern design in the computer to the creation of functional patterns.

Three key issues in this automated process planning problem are studied in detail in this dissertation.

1) The layer thickness has a significant effect on the surface quality of the final part, and more importantly could determine whether or not a catastrophic failure occurs during machining. A group of features related to thin material machining including local peaks and valleys, up and down-facing flats and shallow slope surface were defined. Methods for detecting heights of these features have also been studied. Given a set of feature heights to avoid, slab thickness, pattern material, glue and tool parameters, the system was able to determine the layer placement that best avoids these critical feature transitions. The system has been implemented with both software and

hardware and has been tested with a set of components that incorporate all feature types and issues. In addition, the system has been successfully used to create a variety of patterns, including a considerably large and complicated pattern for a steel prototype. A successful solution to the glue exposure, material fracturing and chipping problems ensured good final part quality in the proposed RPM system.

2) In the RPM process, each layer is deposited and machined separately with different geometry on it. Therefore, different cutting tools, machining parameters and machining operations can save processing time and improve quality. In the tool size and machining parameter selection research, 3 sub-problems were studied in detail. First, a machining strategy for the overall system was determined. Second, the Stepdown parameter for both a spherical end mill cutter and flat end mill cutter were studied in both rough and finish cutting operations. Third, a tool size selection algorithm based on both accessibility and machining efficiency was proposed for the selection of tools for rough and finish cutting. The input to the algorithm was a slice file from the CAD model. Based on the accessibility and machining efficiency analysis, an approach to select machining operations and tool sizes was developed. The set of tools included a rough cutting flat end mill cutter, a finish cutting spherical end mill cutter, and optional semi-rough cutting flat end mill cutter. The successful implementation of the tool size and machining parameter selection model improved rapid sand casting pattern quality and saved machining time.

3) CNC machining is the main material removal and geometry forming operation in the RPM process; therefore, understanding the effective cutting force is critical for process planning. In this work, popular cutting force models were reviewed, and ultimately the edge cutting force model, which is a mechanics cutting force model,

was adopted to calculate cutting force in the RPM process. This mechanics cutting force model analyzes helical milling with an oblique cutting operation, and obtains cutting force coefficients from orthogonal cutting force data. Based on the cutting force data, two key problems, the thin material machining problem and layer thickness & tool size interaction problem were analyzed. A cantilever beam model was used to represent the thin material machining condition, and a minimum layer thickness model was presented. When the raw material slab thickness restriction was resolved in the RPM process, the layer thickness decision problem and tool size selection problem interacted with each other in terms of cutter deflection. Based on cutter deflection data, a combined layer thickness & tool size model was presented to solve the layer thickness and tool size interaction problem. The study of the thin material machining failure mode based on mechanics analysis helps to reveal that bending causes fracture failure when machining thin materials during the RPM process. The development of a minimum layer thickness model reduces or eliminates fracture failure. The combined layer thickness and tool size model helps to optimize both layer thickness and tool size selection solutions, so that machining time savings can be achieved.

Large and complex sand casting patterns have been successfully created by the RPM system; however, there exist limitations to this approach and opportunities for future research.

In this work, the pattern geometry is decomposed into layers along the building orientation (z axis) of the system. For large sand casting patterns, this geometry decomposition solution may not be optimal, because the geometry on each single layer may also be complex. As a possible improvement, the idea of feature based machining

could be integrated into the system to decompose the target part geometry in terms of both features and layers.

Target parts of this system are sand casting patterns without overhang structure. Additional research could also be concentrated on creating overhang structures with this system. This improvement will make this system a general 3D printer for large parts, and not just patterns.

BIBLIOGRAPHY

Akula, S. Karunakaran, K. P. (2006). Hybrid adaptive layer manufacturing: An intelligent art of direct rapid tooling process. *Robotics and Computer Integrated Manufacturing*, 22(2), 113-123.

Altintas, Y. Spence, A. (1991). End milling force algorithm for CAD systems. *Annals of the CIRP*, 40(1), 31-34.

Altintas, Y. (2000). *Manufacturing Automation: Metal cutting Mechanics. Machine Tool Vibration and CNC Design*. New York: Cambridge University Press.

Altintas, Y. (2001). Analytical prediction of three dimensional chatter stability in Milling. *JSME International Journal*, 44(3), 717-723.

AFS (1970). Pattern Maker's Manual. *American Foundrymen's Society*.

Arezoo, B. Ridgway, K. Al-Ahmari, A. M. A. (2000). Selection of cutting tools and conditions of machining operations using an expert system. *Computers in Industry*, 42(1), 2000.

Armarego, E.J.A. Brown, R.H. (1969). *The machining of Metals*. Prentice-Hall.

Armarego, E. J. A. Witfield, R. C. (1985). Computer based modeling of popular machining operations for force and power prediction. *Annals of the CIRP*, 34(1), 65~69.

Arya, S. Cheng, S. W. Mount, D. M. (1998). Approximation algorithms for multiple tool milling. *Proceedings of the Fourteenth Annual Symposium on Computational Geometry* 297-306.

Bae, S. H. Ko, K. Kim, B. H. Choi, B. K. (2003). Automatic feedrate adjustment for pocket machining. *Computer-Aided Design*, 35(5), 495-500.

Bala, M. Chang, T. C. (1991). Automatic cutter selection and optimal cutter path generation for prismatic parts. *International Journal of Production Research*, 29(11), 2163-2176.

Balasubramanima, M. Joshi, Y. Engels, D. Sarma, S. Shaikh, Z. (2001). Tool selection in three-axis rough machining. *International Journal of Production Research*, 39(18), 4215-4238.

Bellini, A. Guceri, S. (2003). Mechanical characterization of parts fabricated using fused deposition modeling. *Rapid Prototyping Journal*, 9(4), 252-264.

Binnard, M. Cutkosky, M. (1998). Building block design for layered shape manufacturing. *Proceedings-1998 ASME Design Engineering Technical Conference*, 1-9.

Boston, O. W. Gilbert, W. W. Kaiser, K. B. (1937). Power and forces in milling SAD 3150 with helical mills. *Transaction of the ASME*, 59(2), 545.

Bravo, U. Altuzarra, O. Lopez de Lacalle, L. N. Sanchez, J. A. Campa, F.J. (2005). Stability limits of milling considering the flexibility of the workpiece and the machine. *International Journal of Machine Tools & Manufacture*, 45(15), 1669-1680.

Broek, J.J. Horváth, I. Smit, B. Lennings, A.F. Rusák, Z. Vergeest, J.S.M. (2002). Free-form thick layer object manufacturing technology for large-sized physical models. *Automation in Construction*, 11(3), 335-347.

Budak, E. Altintas, Y. (1995). Analytical prediction of chatter stability in milling Part I : General Formulation. *Proceedings of the ASME Dynamic Systems and Control Division*, 57(1), 545 -556.

Budak, E. Altintas, Y. (1995). Analytical Prediction of Chatter Stability in Milling Part II : Application of the General Formulation to common milling systems. *Proceedings of the ASME Dynamic Systems and Control Division*, 57(1), 557 -565.

Budak, E. Altintas, Y. Armarego, E.J.A (1996). Prediction of cutting force coefficients from orthogonal cutting data. *Transaction of the ASME*, 118(2), 216~224.

Cameron Jr. (1989). US Patent 4,811,962.

Cawley, J. D. Heuer, A. H. Newman, W. S. Mathewson, B. B. (1996). Computer-aided manufacturing of laminated engineering materials. *American Ceramic Society Bulletin*, 75(5), 75-79.

Chamberlain, M. A. Joneja, A. Chang, T. C. (1993). Protrusion features handling in design and manufacturing planning. *Computer Aided Design*, 25(1), 19-28.

Chang, Y.C. Pinilla, J. M. Kao, J.H. Dong, J. Ramaswami, K. Prinz, F.B. (1999). Automated layer decomposition for additive/subtractive solid freeform fabrication. *Proceedings of the Solid Freeform Fabrication Symposium*, 111-120.

Chazelle, B. (1983). The polygon containment problem. *Advances in Computing Research, Vol. I: Computational Geometry*, 1 - 33.

Chen, Y. H. Lee, Y. S. Fang, S. C. (1998). Optimal cutter selection and machine plane determination for process planning and NC machining of complex surfaces. *Journal of Machining Systems,* 17(5), 371-388.

Chen, Y.H. Song, Y. (2001). The development of a layer based machining system. *Computer Aided Design*, 33(4), 331-342.

Choi, S. H. Kwok, K. T. (2002). Hierarchical slice contours for layered-manufacturing. *Computers in Industry*, 48(3), 219-239.

Chua, M. S. Rahman, M. Wong, Y. S. Loh, H. T. (1993). Determination of optimal cutting conditions using design of experiments and optimization techniques. *International Journal of Machine Tools & Manufacture*, 33(2), 297-305.

Cormier, D. Taylor, J. B. (2001). A process for solvent welded rapid prototype tooling. *Robotics and Computer Integrated Manufacturing*, 17(1-2), 151-157.

Davies, M. A. Balachandran, B. (2000). Impact dynamics in milling of thin-walled structures. *Nonlinear Dynamics*, 22(4), 375-392.

Depince, P., Hascoet, J. Y. (2006). Active integration of tool deflection effects in end milling. Part I. Prediction of milled surfaces. *International Journal of machine tools & manufacture*, 46(9), 937-944.

Devor, R. E. Kline, W. A. (1980). A mechanistic model for the force system in end milling. *Proceeding of NAMRC* 8^{th}, 297-303.

Dippon, J. Ren, H. Ben Amara, F. Altintas, Y. (2000). Orthogonal cutting mechanics of medium density fiberboards. *Forest Products Journal*, 50(7-8), 25-30.

D'Souza, R. M. (2006). One setup level tool selection for 2.5-D pocket milling. *Robotics and Computer Integrated Manufacturing*, 22(3), 256-266.

Engin, S. Altinatas, Y. Amara, F. B. (2000). Mechanics of routing medium density fiberboard. *Composites and manufactured products*, 50(9), 65~69.

Engin, S. Altintas, Y. (2001). Mechanics and dynamics of general milling cutters: Part I: helical end mills. *International journal of machine tools and manufacture*, 41(15), 2195~2212.

Frank, M. C. Wysk, R. A. Joshi, S. B. (2004). Rapid planning for CNC milling – a new approach for rapid prototyping. *Journal of Manufacturing Systems*, 23(3), 242-255.

Hague, R. D'Costa, G. Dickens P.M. (2001). Structural design and resin drainage characteristics of QuickCast 2.0. *Rapid Prototyping Journal*, 7(2), 66-72.

Hann, V. (1983). *Kinetic de Schaftrasens*. Ph.D dissertation, Aschen: Technischen Hochschule.

He, N. Wang, Z. G. Jiang, C. Y. Zhang, B. (2003). Finite element method analysis and control stratagem for machining deformation of thin-walled components. *Journal of Material Processing Technology*, 139(1-3), 332-336.

Horvath, I. Kovacs, Z. Vergeest, J. S. M. Broek, J. J. Smit, A. (1999). Free-form cutting of plastic foams: a new functionality for thick-layered fabrication of prototypes. *Proceedings of the TCT' 98 Conference*, 229-237.

Hur, J.H. Lee, K. Zhu-hu Kim, J. (2002). Hybrid rapid prototyping system using machining and deposition. *Computer Aided Design*, 34(10), 741-754.

Iwabe, H. Natori, S. Masuda, M. Miyaquchi, T. (2004). Analysis of surface generation mechanism of ball end mill based on deflection by FEM. *JSME International Journal, Series C: Mechanical Systems, Machine Elements and Manufacturing*, 47(1), 8-13.

Jacobs, P.F. (1995). QuickCast 1.1 and rapid tooling. *Proceedings of 4th European Conference on Rapid Prototyping & Manufacturing*, 1-27.

Jalili Saffar, R. Razfar, M. R. Zarei, O. Ghassemieh, E. (2008). Simulation of three-dimension cutting force and tool deflection in end milling operation based on finite element method. *Simulation Modeling Practice and Theory*, 16(10), 1677-1688.

Joo, J. Cho, H. Yun, W. (1997). Efficient feature-based process planning for sculptured pocket machining. *Computers &Industrial Engineering*, 33(3-4), 493-496.

Karapatis, N.P. Van Griethuysen, J.P.S. Glardon, R. (1997). Injection molds behavior and lifetime characterization. *Proceedings of the Solid Freeform Fabrication Symposium*, 317-324.

Kawola, J. (2003). Zcast direct metal casting from data to cast aluminum in 12 hours. *Website: http://www.3dprint.no*, Last accessed: October, 2008.

Kim, G. M. Kim, B. H. Chu, C.N. (2002). Estimation of cutter deflection and form error in ball-end milling processes. *International Journal of Machine Tools & Manufacture*, 43(9), 917-924.

King, D. Tansey T. (2003). Rapid tooling: selective laser sintering injection tooling. *Journal of Materials Processing Technology*, 132(1-3), 42-48.

Kline, W.A. Devor, R. E. Shareef, I.A. (1982). The prediction of surface accuracy in end milling. *Transaction of the ASME Journal of Engineering for Industry*, 104, 272-278.

Koenigsberger, F. Tlusty, J. (1967). *Machine Tool Structure-Vol. 1: Stability Against Chatter*. Pergamon Press.

Kops, L. Vo, D. T. (1990). Determination of equivalent diameter of an end mill based on its compliance. *Annals of the CIRP*, 39(1), 93-96.

Lacerda, H. B. Lima, V. T.(2004). Evaluation of cutting forces and prediction of chatter vibrations in milling. *Journal of the Brazil Society of Mechanical Science & Engineering*, XXVI (1) , 74-81.

Lee, C.W. Chua, C.K. Cheah, C.M. Tan, L.H. Feng, C. (2004). Rapid investment casting: direct and indirect approaches via fused deposition modeling. *International Journal of Advanced Manufacturing Technology*, 23(1-2), 93-101.

Lee, Y. S. Choi, B. K. Chang, T. C. (1992). Cut distribution and cutter selection for sculptured surface cavity machining. *International Journal of Production Research*, 30(6), 1447-1470.

Lee, Y. S. Chang, T. C. (1994). Using virtual boundaries for the planning and machining of protrusion freeform features. *Computers in Industry*, 25(2), 173-187.

Lee, Y. S. Chang, T. C. (1995). Application of computational geometry in optimizing 2.5D and 3D NC surface machining. *Computers in Industry*, 26(1), 41-59.

Leong, K.F. Chua, C.K. Ng, Y.M. (1996). Study of stereolithography file errors and repair: part 1- generic solution. *International Journal of Advanced Manufacturing Technology*, 12(6), 407- 414.

Leong, K.F. Chua, C. Ng, Y. M. (1996). Study of stereolithography file errors and repair: part 2-special cases. *International Journal of Advanced Manufacturing Technology*, 12(6), 415- 422.

Liew, L. S. Maekawa, K. Lida, S. Suzuki T. (2003). The application of the brazing process in Selective Laser Sintering fabricated parts. *JSME International Journal, Series A: Solid Mechanics and Material Engineering*, 46(3), 506-511.

Lim, T. Corney, J. Clark, D. E. R. (2000). Exact tool sizing for feature accessibility. *International Journal of Advanced Manufacturing Technology*, 16(11), 791-802.

Lin, A. C. Gian, R. (1999). A multiple-tool approach to rough machining of sculptured surfaces. *The International Journal of Advanced Manufacturing Technology*, 15(6), 387-398.

Link, G. R. Fessler, J. Nickel, A. Prinz, F. (1998). Rapid tooling die cast inserts using shape deposition manufacturing. *Materials and Manufacturing Processes*, 13(2), 263-274.

Liu, Z. Q Venuvinod, P. K. (1999). Error compensation in CNC turning solely from dimensional measurements of previously machined parts. *Annals of the CIRP*, 48(1), 429-432.

Lo, C. C. Hsiao, C. Y. (1998). CNC machine tool interpolator with path compensation for repeated contour machining. *Computer Aided Design*, 30(1), 55-62.

Luo, R.C. Chang, Y.C. Tzou, J.H. (2001). The development of a new adaptive slicing algorithm for layered manufacturing systems. *Proceedings of the 2001 IEEE International Conference on Robotics & Automation*, 1334-1339.

Luo, X. M. Frank, M. C. (2009). A layer thickness algorithm for Additive/Subtractive Rapid Pattern Manufacturing. *Rapid Prototyping Journal, (*Accepted).

Luo, X. M. Frank, M. C. (2009). A tool size and machining parameter selection algorithm for Additive/Subtractive Rapid Pattern Manufacturing. *Rapid Prototyping Journal*, (To be submitted).

Mathews, J.H. Fink, K.D. (2004). *Numerical methods: using Matlab*. Prentice hall.

MDF Standard (1999). *China: GB/T 11718-1999*.

Merchant, M. E. (1944). Basic Mechanics of the metal cutting process. *Transaction of the ASME Journal of Applied Mechanics*, A11, 168-175.

Merrit, H. E. (1965). Theory of self-exited machine tool chatter. *Transaction of the ASME Journal of Engineering for Industry*, 87, 447-454.

Merz, R. Prinz, F.B. Ramaswami, K. Terk, M. Weiss, L.(1994). Shape deposition manufacturing. *Proceedings of the Solid Freeform Fabrication Symposium*, 1-8.

Michaels, S. Sachs, E. M. Cima, M. J. (1992). Metal parts generation by three dimensional printing. P*roceedings of the Solid Freeform Fabrication Symposium*, 244-250.

Millit webpage (2007). Millit - Rapid Prototyping durch Fräsen. *http://www.millit.net/*, November, 2007.

MillPro webpage (1998). Machine tool testing software and machining problem diagnosis software. *http://www.maline.com*, March, 2009.

Mueller, B. Kochan, D. (1999). Laminated object manufacturing for rapid tooling and patternmaking in foundry industry. *Computers in Industry*, 39(1), 47-53.

Nadjakova, I. Mcmains, S. (2004). Finding an optimal set of cutter radii for 2D pocket machining. *Proceedings of International Mechanical Engineering Congress and RD&D Expo*, 1-8.

Naitove, N.H. (1996). Faster, bigger desktop modeler. *Plastics Technology*, 42(12), 27.

Obara, H. Watanabe, T. Osumi, T. Hatano, M. Ninomiya, E. (2003). A Method to Machine Three-Dimensional Thin Parts. *Journal of the Japan Society for Precision Engineering*, 69(3), 375-379.

Opitz, H. Bernardi, F. (1970). Investigation and calculation of the chatter behavior of lathe and milling machines. *Annals of the CIRP*, 18, 335~343.

Pandey, P.M. Reddy, N.V. Dhande, S.G. (2003). Slicing procedures in layered manufacturing: a review. *Rapid Prototyping Journal*, 9(5), 274-288.

Perng, D. B. Cheng, C. T. (1994). Feature based process plan generation from 3D DSG inputs. *Computers & Industrial Engineering*, 26(3), 423-435

Pham, D. T. Dimov, S. S. Lacan, F. (2000). The Rapid Tool process: technical capabilities and applications. *Proceedings of the Institution of Mechanical Engineers, Part B: Journal of Engineering Manufacture*, 214(2), 107-116.

Pinilla, J.M. Kao, J. Prinz, F.B. (1998). Process planning and automation for additive/subtractive solid freeform fabrication. *Proceedings of the Solid Freeform Fabrication Symposium*, 245-258.

Rad, M. T. Bidhendi, I. M. (1997). On the optimization of machining parameters for milling operations. *International Journal of Machine Tools & Manufacture*. 37(1), 1-16.

Ramaswami, K. Yamaguchi, Y. Prinz, F. B. (1997). Spatial partitioning of solids for solid freeform fabrication. *Proceedings of the Fourth ACM Symposium on Solid Modeling and Applications*, 346-353.

Rao, V. S. Rao, P. V. M. (2006). Tool deflection compensation in peripheral milling of curved geometries. *International Journal of Machine Tools & Manufacture*, 46(15), 2036-2043.

Perng, D. B. Cheng, C. T. (1994). Feature based process plan generation from 3D DSG inputs. *Computers & Industrial Engineering*, 26(3), 423-435

Ribeiro, M. V. Coppini, N. L (1999). An applied database system for the optimization of cutting conditions and tool selection. *Journal of Materials Processing Technology*, 92-93, 371-374.

Ryu, S. H. Lee, H. S. Chu, C. N. (2003). The form error prediction in side wall machining considering tool deflection. *International Journal of Machine Tools & Manufacture*, 43(14), 1405-1411.

Sabberwal, A. J. P. (1961). Chip Section and cutting force during the milling operation. *Annals of the CIRP*, 10, 197-203.

Sabourin, E. Houser, S. A. Bohn, J. H. (1997). Accurate exterior, fast interior layered manufacturing. *Rapid Prototyping Journal*, 3(2), 44-52.

Salgado, M. A. Lopez de Lecalle, L. N. Lamikiz, A. Munoa, J. Sanchez, J. A. (2005). Evaluation of the stiffness chain on the deflection of end-mills under cutting forces. *International Journal of Machine Tools & Manufacture*, 45(6), 727-739.

Schaaf, W. (2000). Robotyping-new rapid prototyping processes for sand casting moulds using industrial robots. *Assembly Automation*, 20(4), 321-329.

Smith, S. Tlusty J. (1988). Modeling and simulation of the milling process. *Proceeding of Winter Annual Meeting of the American Society of Mechanical Engineer*, 17-26.

Smock, D. (1995). New moldmaking system slice Art-to-Part cycles. *Plastic World*, 53(7), 38-42.

Song, Y.A. Park, S. Choi, D. Jee, H. (2005). 3D welding and milling: part I – a direct approach for freeform fabrication of metallic prototypes. *International Journal of Machine Tools and Manufacture*, 45(9), 1057-1062.

Song, Y.A. Park, S. Chae, S.W. (2005). 3D welding and milling: part II – optimization of the 3D welding process using an experimental design approach. *International Journal of Machine Tools and Manufacture*, 45(9), 1063-1069.

Song, Y. Chen, Y.H. (1999). Feature based robot machining for rapid prototyping. *Proceedings of the Institution of Mechanical Engineers, Part B: Journal of Engineering Manufacture*, 213(5), 451–459.

Sun, G. P. Sequin, C. H. Wright, P. K. (2001). Operation decomposition for freeform surface features in process planning. *Computer-Aided Design*, 33(9), 621-636.

Sutherland, J. W. Devor, R. E. (1986). An improved method for cutting force and surface error prediction in flexible end milling systems. *Transaction of the ASME Journal of Engineering for Industry*, 108(4), 269-279.

Tang, Y. Fuh, J.Y.H. Loh, H.T. Wong, Y.S. Lu, L.(2003). Direct laser sintering of a silica sand. *Materials & Design*, 24(8), 623-629.

Taylor, F. W.(1907). *On the Art of Cutting Metals*. Transaction of the ASME, 28.

Taylor, J. B. Cormier, D. R. Joshi, S. Venkataraman, V. (2001). Contoured edge slice generation in rapid prototyping via 5-axis machining. *Robotics and computer integrated manufacturing*, 17(1-2), 13-18.

Tlusty, J. MacNeil, P. (1975). Dynamics of cutting forces in end milling. *Annals of the CIRP*, 24(1), 21-25.

Tlusty, J. (1985). *Machine dynamics, handbook of high speed machining technology*. New York: Chapman and Hall.

Tlusty, J. (1986). Dynamics of high-speed milling. *Transaction of the ASME Journal of Engineering for Industry*, 108(2), 59-67.

Tlusty, J. Hernadez, I. Smith, S. Zamudio, c. (1987). High speed high power spindles with roller bearings. *Annals of the CIRP*, 36(1),267-272.

Tobias, S. A (1965). *Machine tool Vibration*. Blackie and Sons Ltd.

Trent, E. M.(1977). *Mteal cutting*. Butterworths.

Tyberg, J. Bohn, J. H. (1998). Local adaptive slicing. *Rapid Prototyping Journal*, 4(3), 118-127.

Veeramani, D. Gau, Y. S. (1997). Selection of an optimal set of cutting-tool sizes for 2 ½ D pocket machining. *Computer Aided Design*, 29(12), 869-877.

Veeramani, D. Gau, Y. S. (2000). Cutter-path generation using multiple cutting-tool sizes for 2 ½ D pocket machining. *IIE transactions*, 32(7), 661-675.

Vouzelaud, F. A. Bagchi, A. (1992). Adaptive laminated machining for prototyping of dies and molds. P*roceedings of the Solid Freeform Fabrication Symposium*, 291-300.

Wang W. P. (1988). Solid modeling for optimizing metal removal of three-dimensional NC end milling. *Journal of Manufacturing Systems*, 7(1), 57-65.

Wang, W. Conley, J.G. Stoll, H.W. (1999). Rapid tooling for sand casting using laminated object manufacturing process. *Rapid Prototyping Journal*, 5(3), 134-141.

Wang, J. Armarego, E. J. A. (1995). Optimization strategies and CAM software for multiple constraint face milling operations. *Proceedings of 6th International Conference on Manufacturing Engineering*, 535-540.

Wang, Y. Ma, H. J. Gao, C. H. Xu, H. G. Zhou, X. H. (2005). A computer aided tool selection system for 3D die/mould-cavity NC machining using both a heuristic and analytical approach. *International Journal of Computer Integrated Manufacturing*, 18(8), 686-701

Weiss, L. Prinz, F. (1998). Novel applications and implementations of shape deposition manufacturing. *Naval Research Reviews*, 1(3), 19-26.

Yang, D. C. H. Han, Z. (1999). Interference detection and optimal tool selection in 3-axis NC machining of free-form surfaces. *Computer-Aided Design*, 31(5), 303-315.

Yang, Z.Y. Chen, Y.H. Sze, W.S. (2002). Layer-based machining: recent development and support structure design. *Proceedings of the Institution of Mechanical Engineers, Part B: Journal of Engineering Manufacture*, 216(7), 979-991.

Yang, Z.Y. Chen, Y.H. Sze, W.S. (2002). Layer-based machining: Recent development and support structure design. *Proceedings of the Institution of Mechanical Engineers, Part B: Journal of Engineering Manufacture*, 216(7), 979-991.

Yao, Z. Y. Gupta, S. K. Nau, D. S. (2001). A geometric algorithm for finding the largest milling cutter. *Journal of Manufacturing Processes*, 3(1), 1-16.

Yao, Z. Y. Gupta, S. K. Nau, D. S. (2003). Algorithm for selecting cutters in multi-part milling problems. *Computer-Aided Design*, 35(9), 825-839.

Yazar, Z. Koch, K. F. Merrick, T. Altan, T. (1994) Feed rate optimization based on cutting force calculations in 3-axis milling of dies and moulds with sculptures surfaces. *International Journal of Machine Tools & Manufacture,* 34(3), 365-377

Zorev, N. N. (1966). *Metal Cutting Mechanics*. Pregamon Press.